Technische Universität München

TUM School of Life Sciences

Role of the t(4;11) fusion proteins MLL/AF4 and AF4/MLL for survival and growth of patient-derived xenograft leukemia cells *in vivo*

Kerstin Völse

Vollständiger Abdruck der von der TUM School of Life Sciences der Technischen Universität München zur Erlangung des akademischen Grades eines

Doktors der Naturwissenschaften (Dr. rer. nat.)

genehmigten Dissertation.

Vorsitzender: Prof. Dr. Wolfgang Wurst

Prüfer der Dissertation:

1. Prof. Dr. Arnd Kieser
2. Prof. Dr. Bernhard Küster

Die Dissertation wurde am 30.11.2020 bei der Technischen Universität München eingereicht und durch die TUM School of Life Sciences am 04.05.2021 angenommen.

Parts of this work have been published in:

M. Carlet*, **K. Völse***, J. Vergalli, M. Becker, T. Herold, A. Arner, D. Senft, V. Jurinovic, W.-H. Liu, Y. Gao, V. Dill, B. Fehse, C. D. Baldus, L. Bastian, L. Lenk, D. M. Schewe, J. W. Bagnoli, B. Vick, J. P. Schmid, A. Wilhelm, R. Marschalek, P. J. Jost, C. Miehting, K. Riecken, M. Schmidt-Supprian, V. Binder, I. Jeremias

"*In vivo* inducible reverse genetics in patients' tumors to identify individual therapeutic targets"

Nature Communications 2021; 12(1):5655, doi: 10.1038/s41467-021-25963-z

* These authors share first authorship.

Table of contents

List of abbreviations

AF4	ALL1-fused gene from chromosome 4
AF5q31	ALL1-fused gene from 5q31
AF9	ALL1-fused gene from chromosome 9
AF10	ALL1-fused gene from chromosome 10
AHP	Acute hepatic porphyria
AIFM2	Apoptosis-inducing factor 2
AL	Acute leukemia
ALF	AF4, LAF4 and FMR2
ALL	Acute lymphoblastic leukemia
AML	Acute myeloid leukemia
AURKB	Aurora kinase B
BBC3	BCL2 Binding Component 3
BCR	Breakpoint cluster region
BLI	Bioluminescence imaging
BM	Bone marrow
BRIP1	BRCA1 Interacting Protein C-Terminal Helicase 1
CBP	CREB Binding Protein
cDNA	Complementary DNA
CENPA	Centromere Protein A
CDC6	Cell Division Cycle 6
CDK2	Cyclin Dependent Kinase 2
CD164	Cluster of differentiation 164
CRISPR	Clustered Regularly Interspaced Short Palindromic Repeats
CtBP	C-terminal-binding protein
dnTASP1	Dominant negative Tapase1
Dot1	Disruptor of telomeric silencing 1-like
DSB	Double-strand break
dsRNA	Double-stranded RNA
EF-1α	Eukaryotic translation elongation factor 1 alpha
eFFly	Enhanced firefly luciferase
eGFP	Enhanced GFP

EGR	Early Growth Response
ELL	Eleven-nineteen Lys-rich leukemia
ENL	Eleven-nineteen leukemia
ER	Estrogen receptor
FACS	Fluorescence-activated cell sorting
FMR2	Fragile X mental retardation 2
FSC	Forward scatter
GEPDX	Genetically engineered PDX
GFP	Green fluorescent protein
GLuc	Gaussia luciferase
GOI	Gene of interest
GSEA	Gene set enrichment analysis
hATTR	Hereditary transthyretin amyloidosis
HCF	Host cell factor
HLA	Human leucocyte antigen
HOXA	Homeobox A
HSPC	Hematopoietic stem/progenitor cell
Hsp90	Heat shock protein 90
H2AFX	H2A histone family member X
IL-2	Interleukin 2
iRFP	Infrared fluorescent protein
KD	Knockdown
LAF4	Lymphoid nuclear protein related to AF4
LDL	Low density lipoprotein receptor
LEDGF	Lens epithelium-derived growth factor
loxP	Locus of X-over of bacteriophage P1
LSPC	Lin−/Sca1+ purified cell
luc	Luciferase
MACE	Massive Analysis of cDNA Ends
MACS	Magnetic cell separation
MCEF	Major CDK9 elongation factor-associated protein
MCM	Minichromosome Maintenance Complex Component
MEF	Mouse embryonic fibroblasts
MEN1	Menin

MFI	Mean fluorescent intensity
miRNA	microRNA
MLL	Mixed lineage leukemia
MRD	Minimal residual disease
mRNA	Messenger RNA
mTagBFP	Monomeric blue fluorescent protein
NGFR	Nerve growth factor receptor
NLS	Nuclear localization signal
NK	Natural killer
NOD	Non-obese diabetic
nt	Nucleotide
PcG	Polycomb group
PDK1	Pyruvate Dehydrogenase Kinase 1
PDX	Patient-derived xenograft
PECAM1	Platelet endothelial cell adhesion molecule 1
PHD	Plant homeodomain
PLCG1	Phospholipase C Gamma 1
POLE2	DNA Polymerase Epsilon 2
Pol II	Polymerase II
pre-miRNA	Precursor mi-RNA
pri-miRNA	Primary miRNA
Prkdc	Protein kinase, DNA-activated, catalytic subunit
P-TEFb	Positive transcription elongation factor b
qRT-PCR	Quantitative real-time PCR
RISC	RNA induced silencing complex
RNA	Ribonucleic acids
RNAi	RNA interference
RNU5D-1	RNA, U5D Small Nuclear 1
RSK	Ribosomal Protein S6 Kinases
RT	Room temperature
SCID	Severe combined immunodeficiency
SEC	Super elongation complex
SET	Su(var)3–9/Enhancer of zeste/trithorax
SFFV	Spleen focus-forming virus

SIAH	Seven in absentia homologue
shRNA	Short-hairpin RNA
siRNA	Small interfering RNA
SNL	Subnuclear localization signals
SPHK1	Sphingosine Kinase 1
SSC	Side scatter
ssRNA	Single-stranded RNA
TAD	Transactivation domain
TAM	Tamoxifen
Taspase1	Threonine aspartase 1
TFIIA	Transcription initiation factor IIA
TGF	Transforming growth factor
TP53INP1	Tumor Protein P53 Inducible Nuclear Protein 1
TUBB4B	Tubulin Beta 4B Class IVb
UBE2C	Ubiquitin Conjugating Enzyme E2 C
UTR	Untranslated region
V(D)J	Variable-diversity-joining
VEGFR2	Vascular Endothelial Growth Factor Receptor 2

List of figures

List of tables

Abstract

Acute leukemia, a disease of the hematopoietic system, is characterized by a block of differentiation and an accumulation of immature blood cells. MLL rearrangements are frequently detected in childhood acute lymphoblastic leukemia (ALL). Among them, patients with a t(4;11) rearrangement have a high risk leukemia with bad prognosis and new therapeutic options are definitively needed. Although intensive research was performed so far to understand the function of this translocation, many questions remain open. In this project, I investigated the importance of the two chimeric fusion proteins MLL/AF4 and its reciprocal AF4/MLL for tumor maintenance in patients' tumor cells *in vivo*.

To achieve precise targeting of the fusion proteins, breakpoint specific short-hairpin (sh) ribonucleic acids (RNAs) were designed and expressed by previously established constitutive and inducible knockdown (KD) systems. In order to optimize the running technique and increase the KD efficiency, the inducible KD system was improved using on the one hand a stronger miR-30-based backbone and on the other hand shRNA concatamers. In addition to RNA interference (RNAi), a dominant negative Tapase1 was expressed to molecularly inhibit the reciprocal AF4/MLL fusion protein. In addition to leukemic cell lines, patient-derived xenograft (PDX) leukemia cells were used for *in vivo* experiments as a highly clinically related model system.

The experiments performed here revealed no essential function of AF4/MLL in established leukemia, despite inhibition of AF4/MLL by dnTASP1 expression induced alterations of cell cycle related genes, as detected by gene expression analysis. Analysis of the second fusion protein MLL/AF4 revealed, in contrast to the reciprocal AF4/MLL fusion protein, an essential function of MLL/AF4 for leukemia maintenance. MLL/AF4 played a clearly essential role upon constitutive KD using a breakpoint specific shRNA. More importantly and directly mimicking the situation of patients before treatment, even an inducible KD of MLL/AF4 in established patients' t(4;11) leukemia showed an essential function and reduced tumor growth. Accordingly, gene expression profiles showed alterations in proliferation, differentiation and apoptosis upon MLL/AF4 silencing in PDX cells re-isolated from murine bone marrow.

Taken together, MLL/AF4 represents a potent, highly specific target for molecular therapy of t(4;11) leukemia, which is not expressed in healthy cells and might be

addressed by future treatment to improve prognosis and outcome of patients suffering t(4;11) ALL.

Zusammenfassung

Die akute Leukämie, eine Erkrankung des hämatopoietischen Systems, ist durch eine gehemmte Zelldifferenzierung und einer Akkumulierung unreifer Blutzellen gekennzeichnet. Hierbei treten MLL-Rearrangements häufig bei akuten lymphatischen Leukämie (ALL)-Patienten im Kindheitsalter auf. Darunter gehören Patienten mit einer t(4;11) Translokation, die zu einer schweren Form der Leukämie mit schlechter Prognose führt und wofür neue Therapieoptionen dringend benötigt werden. Obwohl intensiv an der Funktion der Translokation geforscht wird, stehen weiterhin viele Fragen offen. In diesem Projekt habe ich die Bedeutung der chimären Fusionsproteine MLL/AF4 und AF4/MLL für die Tumorerhaltung in Patienten abgeleiteten Tumorzellen untersucht.

Um die Fusionsproteine präzise zu inhibieren wurden bruchpunkt spezifische shRNAs designt und mit zuvor etablierten konstitutiven und induzierbaren knockdown (KD) Systemen exprimiert. Um die Technik und die KD Effizienz zu erhöhen, wurde das induzierbare System auf der einen Seite mit Hilfe einer stärkeren miR-30 basierten Kassette und auf der anderen Seite durch shRNA Konkatamerisierung verstärkt. Zusätzlich zu der RNA Interferenz wurde eine dominant negative Taspase1 (dnTASP1) exprimiert um das reziproke AF4/MLL Fusionsprotein zu inhibieren. Für die Versuche wurden zusätzlich zu Zelllinien auch Patienten abgeleitete Xenograft (PDX) Leukämie Zellen als kliniknahes Modellsystem *in vivo* verwendet.

Die hier durchgeführten Versuche zeigten keine essentielle Funktion für AF4/MLL in einer etablierten Leukämie, jedoch führte die Inhibierung von AF4/MLL durch dnTASP1 zu Veränderungen im Zellzyklus, wie in Genexpressionsanalysen gezeigt werden konnte. Bei der Analyse des zweiten Fusionsproteins, MLL/AF4, konnte im Gegensatz zu AF4/MLL eine essentielle Funktion von MLL/AF4 für die Leukämieerhaltung gezeigt werden. Ein konstitutiver KD von MLL/AF4 mit einer bruchpunkt spezifischen shRNA zeigte die essentielle Rolle von MLL/AF4. Mit Hilfe eines induzierbaren KD Systems konnte die Situation der Patienten vor einer Behandlung simuliert werden. Selbst mit diesem System konnte das Wachstum der t(4;11) Leukämiezellen durch einen induzierbaren KD von MLL/AF4 reduziert werden. Genexpressionsanalysen zeigten Veränderungen in der Proliferation, Differenzierung und Apoptose nach MLL/AF4 Inhibierung in PDX Zellen.

Zusammengefasst repräsentiert MLL/AF4 einen wirksamen und hoch spezifischen Kandidaten für die molekulare Therapie von t(4;11) Leukämien, welches nicht in gesunden Zellen exprimiert wird und für zukünftige Therapien genutzt werden könnte, um die Prognose von t(4;11) ALL Patienten zu verbessern.

1. Introduction

1.1 Acute leukemia

Acute leukemia (AL) was first described in the early nineteenth century when cases of patients with altered or uncommon blood were reported (Piller, 2001). The term “leukemia” was established in 1945 by Bennett to describe a disease of the hematopoietic system. Defined by a block of differentiation and proliferation of immature blood cells, AL is the most common childhood cancer accounting for one third of all pediatric cancers (Siegel et al., 2020, Esparza and Sakamoto, 2005). Furthermore, death caused by leukemia is the second most frequent cause of cancer death for men younger than 40 years and women younger than 20 years in the United States (Siegel et al., 2020). In AL, acute lymphoblastic leukemia (ALL) and acute myeloid leukemia (AML) are distinguished according to the lineage that is altered (Fig. 1). AML is a heterogeneous disease mostly present in elderly people while ALL mainly occurs in children.

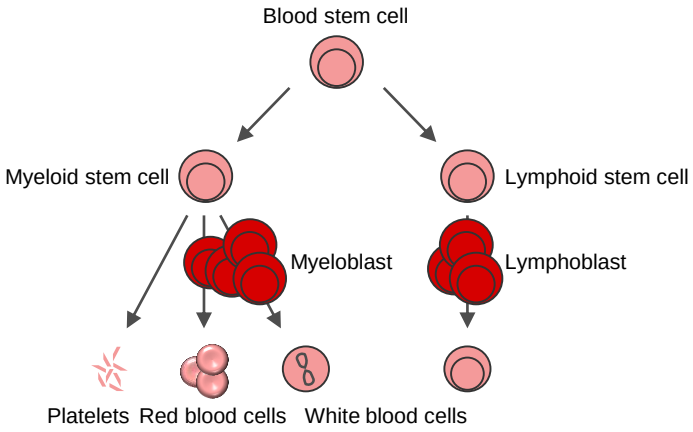

Figure 1: Altered blood cell differentiation in acute leukemia
Blood stem cells normally differentiate into myeloid or lymphoid stem cells and finally into platelets, red blood cells or white blood cells. In acute leukemia, the differentiation process is altered and leads to an accumulation of immature myelo- or lymphoblasts.

1.1.1 Acute lymphoblastic leukemia

According to the Robert-Koch-Institute, ~4.3 cases per 100,000 children under the age of 15 are diagnosed with ALL each year in Germany. These patients have a relatively good prognosis with a five-year overall survival above 90 %, except in defined subgroups (Brenner and Spix, 2003, Pulte et al., 2008). In adults, the prognosis

declines with cure rates of 30 – 40 % for patients over the age of 40, due to frequent relapses (Gökbuget et al., 2012).

In ALL different subtypes are distinguished that are based on the lineage in which the leukemogenic event occurred, B- or T-cell lineage, and on the stage of lymphoid differentiation. 80 % of all ALL cases are precursor B-ALL, 1 – 2 % have a mature B-ALL and 15 – 20 % of patients have a T-ALL (Chiaretti et al., 2014). In some cases, independent from the specific ALL subtype, the initiating leukemogenic event occurred prenatally (Taub et al., 2002). Especially in infants with precursor B-ALL, the mutational load is very low with in average 2.5 mutations per genome, representing the most stable genome across 24 different cancer cohorts among children (Agraz-Doblas et al., 2019). Secondary alterations can be acquired during disease progression (Mullighan et al., 2007).

Alterations found in ALL vary between patients. Loss or gain of whole chromosomes, chromosomal translocations or sequence mutations disturbing for example the lymphoid development, tumor suppression or chromatin modifications are common alterations in ALL patients (Iacobucci and Mullighan, 2017). Due to advances in treatment, many children can be cured, with the exception of some specific alterations resulting in high-risk leukemia. While a high hyperdiploidy with a gain of at least five chromosomes is associated with good prognosis, chromosomal translocations with MLL belong to the high-risk group (Paulsson et al., 2015, Pieters et al., 2007).

1.1.2 Chromosomal translocations in acute leukemia

Chromosomal translocations are frequent alterations in acute leukemia. They occur when at least two double-strand breaks (DSBs) take place simultaneously in separate chromosomes and when free double-strand ends of different chromosomes are ligated (Richardson and Jasin, 2000). DSBs arise either spontaneously during DNA replication, DNA repair and V(D)J recombination or they can be induced by treatment with e.g. topoisomerase II inhibitors like Etoposide leading to DSBs in the *KMT2A* (MLL) gene (Libura et al., 2005).

A translocation results in fusion genes and leads to dysregulated partner genes or to fusion proteins with new biological functions. This process is often an early or initiating event in leukaemogenesis, but usually additional events are required to cause leukemia (Daley et al., 1990, Yuan et al., 2001). The different AL subtypes are characterized by distinct translocations. Identification of chromosomal translocations

is of special interest for risk classification and determination of the therapy intensity. In childhood leukemia, more than 200 genes involved in translocations have been found. However, there are certain predominate genes like *KMT2A*, *TEL* or *AML1* that are found with more than 15 different partner genes after chromosomal translocation (Greaves and Wiemels, 2003). *KMT2A* rearrangements are found especially in infants with ALL younger than one year and are associated with poor prognosis (Pui et al., 2002). In ALL, the major chromosomal translocation is t(4;11), described intensively in the following chapter.

1.2 t(4;11) translocation

The t(4;11) chromosomal translocation is a rearrangement of *KMT2A* and *AFF1* (Gu et al., 1992). *KMT2A* transcribes the mixed lineage leukemia (MLL) protein and *AFF1* the ALL1-Fused Gene from Chromosome 4 (AF4) protein.

A translocation of the *KMT2A* gene occurs in ~80 % of all ALL cases in infants and in ~15 % of all adult ALL cases (Esparza and Sakamoto, 2005). The fusion partner differs regarding the type of leukemia and the age of the patient (Meyer et al., 2018). Until now, 135 different translocation partners could be identified but only 9 account for more than 90 % of all MLL translocations (Meyer et al., 2018).

The most prominent fusion partner in ALL with ~57 % is AF4 regardless of the age of the patients (Fig. 2). Infants with a t(4;11) translocation have a very bad prognosis with survival rates of 10 – 30 % (Isoyama et al., 2002, Pui et al., 2002). There, the t(4;11) translocation is often acquired in utero with only very few further alterations so that the translocation is sufficient to initiate leukemia (Andersson et al., 2015, Ford et al., 1993). As a consequence of the MLL/AF4 translocation two new chimeric fusion proteins are generated, MLL/AF4 and the reciprocal AF4/MLL. These fusion proteins and their newly acquired functions are described in detail in chapter 1.2.3.

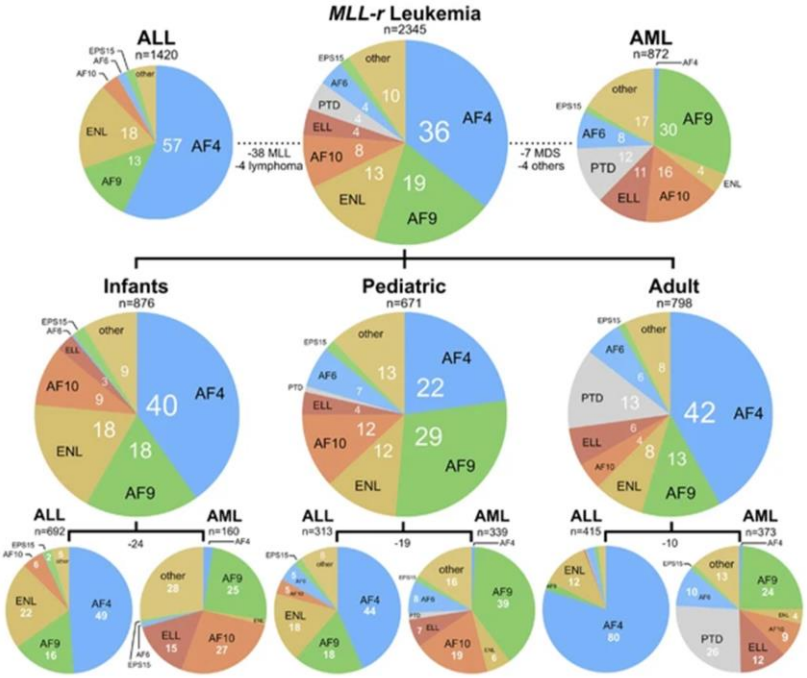

Figure 2: MLL fusion partners according leukemia type and patient age
Most frequent MLL fusion partners of a cohort with 2345 MLL-rearranged acute leukemia patients. Patient were classified as ALL or AML and distributed regarding the age of the patients (infant: 0.03-12 month; pediatric: >12 month-18 years; adult: >18 years). Name of fusion partners are written in black, frequencies are written as white numbers, negative numbers indicate patients that were not classified as ALL or AML subtype (Meyer et al., 2018).

1.2.1 Mixed lineage leukemia (MLL) protein

MLL is a nuclear protein encoded by the *KMT2A* gene, located on chromosome 11 at q23. It shares its function with the *Drosophila* homologue Trithorax as important regulator of development by regulating the *Hox* gene expression (Ernst et al., 2004). MLL is expressed in most fetal and in adult hematopoietic cell types including stem cells and progenitors (Kawagoe et al., 1999). Loss of MLL is lethal, as shown using MLL-deficient mice (Hess et al., 1997, Yagi et al., 1998).

KMT2A consists of 37 exons and encodes the 4,005-amino-acid MLL protein (Marschalek et al., 1997, Nilson et al., 1996). Of note, in ~90 % of all MLL transcripts exon 2 is missing (Meyer et al., 2006). Furthermore, alternative splicing leads to different MLL mRNA transcripts that can change the activity of MLL from being a positive modulator of gene transcription to a transcriptional repressor complex (Ma et al., 1993, Mbangkollo et al., 1995, Rössler and Marschalek, 2013).

MLL has multiple domains (Fig. 3) (Tkachuk et al., 1992). At the N-terminus MLL has three AT-hook motifs for binding AT-rich DNA (Zeleznik-Le et al., 1994). Further, sub-nuclear localization signals (SNL) and a DNA methyltransferase homology domain are

part of MLL. This DNA methyltransferase homology domain recognizes and binds DNA with unmethylated CpG sequences and represses transcription and targets MLL to specific promoter sites like, for example, the promoter of some *HOX* genes (Birke et al., 2002, Ono et al., 2005, Prasad et al., 1995). MLL has four cysteine-rich plant homeodomain (PHD) zinc fingers mediating protein-protein interactions (Fair et al., 2001). At the C-terminus the protein has a transactivation domain and a SET (Su(var)3–9/Enhancer of zeste/trithorax) domain (Tkachuk et al., 1992). The SET domain binds to histone H3, Sbf1, ASH1 and itself and has an intrinsic H3 lysine 4 methylation activity inducing target genes like *HOX* (Rozovskaia et al., 2000, Milne et al., 2002, Nakamura et al., 2002, Hsieh et al., 2003b).

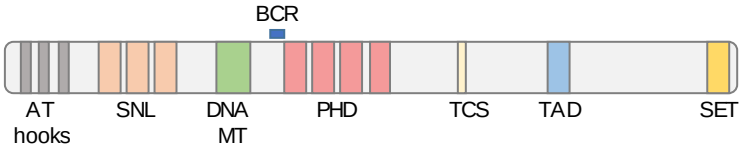

Figure 3: Functional domains of MLL
Depiction of MLL protein domains. (SNL: subnuclear localization signal; DNA MT: DNA methyltransferase homology domain; PHD: cysteine-rich plant homeodomain zinc fingers; TCS: Taspase1 cleavage site; TAD: transactivation domain; SET: Su(var)3–9/Enhancer of zeste/trithorax domain; BCR: breakpoint cluster region).

The MLL protein is post-translationally cleaved by the threonine aspartase 1 (Taspase1) between amino acid positions 2666/2667 and 2718/2719 next to the transactivation domain resulting in a 320 kDa N-terminal and a 180 kDa C-terminal fragment (Hsieh et al., 2003b, Hsieh et al., 2003a). These fragments immediately heterodimerize to form a stable complex and translocate into the nucleus, where MLL assembles into a supercomplex composed of at least 29 proteins that remodels, acetylates, deacetylates and methylates free histones and nucleosomes (Yokoyama et al., 2004, Nakamura et al., 2002). The N-terminal MLL fragment possesses transcriptional repression activity mediated by transcriptional co-regulators like Host cell factor 1 and 2 (HCF-1, HCF-2), by co-repressors C-terminal-binding protein (CtBP) and Polycomb group (PcG) proteins or by histone deacetylases (Xia et al., 2003, Yokoyama et al., 2004). The C-terminal MLL fragment can activate transcription for example through the recruitment of the co-activator CREB Binding Protein (CBP) with histone acetyltransferase activity leading to acetylation of histones H3 and H4 at target genes (Ernst et al., 2001, Yokoyama et al., 2004).

Over 100 fusion partners were found for MLL, but the most frequent MLL fusion partners are AF4, ALL1-fused gene from chromosome 9 (AF9), ALL1-fused gene from

chromosome 10 (AF10) and eleven-nineteen leukemia (ENL) all belonging to the 1.5 MDa super elongation complex (SEC) (Lin et al., 2010). The function of SEC and the importance of the complex for the fusion proteins are described below.

1.2.2 ALL1-Fused Gene From Chromosome 4 (AF4) protein

AF4 is encoded by *AFF1* and located on chromosome 4 at q21 (Chen et al., 1993, Gu et al., 1992). It consists of 23 exons with four alternative first exons, 1a1, 1a2, 1b and 1c and is translated into a 131 kDa protein, mainly located in the nucleus (Nilson et al., 1997). AF4 belongs to the ALF (AF4, LAF4 and FMR2) family including the fragile X mental retardation 2 (FMR2), the lymphoid nuclear protein related to AF4 (LAF4) and the ALL-1 fused gene from 5q31 (AF5q31, also named major CDK9 elongation factor-associated protein (MCEF)). The ALF family share a N- and C-terminal homology domain, a serine-rich transactivation domain (TAD), a nuclear localization signal (NLS) and a ALF homology domain (Fig. 4). The ALF homology domain promotes proteasomal degradation by interaction with the ubiquitin ligase seven in absentia homologue (SIAH) (Nilson et al., 1997, Prasad et al., 1995, Bursen et al., 2004).

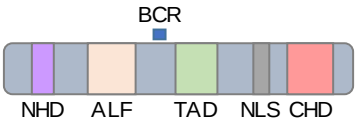

Figure 4: Functional domains of AF4
Depiction of AF4 protein domains. (NHD: N-terminal homology domain; ALF: ALF homology domain; TAD: transactivation domain; NLS: nuclear localization signal; CHD: C-terminal homology domain; BCR: breakpoint cluster region).

AF4 is widely expressed in hematopoietic and non-hematopoietic cells; especially high expression levels are found in the lymphoid system (Chen et al., 1993, Frestedt et al., 1996, Isnard et al., 1998). Inactivation of AF4 by homologous recombination in mice influences the development of B and T cells showing a critical function for lymphoid development (Isnard et al., 2000). Overexpression of Af4 was studied using a robotic mouse generated by phenotype-based mutagenesis. Here, a point mutation in the ALF domain led to overexpression of Af4 resulting in cerebellar ataxia and Purkinje cell loss as well as in abnormalities in T cell development (Isaacs et al., 2003).

The AF4 protein is part of the transcriptional regulatory chromatin remodeling complex called SEC. Beside AF4 it includes AF9, AF10, ENL, the eleven-nineteen Lys-rich leukemia (ELL) family member ELL1, ELL2, ELL3 and the positive transcription elongation factor b (P-TEFb) (Bitoun et al., 2007, Lin et al., 2010). SEC regulates gene

transcription by P-TEFb mediated RNA Polymerase II (Pol II) activation. Further, SEC mediates disruptor of telomeric silencing 1-like (Dot1) recruitment leading to H3K79 methylation and to an open chromatin structure (Bitoun et al., 2007). Thus, not only MLL but also AF4 play an important role in gene regulation.

1.2.3 MLL/AF4 and AF4/MLL fusion proteins

The t(4;11) translocation can lead to the expression of two chimeric fusion proteins, MLL/AF4 and AF4/MLL alongside the wildtype MLL and AF4 proteins. MLL/AF4 consists of the N-terminal part of MLL and the C-terminal part of AF4, while for AF4/MLL it is the other way round.

Translocations occur in specific breakpoint cluster regions (BCR). The main BCR in the *KMT2A* gene is in the introns between exon 9 and 11 (Meyer et al., 2013). Only ~6.5 % of the patients with MLL rearrangement have a MLL breakpoint outside the BCR (Meyer et al., 2018). The BCR of *AFF1* is between exon 3 and 7 (Nilson et al., 1997). This implies that in general MLL/AF4 consists of the N-terminal part of MLL with AT-hook motifs, subnuclear localization signals and a DNA methyltransferase homology domain fused to the C-terminal part of AF4 having a transactivation domain, a C-terminal homology domain and a nuclear localization signal (Fig. 5). In contrast, AF4/MLL consists of the N-terminal part of AF4 with the N-terminal homology domain and the ALF homology domain and is combined with the C-terminal part of MLL with PHD zinc fingers, a Taspase1 cleavage site, a transactivation and a SET domain. The resulting fusion proteins are characterized by new biological functions.

In detail, the missing C-terminal part of MLL in MLL/AF4 affects the methylation pattern and the target gene activity as the SET domain is lost. However, gene expression profiles of leukemia patient cells showed that MLL/AF4 is capable of activating MLL target genes like the HOX genes *HOXA4*, *HOXA5* and *HOXA9* as well as *MEIS1* which encodes a cofactor for HOX proteins (Milne et al., 2002, Armstrong et al., 2002, Yeoh et al., 2002, Rozovskaia et al., 2001). This expression profile was observed in MLL translocated leukemia patients independent from the specific fusion partner. The N-terminal part of MLL is able to bind to MLL target genes by associating with Menin (MEN1) and lens epithelium-derived growth factor (LEDGF, also named PC4 and SFRS1 interacting protein 1). The C-terminal part of AF4 interacts with the other common MLL fusion partner AF9, AF10, ENL and DOT1L. This interaction stabilizes

the SEC machinery at MLL target genes and leads to overexpression of these genes (Lin et al., 2010, Krivtsov et al., 2008).

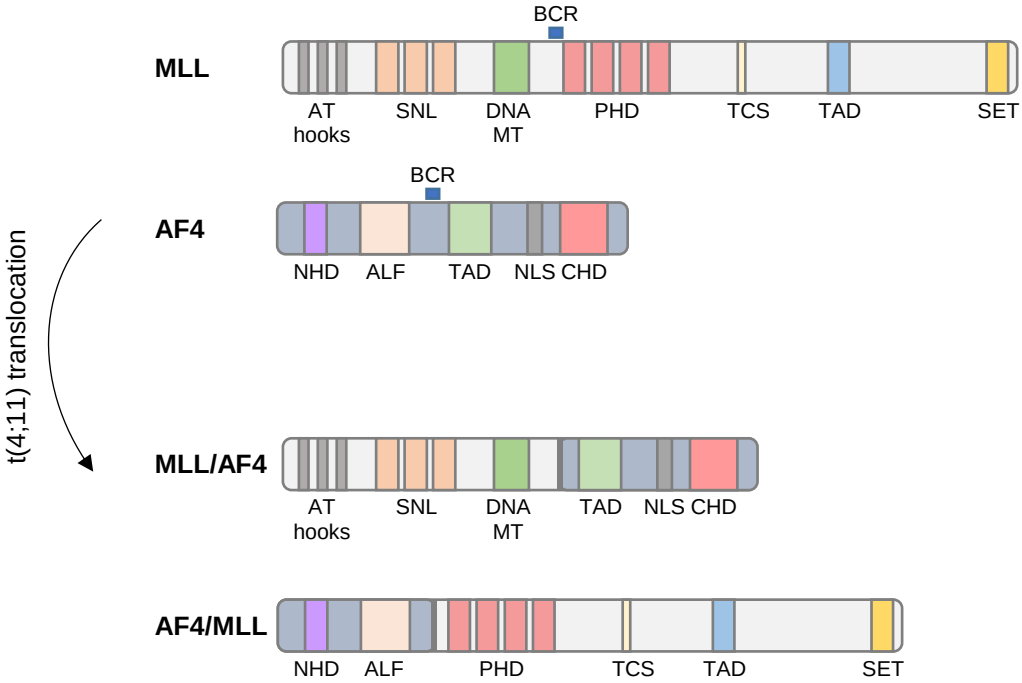

Figure 5: Functional domains of MLL and AF4 in wildtype and fusion proteins
MLL and AF4 protein domains are depicted in native proteins and after t(4;11) translocation. (SNL: subnuclear localization signal; DNA MT: DNA methyltransferase homology domain; PHD: cysteine-rich plant homeodomain zinc fingers; TCS: Taspase1 cleavage site; TAD: transactivation domain; SET: Su(var)3–9/Enhancer of zeste/trithorax domain; BCR: breakpoint cluster region; NHD: N-terminal homology domain; ALF: ALF homology domain; NLS: nuclear localization signal; CHD: C-terminal homology domain).

The reciprocal AF4/MLL fusion protein is cleaved by Taspase1 at the C-terminal part of MLL. The cleaved protein heterodimerizes and competes with the endogenous MLL for binding partners to form a supercomplex and leads to a new H3K4 and H3K79 methylation pattern resulting in aberrant gene expression (Benedikt et al., 2011). Wildtype AF4 is degraded after each cycle of transcriptional elongation by interaction with SIAH. However, for the AF4/MLL fusion protein, the ubiquitin ligase is not able to initiate the degradation leading to a prolonged protein half-life of 72 – 96 h (Bursen et al., 2004).

It remains unclear whether MLL/AF4, AF4/MLL or both fusion proteins are essential for the development and maintenance of a t(4;11) leukemia. While all patients with a t(4;11) translocation express MLL/AF4, only 50 – 80 % express both fusion proteins (Agraz-Doblas et al., 2019, Kowarz et al., 2007, Trentin et al., 2009, Downing et al., 1994, Reichel et al., 2001). Different groups have generated Mll/AF4 knock-in mouse models or MLL/AF4 expressing cord blood cells using CRISPR/Cas9 which result in

B-cell lymphoma and leukemia (Chen et al., 2006, Krivtsov et al., 2008, Secker et al., 2019). Furthermore, inhibition of MLL/AF4 by siRNA in t(4;11) cell lines led to impaired proliferation and clonogenicity (Thomas et al., 2005). In contrast, Lin−/Sca1+ purified cells (LSPCs) retrovirally transduced with MLL/AF4 were not capable of inducing leukemia in mice (Bursen et al., 2010). However, LSPCs transduced with AF4/MLL could induce ALL in mice (Bursen et al., 2010), while AF4/MLL expression in neonatal CD34+ hematopoietic stem/progenitor cells (HSPCs) did not initiate leukemia (Prieto et al., 2017). Nevertheless, a transient AF4/MLL KD in cell line did not show any changes in proliferation, cell cycle or apoptosis (Kumar et al., 2011b). Moreover, a cooperation of MLL/AF4 and AF4/MLL during hematopoietic development was described and co-transfection of cell lines with MLL/AF4 and AF4/MLL increased resistance against apoptotic triggers and enhanced the cell cycling capacity (Bueno et al., 2019, Gaussmann et al., 2007). Recently, Agraz-Doblas et al. (2019) published that HOXA genes were exclusively expressed in t(4;11) leukemia patients with AF4/MLL expression. These patients had a significantly better 4-year overall survival with 73.7 % compared to 25.2 % of t(4;11) leukemia patients without AF4/MLL expression (Agraz-Doblas et al., 2019). The reason for the prolonged survival by AF4/MLL expression is unknown.

In summary, it is still under discussion which impact both fusion proteins have for the development and maintenance of leukemia and further investigations are required.

1.3 Proteases in cancer

Proteases are enzymes that regulate physiological processes like gene expression, differentiation and cell death by determining the overall turnover of proteins. They are able to hydrolyze peptide bonds between amino acids and are responsible e.g. for protein degradation to recycle or inactivate proteins or to destroy misfolded ones. In humans, more than 600 proteases are known and are classified as aspartic, cysteine, glutamic, metallo, asparagine, serine and threonine proteases (Barrett et al., 2001, Ordóñez et al., 2009).

Proteases play a critical role in cancer as they can control tumor invasion, angiogenesis and metastasis. Tumor cells can induce expression of proteases in neighboring cells to increase the nutrient and oxygen supply (Yang et al., 2009). Due to upregulation of proteases during cancer progression, proteases are ideal therapeutic targets and inhibitors are developed for cancer therapy.

Here, the role of a specific threonine protease, the threonine aspartase 1, is described more in detail, as it is necessary for the cleavage of MLL and of the reciprocal fusion protein AF4/MLL.

1.3.1 Threonine aspartase 1

The threonine protease Taspase1 is encoded by the *taspase1* gene located on chromosome 12 at p12. It encodes a 420 amino acid proenzyme that gets autoproteolytically processed after dimerization into a 28 kDa α and 22 kDa β subunit which assemble afterwards in catalytically active homo- (αβ) or heterodimers (αββα) (Hsieh et al., 2003b). With an endopeptidase activity, it recognizes a conserved peptide motif with aspartate residues (Hsieh et al., 2003b, Sabiani et al., 2015).

A genome-wide bioinformatics prediction resulted in 27 putative targets for Taspase1 (Bier et al., 2011). These putative targets are involved in DNA repair, cell cycle, transcription, transport and developmental and metabolic processes and are known to play a role in tumorigenesis. Additionally, Taspase1 is overexpressed in different types of cancer representing an interesting target for therapy (Bier et al., 2011, Chen et al., 2010). However, only few Taspase1 target proteins are confirmed: MLL, MLL4, the transcription initiation factor IIA (TFIIA) and the reciprocal AF4/MLL fusion protein (Bursen et al., 2004, Hsieh et al., 2003b, Zhou et al., 2006). MLL is cleaved by Taspase1 at two highly conserved sites, CS1 and CS2, heterodimerize and form a stable multiprotein complex (Hsieh et al., 2003b). Moreover AF4/MLL is processed by Taspase1 leading to a stable multiprotein complex that is resistant against SIAH-mediated degradation (Krämer et al., 2013). Therefore, Taspase1 functions in t(4;11) leukemia as an oncoprotein and represents an interesting therapeutic candidate.

In Taspase1 deficient mice, an impaired proliferation of mouse embryonic fibroblasts (MEFs) and a reduction of thymocytes were observed (Takeda et al., 2006). Inhibition of Taspase1 by RNAi or small molecule inhibitors in adult mice had no adverse side effects (Chen et al., 2012, Hsieh et al., 2003b). There, uncleaved MLL led to reduced histone H3 methyl transferase activity and reduced HOX expression (Takeda et al., 2006, Hsieh et al., 2003b). Further *in vitro* studies showed impaired proliferation of different cancer cell lines upon Taspase1 KD (Chen et al., 2010).

Taken together, Taspase1 is overexpressed in different cancers and plays an important role especially in t(4;11) leukemia as it generates a stable AF4/MLL protein. Therefore, Taspase1 is of high interest for putative cancer therapy.

1.3.2 Dominant negative Taspase1

As Taspase1 represents a potential therapeutic target, different inhibitors or small molecules to inhibit Taspase1 have been developed in recent years (Chen et al., 2012, Hsieh et al., 2003b). Sabiani et al. (2015) created a dominant negative Taspase1 (dnTASP1) by site-directed mutagenesis (C163E and S291A) to specifically inhibit and analyze the function of AF4/MLL. Upon dimerization of dnTASP1 with a wildtype Taspase1 monomer, the S291A mutation impaired hydrolyzation between D233 and T234 of dnTASP1 while mutation at site C163E blocked positioning of S291 in the dimerized wildtype Taspase1. Thus, dimerization with dnTASP1 results in enzymatically inactive heterodimers (Sabiani et al., 2015).

The function of dnTASP1 was tested in MLL and AF4/MLL transfected HEK-293T cells *in vitro*. While in cells expressing wildtype Taspase1, cleaved fragments of MLL and AF4/MLL could be detected by western blot, no cleaved products could be observed in dnTASP1 transfected cells (Sabiani et al., 2015). Furthermore, expression of dnTASP1 had only minor effects on MLL dependent HOX expression, as unprocessed MLL is still sufficient to induce transcription of target genes (Hsieh et al., 2003a, Sabiani et al., 2015). Therefore, the normal cell physiology is not significantly impaired by dnTASP1 expression. In contrast, inhibition of AF4/MLL cleavage by dnTASP1 resulted in fast protein degradation mediated by SIAH, a process which might have a significant impact for the treatment of t(4;11) leukemia (Sabiani et al., 2015).

In conclusion, Sabiani et al. (2015) generated a dominant negative Taspase1 variant by site-directed mutagenesis that has no overt significant effect on normal cell physiology but prevents dimerization of AF4/MLL fragments and therefore induces degradation of the fusion protein.

1.4 RNA interference

RNAi is a technique allowing specific gene silencing by inducing messenger RNA (mRNA) degradation using double-stranded RNA (dsRNA). It was first discovered in *Caenorhabditis elegans* in 1993 by detecting a small RNA, lin-4, regulating the gene *lin-14* that is partially complementary to the lin-4 RNA (Lee et al., 1993, Wightman et al., 1993). A few years later in 1998, the term RNA interference was introduced after the discovery of Fire et al. (1998): injecting dsRNA in *C. elegans* led to specific gene silencing. Since then over 300 microRNAs (miRNAs) have been discovered in the human genome regulating cell differentiation and development (Cullen, 2005).

Nowadays, RNAi is widely used to study the function of selected genes and as potential method for disease therapy.

1.4.1 Inhibition of gene expression by shRNAs

In vertebrates, the post-transcriptional RNAi process relies on ~22 nucleotide (nt), single-stranded RNAs (ssRNAs) guiding a ribonucleoprotein complex to target mRNAs (Fig. 6) (Bartel, 2004, Cullen, 2004). Specifically, these miRNAs are first transcribed by Pol II as primary miRNAs (pri-miRNAs, >1 kb) (Lee et al., 2002, Ohler et al., 2004). After, the pri-miRNA is processed by Drosha, an RNAase III endonuclease generating a ~65 nt precursor mi-RNA (pre-miRNA) hairpin (Lee et al., 2003). This intermediate is then shuttled from the nucleus to the cytoplasm by the nuclear export factor Exportin-5. In the nucleus, the pre-miRNA interacts with another RNase III enzyme called Dicer (Lund et al., 2004, Yi et al., 2003). Dicer removes the hairpin loop and generates 22 nt long short double-stranded miRNAs. These miRNAs interact with the RNA induced silencing complex (RISC), which binds them as ssRNA (Elbashir et al., 2001, Martinez et al., 2002). The RISC complex is able to identify mRNAs that have partial sequence complementarity in the 3' untranslated region (UTR) to the incorporated miRNA and induces their cleavage by Argonaute-2 (Cullen, 2005, Lee et al., 2002). Taken together, RNAi is a post-transcriptional process inducing the silencing of homologous mRNA.

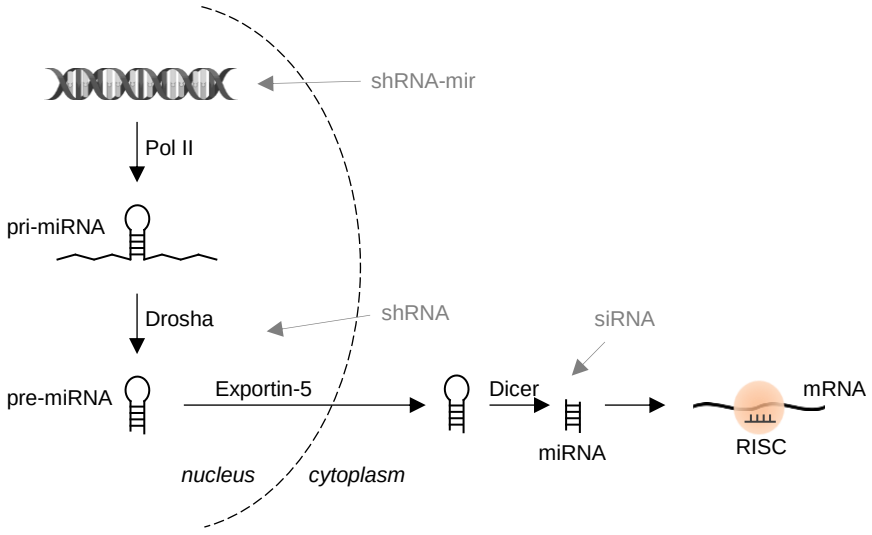

Figure 6: RNA interference
Schematic of RNAi mediated gene silencing. The primary miRNA (pri-miRNA) is transcribed by polymerase II (Pol II) and processed by Drosha generating a precursor miRNA (pre-miRNA). Exportin-5 transports the pre-miRNA into the cytoplasm. Here, Dicer removes the pre-miRNA hairpin loop and generates a double stranded miRNA. The miRNA interacts with the RNA induced silencing complex (RISC) and is incorporated as single strand RNA to target complementary mRNA. Entry sites for artificial gene silencing using shRNA-mir, shRNAs and siRNAs are depicted in grey.

This natural process can be exploited to achieve artificial gene silencing in specific target cells using small interfering RNAs (siRNAs), shRNAs or shRNA-mir. siRNAs are comparable to the natural miRNAs and are directly incorporated into RISC leading to gene specific silencing (Elbashir et al., 2001). They are delivered into cells by transfection or electroporation. Thus, using siRNAs for gene silencing is a fast and easy process, however, only a transient KD is induced and the depletion of stable proteins is challenging (Harborth et al., 2003). Another option for gene silencing is the use of shRNAs that are comparable to pre-miRNAs. shRNAs are introduced by expression plasmids and transcribed by the strong RNA Polymerase III (Brummelkamp et al., 2002, Paddison et al., 2002). However, highly expressed shRNAs compete with natural miRNAs for factors like Exportin-5. This leads to saturation of the endogenous miRNA pathway and is responsible for cell toxicity (Grimm et al., 2006). A third option for artificial RNAi is the use of modified microRNAs, which are comparable to the pri-miRNA. To this aim, Zeng and colleagues developed in 2002 a lentiviral vector where specific shRNA (22mer long) sequences could be embedded into the miR-30 original sequence. Thus, the shRNA-miR-30 cassette is integrated into the genome and is expressed from Pol II, like the natural pri-miRNA. Thus, a stable, effective and tissue specific KD is achieved, avoiding cell toxicity (Dickins et al., 2005, Silva et al., 2005, Zeng et al., 2002).

In conclusion, numerous techniques were developed in the last years to induce gene silencing, among those the stable KD by miR-30 based shRNA-mir is widely used for functional studies (Liao and Tang, 2016).

1.4.2 Inducible Cre-ER^{T2} system

Stable shRNA expression results in long term gene silencing and has several advantages, as it is cost effective, has the ability to inhibit stable proteins and allow performing long-term studies. Nevertheless, the system has some drawbacks, as it cannot be used to analyze gene inhibition at defined time points and to study essential genes, especially *in vivo*. To overcome these limitations, different inducible RNAi systems were generated including Cre-loxP, tetracycline-, ecdysone- and lactose-inducible systems (Ait-ali et al., 2003, Gatz et al., 1992, Mett et al., 1993, Wiznerowicz and Trono, 2003).

Cre-loxP is a site-specific recombinase system. Cre is a 38 kDa recombinase protein originally found in bacteriophage P1 (Hoess et al., 1982). It binds to the locus of X-over

of bacteriophage P1 (loxP) sites that consist of 34 bp nucleotide sequences and mediates recombination between loxP sites (Guo et al., 1997). If the loxP sites are placed in the same direction, the intervening DNA sequence is excised and one loxP site is deleted in the genome. This results in an irreversible deletion of a specific part of DNA. If the loxP sites are oriented anti-parallel, Cre induces an inversion of the DNA sequence in between. This inversion is reversible and can direct the DNA sequence in the opposite direction upon recombination (Hoess et al., 1982). Further, loxP sites can be placed on different chromosomes to generate specific chromosomal translocations. To create an inducible Cre-loxP system, Cre was fused to a mutated estrogen receptor (ER) that does not bind it's natural ligand 17β-estradiol at normal concentrations but responds to tamoxifen (TAM), resulting in a TAM-dependent Cre recombinase (Cre-ER^T) (Metzger et al., 1995, Feil et al., 1996, Zhang et al., 1996). Feil et al. (1997) improved the system by further mutations in the Cre ligand-binding domains leading to Cre-ER^{T2} with a G400V/M543A/L544A triple mutation and a 3 to 4-fold increased sensitivity to TAM, thus reducing putative toxicity in mice (Feil et al., 1997). When using the system without TAM, Cre-ER^{T2} is inactive and binds to heat shock protein 90 (Hsp90) in the cytoplasm. In the presence of TAM, TAM binds to Cre-ER^{T2}, displaces the heat shock proteins and induces translocation of Cre-ER^{T2} to the nucleus (Mattioni et al., 1994). Once in the nucleus, Cre-ER^{T2} catalyzes DNA recombination at inserted loxP sites. Thus, induction of Cre-ER^{T2} by TAM enables regulating the expression of specific loxP directed target genes at defined time points.

The Cre-ER^{T2} system is widely used for genetic manipulations. Stern et al. (2008) developed a Cre-ER^{T2} mediated shRNA expression construct (Fig. 7). To this aim, they used two mutated loxP pairs, which are unable to recombine with each other (Oberdoerffer et al., 2003). The construct contain a puromycin resistance and the surface marker Thy1.1 in sense orientation flanked by two different loxP sites. Additionally, the green fluorescent protein (GFP) and the miR-30 RNAi construct are located in antisense orientation followed by two loxP sites in the opposite direction to the first loxP sites. Irreversible recombination requires two steps: First, Cre-ER^{T2} induces a reversible inversion leading to two different intermediate constructs. Second, the following recombination deletes the puromycin resistance, Thy1.1 and a loxP site preventing reversion to the original construct. Thus, at the end GFP and the miR-30 RNAi construct are expressed. This process was termed "flipping" by Stern et al. (2008).

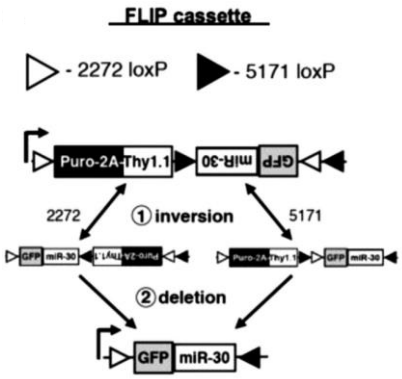

Figure 7: Cre-ER^{T2} mediated RNA interference
Inducible shRNA expression construct mediated by a Cre-loxP system. The depicted construct consists of a puromycine resistance (Puro-2A) and the surface marker Thy1.1 in sense orientation and GFP and a miR-30 cassette in antisense orientation. Two mutated loxP pairs allow stable and irreversible recombination in a two step pathway. First, a reversible inversion occurs in the presence of Cre-ER^{T2} leading to two different intermediate constructs. Second, the puromycine resistance and the surface marker Thy1.1 are deleted due to the flanked loxP pair. Thus, expression of GFP and the miR-30 cassette are induced by Cre-ER^{T2} (Stern et al., 2008)

Using the above described FLIP constructs, transgenic cells can be selected by selection markers (e.g. resistance marker or fluorophores) and shRNA coupled to transgenic markers can be induced at defined time points. Hence, even genes, which are essential for cells' development, can be investigated *in vivo*.

1.4.3 Increased inhibition by optimized shRNAs

The miR-30 based constitutive KD was so far widely used for different kind of studies as it is a very effective method resulting in high KD efficiencies (Liao & Tang, 2016). Nevertheless, in some cases, for example when the shRNA is expressed from a single genomic copy, even potent shRNAs are not able to induce a strong KD (Fellmann et al., 2011). Moreover, when targeting specific mutations or translocations weaker shRNAs are designed due to limitations in the design of the target site, thus resulting in low KD efficiencies. To overcome these limitations and increase gene silencing by shRNAs different groups tried to optimize the technique.

One option to increase the shRNA KD efficiency is to use an optimized version of the miR-30 cassette. The miR-30 cassette used for artificial shRNA expression differs from the natural human MIR30A e.g. by the introduction of EcoRI and XhoI restriction sites for shRNA cloning. Fellmann et al. (2013) reverted all alterations, individually, to analyze their impact on the shRNA efficiency. They realized that in the miR-30 cassette, the EcoRI cloning site was placed in a conserved region of the basal stem. Repositioning this restriction site to a non-conserved region increased the KD

efficiency and led to a 10 - 30 fold higher shRNA expression (Fellmann et al., 2013). This optimized backbone was termed miR-E and can be easily used in RNAi studies.
Another possibility to improve gene silencing is by shRNA concatamerization. Naturally, some miRNAs exist in clusters of identical or different miRNAs (Lagos-Quintana et al., 2001). Sun et al. (2006) developed an artificial miRNA cluster by shRNA concatamerization. It was shown that the pre-miRNA is generated efficiently when it has, beside its own 65 nt hairpin structure, a minimum of 22 nt single-stranded RNA extensions outside the hairpin (Zeng and Cullen, 2005). Based on this observation, Sun et al. (2006) extended miR-30 hairpins to 118 nt, plus an artificial sequence carrying the cloning sites. This strategy allows to connect multiple hairpins *via* an artificial sequence; thus, using two or three shRNA copies enhanced the KD efficiency compared to a single shRNA (Sun et al., 2006). In addition, shRNAs targeting different genes can be concatamerized resulting in multiple KDs in parallel.
In summary, the use of a more potent miR-30-based cassette and concatamerization of numerous shRNAs can be used as strategy to increase the KD efficiency especially when shRNAs are expressed from a single genomic copy or when the shRNA sequence is weak, due to design related limitations.

1.5 Patient-derived xenograft mouse model of acute leukemia

Studying a disease relies highly on the model system used. As cell lines frequently have additional, unphysiological mutations, lack the heterogeneity of the disease and do not represent all clinical subtypes, patient cells or mouse models are often used for clinical investigations (Leroy et al., 2014). Patient cells are ideal models as they reflect the disease preserving tumor heterogeneity; however, primary cell material is limited and primary ALL cells cannot be cultured over long period *in vitro* thus restricting experimental settings. To overcome this problem, PDX mouse models were developed *via* engraftment of patient-derived cells into immunocompromised mice. Here, the heterogeneity of tumor cells, the characteristics of the disease as well as the gene expression profile are retained (Tentler et al., 2012, Cassidy et al., 2015).
To generate PDX models, immunocompromised mice had to be developed first. The first immunocompromised mice called “nude” were generated in 1962, but the presence of a still functional innate immune system did not allow transplantation of human cells (Flanagan, 1966). Therefore, other types of immunocompromised mice have been developed throughout the years. Mice with a severe combined

immunodeficiency (SCID) lack functional T and B lymphocytes due to mutated Prkdc (protein kinase, DNA-activated, catalytic subunit) (Bosma et al., 1983). In non-obese diabetic (NOD) mice, T lymphocytes infiltrate and destroy pancreatic islets leading to diabetes mellitus (Makino et al., 1980). In addition, further immune abnormalities were observed in NOD mice including impaired function of natural killer (NK) cells, macrophages and dendritic cells as well as loss of the complement system (Kikutani and Makino, 1992). Breeding of NOD and SCID mice led to NOD/SCID mice that have multiple defects in the innate and adaptive immune system but they do not develop diabetes due the lack of T cells (Shultz et al., 1995). To remove some residual NK cell activity, NOD/SCID mice were crossbred with interleukin-2 (IL-2) receptor γ-deficient mice as the γ chain is critical for NK cell development resulting in NSG mice (Notarangelo et al., 2000, Shultz et al., 1995). Finally, in NSG mice normal and malignant human cells can be transplanted with high engraftment capacity (McDermott et al., 2010, Shultz et al., 2005).

PDX models of acute leukemia are generated by injecting patients' leukemia cells isolated from BM aspirates or peripheral blood into immunocompromised mice. PDX cells first engraft in the murine BM, afterward they can infiltrate other organs like spleen and liver. The success rate of generating PDX relies on the disease characteristics. For acute leukemia, the engraftment capacity and overall survival of mice correlates with the prognosis of patients (Woiterski et al., 2013). Cells isolated from patients with relapses or very aggressive leukemia are especially able to engraft into mice (Vick et al., 2015). Acute leukemia PDX cells are then used to study e.g. leukemia stem cells, evolution, interaction of leukemic cells with the microenvironment or minimal residual disease (MRD) (Hope et al., 2004, Woiterski et al., 2013, Ebinger et al., 2016, Patel et al., 2014). Furthermore, PDX models are used for drug tests exploiting the wide variety of different genetic subgroups (Townsend et al., 2016). PDX cells can also be serially re-transplanted to be amplified for *in vivo* and *in vitro* experiments or for repetitive functional studies. Thus, PDX cells get isolated from the murine BM or spleen and are re-injected in immunocompromised mice, a process that do not interfere with the samples' heterogeneity even over serial passages. Only for some samples, subclonal skewing was observed (Vick et al., 2015).

In conclusion, the acute leukemia PDX mouse model is currently the best available model system to study leukemia. It preserves the disease characteristics and growing of PDX cells *in vivo* enables reproducible functional studies.

1.5.1 Genetic engineered PDX mouse models

More recently, several groups including the group that I worked in have established genetic engineering of PDX mouse models. Serially transplantable PDX cells from ALL patients can be genetically engineered using lentiviruses (genetically engineered PDX, GEPDX). Stable genetic modifications of PDX cells enables the *in vivo* follow up of PDX samples, e.g. tumor growth can be monitored reliably in living mice by integrating a luciferase reporter gene for bioluminescence imaging *in vivo* (Jones et al., 2017, Terziyska et al., 2012, Vick et al., 2015). Alternatively, fluorophores like mCherry or surface markers like the nerve growth factor receptor (NGFR) can be used to mark transduced cells. With these, cells can be enriched by fluorescence activated cell sorting or magnetic cell separation or they can be analyzed by flow cytometry (Carlet et al., 2021, Ebinger et al., 2016, Liu et al., 2020, Vick et al., 2015). Importantly for my goal, gene silencing can be performed in PDX cells using knockdown, knockout or knock-in approaches to investigate the function of specific targets (Carlet et al., 2021, Liu et al., 2020).

1.6 Aim of this project

The t(4;11) rearrangement leads to an aggressive type of leukemia with bad prognosis. Upon translocation, two chimeric fusion proteins, MLL/AF4 and AF4/MLL, are generated, with MLL/AF4 always present, while AF4/MLL is restricted to 50 – 80 % of the cases. So far, controversial reports have been published concerning the role of the two fusion proteins in maintaining established leukemias. This question is of major clinical significance as both fusions, if essential, represent attractive therapeutic targets.

In the present project, I aimed to investigate whether MLL/AF4 and/or its reciprocal AF4/MLL might play an essential role for maintaining patients' leukemias alive and growing. Towards this aim and to use a model system highly related to patients, I studied patient-derived xenograft mouse models *in vivo* and designed specific shRNAs against the different break points. I performed translocation-specific knockdown experiments in both a constitutive as well as a Cre-loxP-based inducible approach, the latter preventing undesired knockdown already during cell transplantation and homing that putatively overestimate effects. Beside using shRNAs, I also expressed a dominant negative Taspase1 to inhibit the AF4/MLL fusion protein regardless of the fusion breakpoint.

Using these highly patient related techniques, I aimed at gaining new insights into the function of the fusion proteins MLL/AF4 and AF4/MLL for maintaining established t(4;11) translocated leukemia alive *in vivo*.

2. Material

2.1 Mice

In this project, ALL PDX cells were engrafted into NSG mice. NSG mice have a non-obese diabetes (NOD) severe combined immune deficiency (SCID) combined with an interleukin-2 receptor γ chain knockout, Thus, they are lacking mature B, T and natural killer cells and have deficient cytokine signaling pathways (Shultz et al., 2005).

Table 1: Mice

Name	Description	Provider
NSG	NOD.Cg-Prkdc^{scid} Il2^{rgtm1Wjl}/SzJ	Jackson Laboratory, Bar Harbor, MA, USA

2.2 Cell lines

Table 2: Cell lines

Name	Description	Provider
CCRF-CEM	human T cell leukemia cell line	DSMZ, Braunschweig, Germany
HEK-293T	human embryonal kidney cell line expressing the temperature sensitive mutant of simian virus 40 large T-antigen	DSMZ, Braunschweig, Germany
JURKAT	human T cell leukemia cell line	DSMZ, Braunschweig, Germany
NALM-6	human B cell precursor leukemia cell line	DSMZ, Braunschweig, Germany
REH	human B cell precursor leukemia cell line	DSMZ, Braunschweig, Germany
SEM	human B cell precursor leukemia cell line	DSMZ, Braunschweig, Germany

2.3 Bacterial strains

Table 3: Bacterial strains

Name	Description	Provider
Escherichia coli (*E. coli*) DH5α	F$^-$ ϕ80*lac*ZΔM15 Δ(*lac*ZYA-*arg*F) U169 *rec*A1 *end*A1 *hsd*R17(r_K^-, m_K^+) *pho*A *sup*E44 *thi*-1 *gyr*A96 *rel*A1 λ$^-$	Thermo Fisher Scientific, Waltham, MA, USA

2.4 Plasmids

Table 4: Plasmids

Name	Provider
pMD2.G	Addgene, Cambridge, MA, USA
pMDLg/pRRE	Addgene, Cambridge, MA, USA
pRSV-Rev	Addgene, Cambridge, MA, USA
pCDH-EF1α-eFFly-T2A-mTagBFP	Cloned by Michela Carlet
pCDH-EF1α-eFFly-T2A-eGFP	Cloned by Michela Carlet
pCDH-SFFV-dsRED-miR30_Renilla	Cloned by Jenny Vergalli
pCDH-SFFV-dsRED-miR30_MLL/AF4	Cloned by Birgitta Heckl
pCDH-SFFV-dsRED-miR30_AF4/MLL_SEM1	Cloned by Kerstin Völse for this study
pCDH-SFFV-dsRED-miR30_AF4/MLL_PDX3	Cloned by Kerstin Völse for this study
pCDH-SFFV-dsRED-miR30_AF4/MLL_PDX4	Cloned by Kerstin Völse for this study
pCDH-SFFV-GLuc-T2A-CreERT2-P2A-mCherry	Cloned by Michela Carlet
pCDH-SFFV-GLuc-T2A-CreERT2-P2A-NGFR	Cloned by Wen-Hsin Liu
pCDH-SFFV-FLIP cassette-mTagBFP-eGFP-miR30_Renilla	Cloned by Michela Carlet
pCDH-SFFV-FLIP cassette-mTagBFP-eGFP-miR30_Renilla_Renilla	Cloned by Kerstin Völse for this study
pCDH-SFFV-FLIP cassette-mTagBFP-eGFP-miR30_Renilla_Renilla_Renilla_Renilla	Cloned by Kerstin Völse for this study
pCDH-SFFV-FLIP cassette-mTagBFP-eGFP-miRE_Renilla	Cloned by Kerstin Völse for this study
pCDH-SFFV-FLIP cassette-mTagBFP-eGFP-miRE_Renilla_Renilla	Cloned by Kerstin Völse for this study
pCDH-SFFV-FLIP cassette-mTagBFP-eGFP-miRE_Renilla_Renilla_Renilla_Renilla	Cloned by Kerstin Völse for this study
pCDH-SFFV-FLIP cassette-mTagBFP-eGFP-miR30_MLL/AF4	Cloned by Birgitta Heckl
pCDH-SFFV-FLIP cassette-mTagBFP-eGFP-miR30_MLL/AF4_MLL/AF4	Cloned by Kerstin Völse for this study
pCDH-SFFV-FLIP cassette-mTagBFP-eGFP-miR30_MLL/AF4_MLL/AF4_MLL/AF4_MLL/AF4	Cloned by Kerstin Völse for this study
pCDH-SFFV-FLIP cassette-mTagBFP-eGFP-miRE_MLL/AF4	Cloned by Kerstin Völse for this study
pCDH-SFFV-FLIP cassette-mTagBFP-eGFP-miRE_MLL/AF4_MLL/AF4	Cloned by Kerstin Völse for this study
pCDH-SFFV-FLIP cassette-mTagBFP-eGFP-miRE_MLL/AF4_MLL/AF4_MLL/AF4_MLL/AF4	Cloned by Kerstin Völse for this study
pCDH-SFFV-FLIP cassette-mTagBFP-eGFP-miR30_AF4/MLL_SEM1	Cloned by Kerstin Völse for this study

pCDH-SFFV-FLIP cassette-mTagBFP-eGFP-miR30_AF4/MLL_SEM2	Cloned by Kerstin Völse for this study
pCDH-SFFV-FLIP cassette-mTagBFP-eGFP-miR30_AF4/MLL_SEM3	Cloned by Kerstin Völse for this study
pCDH-SFFV-FLIP cassette-mTagBFP-eGFP-miR30_AF4/MLL_SEM4	Cloned by Kerstin Völse for this study
pCDH-SFFV-FLIP cassette-mTagBFP-eGFP-miR30_AF4/MLL_SEM5	Cloned by Kerstin Völse for this study
pCDH-SFFV-FLIP cassette-mTagBFP-eGFP-miR30_AF4/MLL_PDX1	Cloned by Kerstin Völse for this study
pCDH-SFFV-FLIP cassette-mTagBFP-eGFP-miR30_AF4/MLL_PDX2	Cloned by Kerstin Völse for this study
pCDH-SFFV-FLIP cassette-mTagBFP-eGFP-miR30_AF4/MLL_PDX3	Cloned by Kerstin Völse for this study
pCDH-SFFV-FLIP cassette-iRFP-T-Sapphire-miR30_Renilla	Cloned by Michela Carlet
pCDH-SFFV-FLIP cassette-iRFP-T-Sapphire-miR30_Renilla_Renilla_Renilla_Renilla	Cloned by Kerstin Völse for this study
pCDH-EF1α-dTomato-AF4/MLL sequence(SEM) _reporter	Cloned by Kerstin Völse for this study
pCDH-EF1α-dTomato-AF4/MLL sequence(PDX) _reporter	Cloned by Kerstin Völse for this study
pCDH- EF1α-iRFP-P2A-dnTASP1	Cloned by Kerstin Völse for this study
pCDH- SFFV-iRFP-P2A-dnTASP1	Cloned by Kerstin Völse for this study
pCDH-SFFV-iRFP-miR30_Renilla	Cloned by Kerstin Völse for this study

2.5 Oligonucleotides

Table 5: Oligonucleotides for shRNAs

Name	Sequence 5' → 3'
Ren_s	TCGAGAAGGTATATTGCTGTTGACAGTGAGCGCAGGAATTATAATGCTTATCTATAGTGAAGCCACAGATGTATAGATAAGCATTATAATTCCTATGCCTACTGCCTCGG
Ren_as	ATTCCGAGGCAGTAGGCATAGGAATTATAATGCTTATCTATACATCTGTGGCTTCACTATAGATAAGCATTATAATTCCTGCGCTCACTGTCAACAGCAATATACCTTC
MLL/AF4_s	TCGAGAAGGTATATTGCTGTTGACAGTGAGCGCAAGAAAAGCAGACCTACTCCATAGTGAAGCCACAGATGTATGGAGTAGGTCTGCTTTTCTTTTGCCTACTGCCTCGG
MLL/AF4_as	AATTCCGAGGCAGTAGGCAAAAGAAAAGCAGACCTACTCCATACATCTGTGGCTTCACTATGGAGTAGGTCTGCTTTTCTTGCGCTCACTGTCAACAGCAATATACCTTC
AF4/MLL_PDX1_s	TCGAGAAGGTATATTGCTGTTGACAGTGAGCGACCTTCTCAGTCAGTTGAGGAATAGTGAAGCCACAGATGTATTCCTCAACTGACTGAGAAGGCTGCCTACTGCCTCGG

AF4/MLL_ PDX 1_as	AATTCCGAGGCAGTAGGCAGCCTTCTCAGTCAGTTGAGGAATACATCTGTGGCTTCACTATTCCTCAACTGACTGAGAAGGTCGCTCACTGTCAACAGCAATATACCTTC
AF4/MLL_ PDX 2_s	TCGAGAAGGTATATTGCTGTTGACAGTGAGCGCTCTCAGTCAGTTGAGGAAAAATAGTGAAGCCACAGATGTATTTTTCCTCAACTGACTGAGAATGCCTACTGCCTCGG
AF4/MLL_ PDX 1_as	AATTCCGAGGCAGTAGGCATCAGTCAGTTGAGGAAAAACCATACATCTGTGGCTTCACTATGGTTTTTCCTCAACTGACTGGCGCTCACTGTCAACAGCAATATACCTTC
AF4/MLL_ PDX 3_s	TCGAGAAGGTATATTGCTGTTGACAGTGAGCGCGCCTTCTCAGTCAGTTGAGGATAGTGAAGCCACAGATGTATCCTCAACTGACTGAGAAGGCATGCCTACTGCCTCGG
AF4/MLL_ PDX 3_as	AATTCCGAGGCAGTAGGCATGCCTTCTCAGTCAGTTGAGGATACATCTGTGGCTTCACTATCCTCAACTGACTGAGAAGGCGCGCTCACTGTCAACAGCAATATACCTTC
AF4/MLL_ PDX 4_s	TCGAGAAGGTATATTGCTGTTGACAGTGAGCGCCAGTCAGTTGAGGAAAAACCATAGTGAAGCCACAGATGTATGGTTTTTCCTCAACTGACTGATGCCTACTGCCTCGG
AF4/MLL_ PDX 4_as	AATTCCGAGGCAGTAGGCATCAGTCAGTTGAGGAAAAACCATACATCTGTGGCTTCACTATGGTTTTTCCTCAACTGACTGGCGCTCACTGTCAACAGCAATATACCTTC
AF4/MLL_ PDX 5_s	TCGAGAAGGTATATTGCTGTTGACAGTGAGCGACTTCTCAGTCAGTTGAGGAAATAGTGAAGCCACAGATGTATTTCCTCAACTGACTGAGAAGGTGCCTACTGCCTCGG
AF4/MLL_ PDX 5_as	AATTCCGAGGCAGTAGGCACCTTCTCAGTCAGTTGAGGAAATACATCTGTGGCTTCACTATTTCCTCAACTGACTGAGAAGTCGCTCACTGTCAACAGCAATATACCTTC

Table 6: PCR primer for finger printing of mitochondrial DNA

Name	Sequence 5' → 3'
mtReg-F1	TCCACCATTAGCACCCAAAGC
mtReg-R1	TCGGATACAGTTCACTTTAGC
mtReg-F3	CGCACCTACGTTCAATATTAC
mtReg-R3	GGGTGATGTGAGCCCGTCTAA

Table 7: qPCR primer

Name	Sequence 5' → 3'
HPRT1-fw	TGATAGATCCATTCCTATGACTGTAGA
HPRT1-rev	CAAGACATTCTTTCCAGTTAAAGTTG
MLL_fw (MLL/AF4)	AAGTTCCCAAAACCACTCCTAGT
MLL_rev (MLL)	GATCCTGTGGACTCCATCTGC
AF4_rev (MLL/AF4)	GCCATGAATGGGTCATTTCC
AF4_fw (AF4)	TAGGTCTGCTCAACTGACTGAG
AF4_rev (AF4)	TAGGTCTGCTCAACTGACTGAG
AF4_fw (AF4/MLL)	GCCTTCTCAGTCAGTTGAGGA
AF4_rev (AF4/MLL)	TGGAGAGAGTGCTGAGGATGT

HOXA7_fw	CTGGATGCGGTCTTCAGG
HOXA7_rev	GGTAGCGGTTGAAGTGGAAC
HOXA9_fw	CCCCATCGATCCCAATAA
HOXA9_rev	CACCGCTTTTTCCGAGTG
HOXA10_fw	CCTTCCGAGAGCAGCAAA
HOXA10_rev	TTGGCTGCGTTTTCACCT

2.6 Enzymes

Table 8: Enyzmes

Name	Application	Provider
BamHI HF	Restriction digest	New England Biolabs, Frankfurt am Main, Germany
ClaI	Restriction digest	New England Biolabs, Frankfurt am Main, Germany
EcoRI HF	Restriction digest	New England Biolabs, Frankfurt am Main, Germany
GoTaq G2 DNA Polymerase	PCR	Promega, Madison, WI, USA
NotI HF	Restriction digest	New England Biolabs, Frankfurt am Main, Germany
NsiI HF	Restriction digest	New England Biolabs, Frankfurt am Main, Germany
Phusion High-Fidelity PCR Master Mix	PCR	New England Biolabs, Frankfurt am Main, Germany
Quantiscript Reverse Transcriptase	Reverse Transcription	Qiagen, Venlo, NL
SalI	Restriction digest	New England Biolabs, Frankfurt am Main, Germany
SbfI HF	Restriction digest	New England Biolabs, Frankfurt am Main, Germany
T4 DNA Ligase	Ligation	Thermo Fisher Scientific, Waltham, MA, USA
XbaI	Restriction digest	New England Biolabs, Frankfurt am Main, Germany
XhoI	Restriction digest	New England Biolabs, Frankfurt am Main, Germany

2.7 Antibodies

Table 9: Antibodies

Name	Provider
anti-human CD271 (NGFR)-FITC, clone ME20.4, #345104	Biozol, Eching, Germany
anti-human CD33-PE, clone IV M505, #555450	BD Bioscience, Heidelberg, Germany

anti-human CD38 PE, clone HB7, #345806	BD Bioscience, Heidelberg, Germany
anti-murine CD45-APC, clone 30-F11, #103112	Biolegend, San Diego, CA, USA
mouse IgG1 APC isotype control, clone MOPC-21, #400119	BD Bioscience, Heidelberg, Germany
mouse IgG1 PE isotype control, clone MOPC-21, #400140	Biolegend, San Diego, CA, USA
mouse IgG1 FITC isotype control, clone MOPC-21, #BLD-400107	Biozol, Eching, Germany
anti-FLAG-Tag (DYKDDDDK), clone 1042E, #MAB8529	R&D Systems, Minneapolis, MN, USA
anti-β-Actin, clone AC-15, #NB600-501SS	Novus Biologicals, Centennial, CO, USA
mouse IgG1 APC anti-human CD38, clone HB-7, #356606	Biozol, Eching, Germany

2.8 Commercial Kits

Table 10: Commercial kits

Name	Application	Provider
BCA Protein Assay Kit	Protein concentration	New England Biolabs, Frankfurt am Main, Germany
CloneJET PCR cloning Kit	Cloning	Thermo Fisher Scientific, Waltham, MA, USA
MinElute PCR Purifcation Kit	Purification of PCR product	Qiagen, Venlo, Netherlands
Monarch DNA Gel Extraction Kit	DNA extraction	New England Biolabs, Frankfurt am Main, Germany
Mouse Cell Depletion Kit	Depletion of mouse cells	Miltenyi, Bergisch Gladbach, Germany
NucleoBond Extra Midi	Isolation of plasmid DNA (Midi)	Macherey-Nagel, Duren, Germany
NucleoSpin Gel and PCR Clean-Up	Purification of PCR products, extraction of DNA from agarose gels	Macherey-Nagel, Duren, Germany
NuleoSpin Plasmid Easy Pure	Isolation of plasmid DNA (Mini)	Macherey-Nagel, Duren, Germany
QIAmp DNA Blood Mini Kit	Isolation of genomic DNA	Qiagen, Venlo, Netherlands
QuantiTect Reverse Transcription kit	Reverse transcription	Qiagen, Venlo, Netherlands
RNase-free DNase Set	DNA removal	Qiagen, Venlo, Netherlands
RNeasy Micro Kit	RNA isolation	Qiagen, Venlo, Netherlands
RNeasy Mini Kit	RNA isolation	Qiagen, Venlo, Netherlands

2.9 Chemicals and solutions

Table 11: Chemicals and solutions

Name	Provider
Acetic acid	Carl Roth, Karlsruhe, Germany
Agar-Agar Kobe I	Carl Roth, Karlsruhe, Germany
Agarose	Life Technologies, Carlsbad, CA, USA
Ampicillin (25 mg/ml)	Sigma-Aldrich, St. Louis, MO, USA
Anexate	Hexal, Holzkirchen, Germany
Anti-Mouse Detection Module for Wes	Proteinsimple, San Jose, CA, USA
Anti-Rabbit Detection Module for Wes	Proteinsimple, San Jose, CA, USA
Antisedan Vet	Prodivet pharmaceuticals S.A., Raeren, Belgium
α-Thioglycerol	Sigma-Aldrich, St. Louis, MO, USA
ATP	New England Biolabs, Frankfurt am Main, Germany
Baytril (2.5 %)	Bayer, Leverkusen, Germany
β-mercaptoethanol	Sigma-Aldrich, St. Louis, MO, USA
BSA	Carl Roth, Karlsruhe, Germany
$CaCl_2$	Carl Roth, Karlsruhe, Germany
Cell lysis buffer (10x)	Cell Signaling Technology, Boston, MA, USA
Coelenterazine	Synchem OHG, Felsberg, Germany
Corneregel	Bausch & Lomb, Berlin, Germany
Corn oil	Sigma-Aldrich, St. Louis, MO, USA
CutSmart buffer	New England Biolabs, Frankfurt am Main, Germany
D-Luciferin	Biomol GmbH, Hamburg, Germany
DMEM	Gibco, San Diego, CA, USA
DMSO	Sigma-Aldrich, St. Louis, MO, USA
DNA ladder mix	Thermo Fisher Scientific, Waltham, MA, USA
DNA loading dye	Thermo Fisher Scientific, Waltham, MA, USA
DNase I	Roche, Mannheim, Germany
DNase I Buffer	Roche, Mannheim, Germany
dNTPs (10 mM each)	Biozym, Hessisch Oldendorf, Germany
Domitor vet	Alvetra, Neumünster, Germany
Dormicum	Roche, Mannheim, Germany
EDTA (0.5 M)	Lonza, Basel, Switzerland
Ethanol	Carl Roth, Karlsruhe, Germany
FACS Lysing solution (10x)	BD Bioscience, Heidelberg, Germany
Fentanyl	Piramal, Mumbai, India
Fetal calf serum	Gibco, San Diego, CA, USA
Ficoll	GE Healthcare, Freiburg, Germany
Gentamycin	Lonza, Basel, Switzerland
Glucose (20 %)	Braun, Melsungen, Germany
Glutamine	Gibco, San Diego, USA
Glycerine 98 %	Carl Roth, Karlsruhe, Germany
HCl (32 %)	Merck Millipore, Darmstadt, Germany
Heparin	Ratiopharm, Ulm, Germany

Hepes (1 M)	Gibco, San Diego, USA
IMEM	Gibco, San Diego, USA
Insulin-Transferrin-Selenium (100x)	Gibco, San Diego, USA
Isoflurane	Sigma-Aldrich, St. Louis, MO, USA
Isopropyl alcohol	Merck Milipore, Darmstadt, Germany
K-Acetate	Sigma-Aldrich, St. Louis, MO, USA
KCl	Merck Milipore, Darmstadt, Germany
KH_2PO_4	Merck Milipore, Darmstadt, Germany
LightCycler 480 Probes Master	Roche, Mannheim, Germany
L-Glutamine	Gibco, San Diego, CA, USA
Midori Green	Biozym, Hessisch Oldendorf, Germany
$MnCl_2$	Sigma-Aldrich, St. Louis, MO, USA
MOPS	Sigma-Aldrich, St. Louis, MO, USA
Na_2HPO_4	Sigma-Aldrich, St. Louis, MO, USA
NaCl	Carl Roth, Karlsruhe, Germany
NEBuffer 3.1	New England Biolabs, Frankfurt am Main, Germany
Nitrogen	Linde AG, Pullach, Germany
PBS	Gibco, San Diego, CA, USA
Penicillin/Streptavidin (5,000 U/ml)	Gibco, San Diego, CA, USA
PMSF	Cell Signaling Technology, Boston, MA, USA
Polybrene (2 mg/ml)	Sigma-Aldrich, St. Louis, MO, USA
RPMI-1640	Gibco, San Diego, CA, USA
Selected peptone 140	Gibco, San Diego, CA, USA
Sodium pyruvate (100 mM)	Sigma-Aldrich, St. Louis, MO, USA
StemPro-34 medium	Thermo Fisher Scientific, Waltham, MA, USA
StemPro-34 Nutrient Supplement	Thermo Fisher Scientific, Waltham, MA, USA
StemSpan SFEM	STEMCELL Technologies, Vancouver, BC, Canada
T4 Ligation buffer	Thermo Fisher Scientific, Waltham, MA, USA
Tamoxifen	Sigma-Aldrich, St. Louis, MO, USA
Temgesic	Bayer, Leverkusen, Germany
Tris	Carl Roth, Karlsruhe, Germany
Trypan blue	Sigma-Aldrich, St. Louis, MO, USA
Trypsin (0.05 %)	Gibco, San Diego, CA, USA
Turbofect	Thermo Fisher Scientific, Waltham, MA, USA
Universal ProbeLibrary Probes	Roche, Mannheim, Germany
Yeast extract	Carl Roth, Karlsruhe, Germany

2.10 Buffers and Media

Table 12: Buffers

Name	Ingredients
Annealing buffer	50 mM Hepes 100 mM NaCl pH 7.4
HBG (HEPES buffered glucose)	20 mM HEPES, pH 7.1 5 % glucose w/v

Phosphate buffered saline (PBS)	H_2O 137 mM NaCl 2.7 mM KCl 10 mM Na_2HPO_4 1.8 mM KH_2PO_4
PBS + 0.5 % BSA	
TAE buffer	H_2O 1.8 g Tris/HCl, pH 8.5 1.14 ml acetic acid 0.7 g EDTA
TFB I (transformation buffer I) buffer	H_2O, pH 5.8 100 mM KCl 10 mM $CaCl_2$ 30 mM K-Acetate 50 mM $MnCl_2$ 15 % glycerine
TFB II (transformation buffer II) buffer	H_2O, pH 7.0 10 mM KCl 75 mM $CaCl_2$ 10 mM MOPS 15 % glycerine

Table 13: Media

Name	Ingredients
LB agar	H_2O 1 % Selected peptone 140 0.5 % Yeast extract 1 % NaCl 1.5 % Agar-Agar Kobe I
LB medium	H2O 1 % Selected peptone 0.5 % Yeast extract 1 % NaCl
Medium for cultivation of SEM cells	IMEM 10 % FCS 1 % L-Glutamine
Medium for cultivation of JURKAT, NALM-6 and REH cells	RPMI-1640 10 % FCS 1 % L-Glutamine
Medium for cultivation of HEK-293T cells	DMEM 10 % FCS 1 % L-Glutamine
Medium for cultivation of PDX ALL cells	StemSpan SFEM 10 % FCS 1 % L-Glutamine 1 % Pen/Strep

2.11 Consumables

Table 14: Consumables

Name	Provider
Amicon-Ultra 15 ml centrifugal filter units	Merck Milipore, Darmstadt, Germany
Bacterial tubes	Corning, Corning, NY, USA
BD microfine 1 ml syringe	BD Bioscience, Heidelberg, Germany
Cell culture EasyFlask T75	Thermo Fisher Scientific, Waltham, MA, USA
Cell culture flasks (T25, T75, T175)	Greiner bio-one, Frickenhausen, Germany
Cell strainer (45 mm, 70 mm)	Greiner bio-one, Frickenhausen, Germany
Centrifuge tubes (15 ml, 50 ml)	Greiner bio-one, Frickenhausen, Germany
Cryotubes	Thermo Fisher Scientific, Waltham, MA, USA
Disposable serological pipettes (5 ml, 10 ml, 25 ml, 50 ml)	Greiner bio-one, Frickenhausen, Germany
Eppendorf reagent tubes (0.5 ml, 1.5 ml, 2.0 ml)	Greiner bio-one, Frickenhausen, Germany
Erlenmeyer flasks	SCHOTT AG, Mainz, Germany
FACS tubes (with and without filter)	Corning, Corning, NY, USA
Filterunit Millex-HV 0.45 µm	Merck Millipore, Darmstadt, Germany
Inoculation loops	Sarstedt, Nümbrecht, Germany
LightCycler 480 Multiwell plate 96	Roche, Mannheim, Germany
LS columns	Miltenyi, Bergisch Gladbach, Germany
Microvette, Lithium-Heparin (100 µl)	Sarstedt, Nümbrecht, Germany
Needles RN G32 PST3 51MM	Hamilton, Reno, USA
Nitrile gloves	Starlab, Hamburg, Germany
Petri dishes	Greiner bio-one, Frickenhausen, Germany
Pipette filter tips TipOne	Starlab, Hamburg, Germany
Pipette tips TipOne	Starlab, Hamburg, Germany
QiaShredder	Qiagen, Venlo, NL
Rotilabo syringe filters 0.22 µm	Carl Roth, Karlsruhe, Germany
Sealing Foil for LightCycler 480	Roche, Mannheim, Germany
Surgical disposable scalpel	Braun, Melsungen, Germany
Well plates for tissue culture (6, 12, 24, 48, 96-well)	Corning, Corning, NY, USA
12-230 kDa Wes Separation Module	Proteinsimple, San Jose, CA, USA

2.12 Hardware and Equipment

Table 15: Hardware and Equipment

Name	Provider
BD Calibur	BD Bioscience, Heidelberg, Germany
BD FACS AriaIII	BD Bioscience, Heidelberg, Germany
BD LSRFortessa	BD Bioscience, Heidelberg, Germany

Biological safety cabinet Safe 2020	Thermo Fisher Scientific, Waltham, MA, USA
Calibration Check pH meter HI 221	HANNA Instrument, Vöhringen, Germany
Centrifuge Rotanta 460R	Andreas Hettich GmbH, Tuttlingen, Germany
ErgoOne pipettes	STARLAB, Hamburg, Germany
Freezer (-20 °C)	Siemens, München, Germany
Freezing container Nalgene Mr. Frosty	Sigma-Aldrich, St. Louis, MO, USA
Freezer (-80 °C)	Thermo Fisher Scientific, Waltham, MA, USA
Fridge (4 °C)	Bosch GmbH, Stuttgart, Germany
Gel documentation E-box VX5	Peqlab, Erlangen, Germany
Heating block MixerHC	Starlab, Hamburg, Germany
Incubator Hera Cell 150i	Thermo Fisher Scientific, Waltham, MA, USA
Innova 44 shaking incubator	New Brunswick Scientific, Enfield, CT, USA
IVIS Lumina II Imaging System	Caliper Life Sciences, Mainz, Germany
Laminar Flow SAFE 2000	Thermo Fisher Scientific, Waltham, MA, USA
LightCycler 480 II	Roche, Mannheim, Germany
Light microscope 550 1317	Zeiss, Jena, Germany
Microbiological incubator B 6060	Heraeus, Hanau, Germany
Microcentrifuge 5417C	Eppendorf, Hamburg, Germany
Microwave MW 1226CB	Bomann, Kempen, Germany
Micro Scales Sartorius 2001 MP2	Sartorius AG, Göttingen, Germany
Nanodrop OneC	Thermo Fisher Scientific, Waltham, MA, USA
Neubauer improved counting chamber	Brand, Wertheim, Germany
PerfectBlue Gelsystem Mini S	Peqlab, Erlangen, Germany
Pipette controller Accu-jet pro	Brand, Wertheim, Germany
Power supply PowerPac	Bio-Rad, München, Germany
ProFlex PCR system	Life Technologies, Carlsbad, CA, USA
Quietek CO_2 Induction Systems	Next Advance, Averill Park, USA
Refrigerator	Liebherr, Bulle, Germany
Roller mixer SRT6D	Stuart, Staffordshire, UK
Vortex-Genie 2	Scientific Industries, Bohemia, NY, USA
Water bath	Memmert GmbH, Schwabach, Germany

2.13 Software

Table 16: Software

Name	Provider
Compass for SW 4.0.0	ProteinSimple, San Jose, CA, USA
Endnote X9	Alfasoft GmbH, Frankfurt am Main, Germany
Geneious 11	Biomatters Ltd, Auckland, New Zealand
MyIMouse	Bioslava, Hagenbach, Germany
GSEA 4.0.1	Broad Institute, Cambridge, MA, USA
FlowJo 10	FlowJo LLC, Ashley, OR, USA
GraphPad Prism 7	Graphpad Prism, La Jolla, CA, USA
Microsoft Office	Microsoft Corporation, Tulsa, OK, USA

LightCycler 480 software 1.5.1	Roche, Mannheim, Germany
Living Image Software 4.4	PerkinElmer, Krakow, Poland

3. Methods

3.1 Ethical statements

3.1.1 Patient material

Patients' acute lymphoblastic leukemia cells were obtained from residual material of clinical diagnostic done before treatment. Written informed consent was obtained from all patients and from parents/carers in the cases where patients were minors. The study was performed in accordance with the ethical standards of the responsible committee on human experimentation (written approval by Ethikkommission des Klinikums der Ludwig-Maximilians-Universität München, Ethikkommission@med.unimuenchen.de, April 15/2008, number 068-08; September 24/2010, number 222-10; January 18/2019, number 222-10) and with the Helsinki Declaration of 1975, as revised in 2000.

3.1.2 Animal work

NSG mice were kept under specific pathogen-free conditions with free access to drinking water and food, constant room temperature (RT) and a 12-hour day-night light cycle in the research animal facility of the Helmholtz Zentrum München. All animal trials were performed in accordance with the current ethical standards of the official committee on animal experimentation (written approval by Regierung von Oberbayern, tierversuche@reg-ob.bayern.de, January 15/2016, Az. ROB-55.2Vet-2532.Vet_02-16-7; Az. ROB-55.2Vet-2532.Vet_02-15-193; ROB-55.2Vet-2532.Vet_03-16-56).

3.2 PDX mouse model of acute lymphoblastic leukemia

A PDX mouse model was used by amplifying human acute leukemia cells in immunocompromised NSG mice (Kamel-Reid et al., 1989, Lee et al., 2007, Liem et al., 2004, Shultz et al., 2005, Terziyska et al., 2012, Vick et al., 2015).

3.2.1 Expansion of PDX cells

To expand PDX ALL cells, up to 10 million fresh (see 3.2.12 and 3.2.13) or thawed (see 3.3.2) PDX ALL cells in 100µl sterile filtered PBS were injected intravenously into

6-15 weeks old NSG mice. After injection, Baytril (2,5 %) was added to the drinking water of the mice for 7 days to prevent infections.

Leukemia burden was monitored by blood measurements (see 3.2.4) and by bioluminescence *in vivo* imaging (see 3.2.3). Mice were sacrificed (see 3.2.11) at defined time points for specific experiments, when an advanced leukemia was detected by blood measurement or when clinical signs of illness were observed. PDX ALL cells were isolated out of the murine bone marrow (see 3.2.12) and for some PDX samples out of the spleen as well (3.2.13).

3.2.2 Generation of transgenic PDX cells

Transgenic PDX cells were generated by lentiviral transduction. Therefore, freshly isolated PDX cells out of mice (see 3.2.12 and 3.2.13) or thawed cells (see 3.3.2) were lentivirally transduced (see 3.3.7). 4 days after transduction, transgenic cells were sorted (see 3.3.9) and injected into NSG mice to amplify transgenic PDX cells. Depending on whether all re-isolated PDX cells expressed the transgene, cells were either re-sorted and injected into NSG mice for a second passage or cells were transduced with a further construct or directly used for *in vivo* experiments. In case cells were transduced with a constitutively expressed shRNA, cells were sorted 4 days after transduction and directly used for *in vivo* experiments. In addition, all transgenic cells were frozen for future experiments (see 3.3.3).

3.2.3 Bioluminescence *in vivo* imaging

Leukemia growth was monitored by bioluminescence imaging *in vivo* (Terziyska et al., 2012, Barrett et al., 2011, Bomken et al., 2013, Rabinovich et al., 2008). Therefore, PDX ALL cells were genetically engineered (see 3.2.2) expressing Gaussia luciferase (GLuc) or enhanced Firefly luciferase (eFFly). Mice were anesthetized using isoflurane. Then, substrate of the specific luciferase was injected intravenously. Coelentarazine, substrate for GLuc, was dissolved in methanol containing 32 % HCl (10 mg/ml) and diluted in HBG buffer for injection; then 100 µg Coelentarazine was injected. D-Luciferin, substrate for eFFly, was dissolved in sterile PBS (30 mg/ml); here 4.5 mg/ml D-Luciferin was injected. Images were done directly after substrate injection with the IVIS Lumina II Imaging System (field of view: 12.5 cm, binning: 8, f/stop: 1 and open filter setting) and quantified using Living Image Software 4.4.

3.2.4 Blood measurement for monitoring the leukemia burden

Leukemia burden was monitored by *in vivo* blood measurements. Therefore, around 50µl blood was obtained from the mouse tail vein using a heparin coated glass capillary. The blood was mixed with 5 µl heparin and stained with anti-murine CD45 (1:10) and anti-human CD38 (1:10) antibodies for 30 min in the dark at RT. To lyse erythrocytes, samples were incubated with 1 ml FACS Lysing Solution for 15 min at RT. Then, cells were washed twice with FACS buffer (5 min, 300 g, RT) and measured using the flow cytometer BD LSRFortessa X20 (see 3.3.14). Data were analyzed using the FlowJo software.

3.2.5 Bone marrow aspiration

Bone marrow aspirations were performed in order to quantify PDX cells' distribution overtime in the living mice *in vivo*, thus reducing the amount of animals for an experiment. Mice were anesthetized injecting MMF (medetomidine, midazolam and fentanyl) narcosis intravenously using the composition listed in Table 17.

Table 17: Composition of MMF narcosis used for bone marrow aspirations

Substance	Compound	dosis [mg/ml]
Fentanyl citrate	Fentanyl	0.005
Midazolam	Dormicum	0.5
Medetomidine	Domitor vet	0.05
NaCl (0.9 %)		

Eye ointment was used to prevent drying of the callus during narcosis. Mice fur was shaved around the knee and intrafemoral aspiration was performed using a 25G syringe by extracting BM cells from above the knee joint. Then the antagonist (see Table 18) was injected subcutaneously in the nuchal fold. The cage with the mice was placed on a heating plate and mice were monitored the next hours.

Table 18: Composition of antagonisation

Substance	Compound	dosis [mg/ml]
Buprenorphine	Temgesic	0.01
Flumazenil	Anexate	0.05
Atipamezole	Antisedan Vet	0.25
NaCl (0.9 %)		

3.2.6 Tamoxifen treatment of PDX cells *in vivo*

For Cre-ER^{T2} translocation to the nucleus and induction of RNAi in PDX cells *in vivo*, 4-Hydoxytamoxifen (TAM) was used. TAM was resuspended in 90 % sterile filtered corn oil and 10 % filtered ethanol (20 mg/ml), completely dissolved at 55 °C, and stored for maximum 3 month at -20 °C. Pre-heated (37 °C) TAM was applied orally *via* gavaging. TAM concentrations were adjusted to induce shRNA expression in minimum of 50 % of the cells and were given once at 50 mg/kg for ALL-265 and twice on consecutive days at 100 mg/kg for ALL-707 and ALL-763.

3.2.7 Constitutive transplantation assay *in vivo*

Constitutive transplantation assays were performed to analyze if PDX cells expressing a shRNA against a gene of interest were able to engraft and provoke leukemia in mice. Therefore, PDX cells were transduced with lentiviruses (see 3.3.7) and positively transduced cells were enriched by cell sorting (see 3.3.9). Sorted cells were counted (see 3.3.1) and 4,500 cells were injected intravenously per mouse. Leukemia growth was monitored by *in vivo* imaging (see 3.2.3) every second week. Mice were sacrificed (see 3.2.11) when more than 50 % human blasts were detected in the murine peripheral blood (see 3.2.4). PDX cells were re-isolated out of the murine bone marrow (see 3.2.12) and analyzed by flow cytometry (see 3.3.13).

3.2.8 Competitive constitutive transplantation assay *in vivo*

Competitive constitutive transplantation assays were performed to analyze the growth behavior of cells expressing a shRNA against a gene of interest in comparison to cells expressing a control shRNA in the same mouse. Therefore, PDX cells were transduced with lentiviruses (see 3.3.7) and positively transduced cells were enriched by cell sorting (see 3.3.9). PDX subpopulations (mTagBFP/sh-CTRL + eGFP/sh-CTRL, mTagBFP/sh-CTRL + eGFP/sh-AF4/MLL or mTagBFP/sh-CTRL + eGFP/sh-MLL/AF4) were mixed 1:1 and confirmed by flow cytometry (see 3.3.14). Afterwards, cell mixtures were counted (see 3.3.1) and 4,000 to 50,000 cells were injected intravenously per mouse. Leukemia growth was monitored by *in vivo* imaging (see 3.2.3). Mice were sacrificed (see 3.2.11) when more than 50 % human blasts were detected in the murine peripheral blood in one of the experimental mice (see 3.2.4). PDX cells were re-isolated out of the murine bone marrow (see 3.2.12) and the

subpopulations' distribution in the mixture was analyzed by flow cytometry (see 3.3.14).

3.2.9 Competitive homing assay

Using competitive homing assays, the influence of specific genes on engraftment in the murine bone marrow can be analyzed in the presence of control cells in the same mouse. In order to perform the experiment with an amount of cells that can be re-isolated afterward, cells transgenic for the inducible KD system (see 4.3.2) were amplified (see 3.2.1) before starting the homing assay. PDX subpopulations (mTagBFP/sh-CTRL + iRFP/sh-CTRL or mTagBFP/sh-MLL/AF4 + iRFP/sh-CTRL) were mixed 1:1 and confirmed by flow cytometry (see 3.3.13). Then, PDX cells were treated with 150 nM TAM (see 3.2.6 and 3.3.10), cultured for 10 days *in vitro* (see 3.3.4), counted (see 3.3.1) and injected into mice (2 million cells/mouse) intravenously. Three days after injection, cells were isolated out of the murine bone marrow (see 3.2.12) and enriched using magnetic cell separation (MACS) (see 3.3.8). Finally, the subpopulations' distribution in the mixture was analyzed by flow cytometry (see 3.3.13).

3.2.10 Competitive inducible transplantation assay *in vivo*

Exploiting competitive inducible transplantation assays, shRNA expression can be induced at specific time points *in vivo* by administering TAM, thus resulting in equal recombination of control and target cells in the same mouse. Thus, PDX cells can engraft in mice without any RNAi dependent influences and genes of interest can be analyzed in growing leukemic cells *in vivo* in the presence of control cells. Therefore, PDX subpopulations (mTagBFP/sh-CTRL + iRFP/sh-CTRL or mTagBFP/sh-MLL/AF4 + iRFP/sh-CTRL) were mixed 1:1 and confirmed by flow cytometry (see 3.3.13). Cells were counted (see 3.3.1) and 300,000 cells per mouse were injected intravenously. TAM was administered seven days after transduction (see 3.2.6) to induce recombination. Leukemia growth was monitored by *in vivo* imaging (see 3.2.3) and mice were sacrificed at defined time points (see 3.2.11). Isolated human PDX cells (see 3.2.12) were analyzed for the subpopulations' distribution in the mixture by flow cytometry (see 3.3.13).

3.2.11 Sacrificing mice by CO_2 exposure

Mice were sacrificed using CO_2 either at defined time points during an experiment, when blood measurement showed an overt leukemia or when first clinical signs of illness were observed. Mice were anesthetized using the Quietek CO_2 Induction System with a CO_2 flow rate of 10 % (750 ml/min) for one minute that was followed by an increased CO_2 flow rate of 30 % (2250 ml/min) for four minutes to sacrifice mice. Clinical death was verified before organs were removed.

3.2.12 Isolation of PDX cells from the murine bone marrow

For PDX cell isolation out of the murine BM, femur, tibiae, hips, spine and sternum were crushed in PBS using mortar and pestle. Cells were filtered (70 µm cells strainer) and washed twice with PBS (400 g, 5 min, RT). After this, the cell pellet was resuspended in PBS or the required buffer.

3.2.13 Isolation of PDX cells from the murine spleen

Advanced leukemia led to an enlarged spleen in mice injected with PDX ALL-763 and ALL-265. For PDX cell isolation out of the murine spleen, the spleen was homogenized using a 70 µm cell strainer. Cells were resuspended in PBS and underlaid with ficoll. A gradient centrifugation (400 g, 30 min, no brake, RT) was performed to separate mononuclear cells from plasma, erythrocytes and other particles. The interphase containing mononuclear cells was harvested, washed twice with PBS (400 g, 5 min, RT) and resuspended in PBS or the required buffer.

3.3 Cell culture methods

3.3.1 Cell counting

Cell numbers were determined using a Neubauer counting chamber. Therefore, cells were adequately diluted and mixed 1:10 with trypan blue to differentiate between living (colorless) and dead cells (blue). 10 µl of the cell solution were filled into the chamber for counting. Cell concentration was calculated as follows:

$$\text{cell concentration} = \text{mean of counted cells} * \text{dilution factor} * 10^4 \text{ cells/ml}$$

3.3.2 Thawing of PDX cells and cell lines

Cells were thawed at 37 °C and transferred to 10 ml PBS + 10 % FCS. Cells were centrifuged (400 g, 5 min, RT) and resuspended in the appropriate medium or buffer for *in vivo* or *in vitro* experiments.

3.3.3 Freezing of PDX cells and cell lines

Cells were frozen as aliquots with 5 – 10 x 10^6 cells in 1 ml FCS + 10% DMSO. For this purpose, cells were counted (see 3.3.1), centrifuged (5 min, 400 g, RT) and resuspended in FCS. Then the same volume of freezing medium (80 % FCS + 20 % DMSO) was added dropwise. Cells were transferred in cryotubes and placed in Nalgene Mr. Frosty container to ensure freezing at a rate of 1 °C/min to -80 °C. For long-term storage, cells were transferred to -196 °C.

3.3.4 *In vitro* cultivation of PDX cells and cell lines

PDX cells were cultured with a cell density of 2 x 10^6 cells/ml in prepared StemSpan medium (see 2.10) at 37 °C with 5 % CO_2. Cell lines were maintained with a cell density of 0.5 – 2 x 10^6 cells/ml at 37 °C with 5 % CO_2. There, SEM cells were cultured in prepared IMEM medium (see 2.10), CEM, JURKAT, NALM-6 and REH cells were cultured in prepared RPMI medium (see 2.10). Cells were splitted twice a week to keep steady cell densities. The adherent HEK-293T cell line was cultured in specific 75 cm^2 flasks for adherent cells in prepared DMEM medium (see 2.10). To split cells, the medium was removed, attached cells were washed twice with PBS and cells were detached using 0.05 % trypsin. Afterwards, cells were resuspended in fresh medium and splitted to maintain a cell density of 0.5 – 2 x 10^6 cells/ml.

3.3.5 Lentivirus production

For genetic engineering, a third generation lentivirus system was used (Dull et al., 1998, Zufferey et al., 1999). HEK-293T cells were used as packaging cell line and transfected at a confluency of 50 % - 80 %. The HEK-293T cell medium was exchanged by fresh DMEM media and a transfection solution containing DMEM medium without FCS, 2.4 % turbofect, the packaging plasmids pMD2.G (1.25 mg/ml final concentration), pMDLg/pRRE (5 mg/ml final concentration), pRSV-Rev (2.5 mg/ml final concentration) and the transfer vector (250 ng/ml final concentration) was prepared and incubated for 20 min at RT. The transfection solution was added

dropwise to the cells. The cells were cultured for three days at 37 °C and 5 % CO_2. Then, the supernatant was centrifuged (400 g, 5 min, RT) and filtered (0.45 µm). The virus suspension was concentrated by centrifugation in Amicon-Ultra 15 ml centrifugal filter units (2,000 g, 30 min, RT). The virus titer was determined (see 3.3.6). Virus was used for lentiviral transduction (see 3.3.7) directly or after storage as aliquots at -80 °C.

3.3.6 Lentiviral titer determination

To monitor the quality of produced viruses (see 3.3.5), the virus titer was determined for each virus. Therefore, 0.5 x 10^6 NALM-6 cells were cultured in 0.5 ml medium and transduced with 0.03 µl, 0.1 µl, 0.3 µl, 1 µl, 3 ml or 10 µl virus plus 8 µg/ml polybrene. One day after transduction, cells were washed three times with PBS (400 g, 5 min, RT). Then, 4 days after transduction, the percentage of transduced cells was analyzed by flow cytometry (see 3.3.13). The virus titer was calculated as follows:

$$\text{virus titer} = \left(\frac{\mathrm{F} * \mathrm{Z}}{\mathrm{V}}\right) \mathrm{TU/ml}$$

F = transduced cells [%]; Z = number of cells at infection; V = volume of virus [ml]

3.3.7 Lentiviral transduction

For genetic engineering of cell lines, 1 – 5 x 10^6 cells were cultured in 1 ml of the respective medium with the lentivirus (see 3.3.5) and 8 µg/ml polybrene. One day after transduction, cells were washed three times with PBS (400 g, 5 min, RT). Sorting of transduced cells was done at least four days after transduction (see 3.3.9).

To increase the transduction efficiency, PDX ALL cells were transduced by spinocculation. Therefore, 2 x 10^6 cells were cultured in 1 ml prepared StemSpan medium with the lentivirus (see 3.3.5) and 8 µg/ml polybrene. Then cells were centrifuged in a pre-heated centrifuge (1800 rpm, 45 min, 32 °C) and carefully placed in an incubator at 37 °C and 5 % CO_2. One day after transduction, cells were washed three times with PBS (400 g, 5 min, RT). Sorting of transduced cells was done at least four days after transduction (see 3.3.9).

3.3.8 Enrichment of cells by magnetic cell separation

Human PDX cells were enriched from murine BM cells by negative selection using MACS. PDX cells isolated out of the murine BM (see 3.2.12) were resuspended in 3 ml PBS + 0.5 % BSA and incubated with 100 – 300 µl of mouse cell depletion beads,

depending on the percentage of human cells in the mixture, for 15 min at 4 °C. Two LS columns were placed in a magnet and rinsed with PBS + 0.5 % BSA. 10 ml PBS + 0.5 % BSA was added to the cell solution and was loaded on the LS columns. The LS columns were washed twice with PBS + 0.5 % BSA and the collected flow-through was centrifuged (400 g, 5 min, RT). Cells were resuspended in the required medium or buffer for further usage.

3.3.9 Enrichment of cells using fluorescence-activated cell sorting

Cells expressing different fluorophores (eGFP, iRFP, mCherry, mTagBFP or T-sapphire) could be enriched by fluorescence-activated cell sorting (FACS) using the BD FACS AriaIII. Laser and filter settings are listed in Table 19.

Table 19: Filter settings of the BD FACS AriaIII

Excitation [nm]	Longpass filter [nm]	Bandpass filter [nm]	Parameter
375/405	735	780/60	Qdot710
	610	616/23	Qdot605
	556	584//42	PacOrange
	502	530/30	Cerulan
		450/40	DAPI, mTagBFP
488	655	695/40	PerCP-Cy5.5
	502	530/30	FITC, eGFP
		488/10	SSC
561	735	780/60	PE-Cy7
	630	670/14	PE-Cy5
	600	610/20	mCherry, mKate
		582/15	PE
633	735	780/60	APC-Cy7
		660/20	APC

Before sorting, cells were centrifuged (400 g, 5 min, RT), resuspended in PBS and filtered (35 µm). For sorting, lymphocytes with the respective fluorophore were gated and collected in a FACS tube containing the appropriate medium.

3.3.10 Tamoxifen treatment *in vitro*

For *in vitro* TAM treatment, lyophilized TAM was dissolved in 100 % ethanol to obtain a 5 mM stock solution. Aliquots of the stock solution were prepared and stored at -80 °C for up to three months. For experiments, cell lines were treated with 50 nM TAM and PDX ALL cells were treated with 150 nM TAM *in vitro*.

3.3.11 Competitive constitutive assay *in vitro*

To analyze the growth behavior of cells expressing shRNAs or transgenes, competitive experiments were performed having a control population in the mixture. Therefore, cells were first genetically engineered to express different fluorophores (mTagBFP or eGFP) and then transduced with shRNAs (dsRED) or transgenes (iRFP) (see 3.3.7). Cell populations were mixed 1:1 and 0.5 x 10^6 cells/ml were cultured in the appropriate medium for up to six weeks at 37 °C and 5 % CO_2 with regularly cell splitting to maintain a cell density of 0.5 – 2 x 10^6 cells/ml (see 3.3.4). Cell growth was monitored once to twice a week by flow cytometry (see 3.3.13).

3.3.12 Competitive inducible assay *in vitro*

With competitive inducible assays, shRNA expression can be induced at favored time points by administering TAM leading to equal recombination of control and target cells in a mixture. Cells, distinguishable by the expression of different fluorophores, were mixed 1:1 (mTagBFP/sh-CTRL + iRFP/sh-CTRL or mTagBFP/sh-MLL/AF4 + iRFP/sh-CTRL) with 0.5 x 10^6 cells/ml and treated with TAM (see 3.3.10). Cells were cultured in the appropriate medium for up to five weeks at 37 °C and 5 % CO_2 with regularly cell splitting to maintain a cell density of 0.5 – 2 x 10^6 cells/ml (see 3.3.4). Induced recombination was analyzed three days after TAM and then once to twice a week the subpopulations' distribution in the mixture was monitored by flow cytometry (see 3.3.13).

3.3.13 Flow cytometric analysis

For flow cytometric analysis, the BD LSRFortessa X20 was used to detect different fluorophores (APC, eGFP, iRFP, mCherry, mTagBFP, PE, PerCP-Cy5.5 or T-sapphire). The instrumental settings are listed in Table 20.

Table 20: Filter settings of the BD LSRFortessa X20

Excitation [nm]	Longpass filter [nm]	Bandpass filter [nm]	Parameter
405	750	780/60	BV785
	685	710/50	BV711
	653	670/30	BV650
	600	610/20	BV605
	505	525/70	T-Sapphire, AmCyan, BV510
		450/50	mTagBFP, CFP, BV421
488	685	710/50	PerCP, PerCP-Cy5.5
	505	530/30	GFP, FITC, AlexaFluor 488
		488/10	SCC
561	750	780/60	PE-Cy7
	685	710/50	PE-Cy5.5
	635	670/30	PE-Cy5
	600	610/20	mCherry, PE-Texas Red
	505	585/15	DsRED, PE
640	750	780/60	APC-Cy7
	690	730/45	iRFP720, Alexa Fluor 700
		670/30	APC

Cells were first gated on living cells using forward scatter against side scatter (FSC/SSC) and second on the respective fluorophores (Fig. 8).

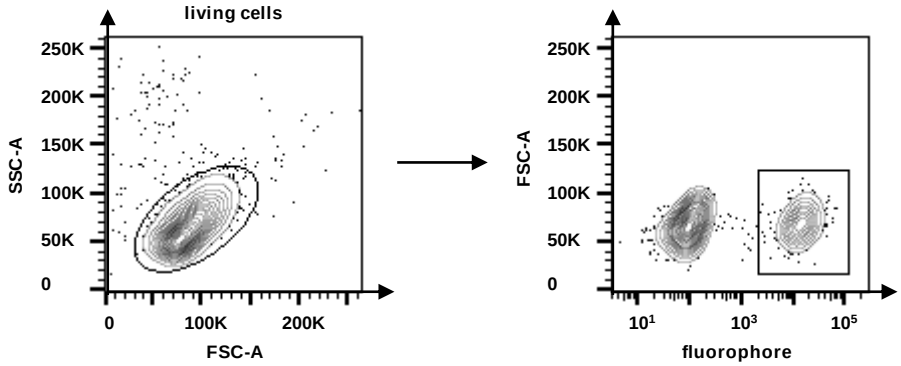

Figure 8: Gating strategy for flow cytometric analysis.
Living cells were gated using forward scatter against side scatter (FSC/SSC). Then cells were gated on the fluorophore of interest. Here, NALM-6 cells were transduced with a mTagBFP expressing construct.

3.4 Microbiological methods

3.4.1 Generation of competent *E. coli* DH5α

Competent *Escherichia coli* (*E. coli*) DH5α were generated for transformation of plasmid DNA. 1 ml of an overnight culture of competent *E. coli* DH5α was used to inoculate 100 ml LB medium (see 3.4.2). At an OD_{600} of 0.4 - 0.5 nm, the culture was cooled on ice. Cells were centrifuged (4,000 g, 5 min, 4 °C), resuspended in 15 ml

TFB I buffer and incubated for 5 min on ice. Cells were centrifuged again (4,000 g, 5 min, 4 °C) and resuspended in 4 ml TFB II buffer. Aliquots with 50 µl bacteria suspension were stored at -80 °C.

3.4.2 Culture of *E. coli* DH5α

E. coli DH5α were cultured in LB medium at 37 °C. After transformation (see 3.4.3), bacteria were cultured in LB medium or LB agar plates containing 50 µg/ml ampicillin.

3.4.3 Heat shock transformation of plasmid DNA into *E. coli* DH5α

For heat shock transformation of plasmid DNA into *E. coli* DH5α, 50 µl bacteria suspension, stored at -80 °C (see 3.4.1), was thawed on ice. 50 – 100 ng plasmid DNA (see 3.5.9) or 5 µl of a ligation mixture (see 3.5.7) was added and the suspension was incubated for 30 min at 4 °C. Heat shock was performed at 42 °C for 60 sec followed by incubation on ice for 2 min. 400 µl LB medium was added and cells were incubated for 60 min at 37 °C under shaking. Cells were centrifuged (13,000 rpm, 1 min, RT), resuspended in 70 µl LB medium, plated on LB agar plates containing 50 µg/ml ampicillin and incubated at 37 °C overnight.

3.4.4 Single colony picking

Single colonies from transformed *E. coli* DH5α (see 3.4.3) were picked from agar plates and cultured in LB medium containing 50 µg/ml ampicillin at 37 °C overnight. Then, plasmid DNA was isolated (see 3.5.9).

3.5 Molecular biology methods

3.5.1 Polymerase chain reaction

Polymerase chain reaction (PCR) was performed to amplify a coding sequence of interest according the composition shown in Table 21.

Table 21: Composition for polymerase chain reaction

Compound	Volume/amount
Phusion High-Fidelity PCR Master Mix	1x
cDNA or Plasmid DNA	50-100 ng
Forward Primer	25 pmol
Reverse Primer	25 pmol
H_2O	up to 50 µl

The PCR program is depicted in Table 22. Annealing temperature and elongation time were adjusted for each PCR according to the melting temperatures of the respective primers and the DNA fragment length of the PCR product.

Table 22: Polymerase chain reaction program

Temperature	Time	Cycles
95 °C	2 min	1
95 °C	0.5 min	
50 – 60 °C	1 min	35
72 °C	0.5 min/kb	
72 °C	5 min	1
4 °C	∞	

3.5.2 Purification of PCR products

PCR products were purified using the NucleoSpin Plasmid EasyPure Kit according to manufacturer's protocol. DNA concentration was determined using Nanodrop and DNA was stored at -20 °C.

3.5.3 Agarose gel electrophoresis

DNA fragments were separated according to their size using agarose gel electrophoresis. To prepare 0.5 – 1.5 % agarose gels, agarose powder was dissolved in 1x TAE buffer by heating. After cooling down to 50 – 55 °C, 0.01 % Midori Green was added. The agarose solution was allowed to dry in a gel chamber with a comb. DNA ladder and samples, mixed with 1x DNA loading dye, were loaded into the gel pockets. DNA separation was performed in 1x TAE buffer at 100 V for 30 – 40 min and analyzed using a gel documentation station. For DNA extraction, appropriate bands were cut out (see 3.5.4).

3.5.4 DNA extraction from agarose gels

For DNA extraction after agarose gel electrophoresis (see 3.5.3), DNA agarose gel slices were first cut out. Then, DNA was extracted using the NucleoSpin Gel and PCR Clean-Up Kit according to manufacturer's protocol. DNA concentration was determined using Nanodrop. Samples were stored at -20 °C.

3.5.5 Restriction enzyme digest

Plasmid DNA was digested using restriction enzymes listed in Table 8. The composition of the restriction digestion mixture is depicted in Table 23.

Table 23: Composition of restriction digestion mixture

Component	Volume/amount
Plasmid DNA	2 µg
Restriction enzyme	5 – 10 U
Restriction enzyme buffer	1x
H_2O	up to 20 µl

The mixture was incubated 1 – 3 h at 37 °C for restriction digestion. Then, digested DNA was separated by agarose gel electrophoresis and DNA was extracted for further cloning.

3.5.6 Annealing of oligonucleotides

shRNAs were ordered as synthesized complementary oligonucleotides and were annealed to double-stranded DNA with the composition described in Table 24.

Table 24: Composition for annealing of oligonucleotides

Compound	Volume/amount
Sense oligonucleotide	100 pmol
Anti-sense oligonucleotide	100 pmol
Annealing buffer	18 µl

Annealing was performed in a thermocycler using the settings listed in Table 25.

Table 25: Cycler program for oligonucleotide annealing

Temperature	Time
90 °C	5 min
70 °C	10 min
70 °C to 37 °C	ramp down -0.5°C/20 s
16 °C	20 min
4 °C	30 min

Annealed oligonucleotides were used for ligation into a plasmid backbone (see 3.5.7) and were stored at -20 °C.

3.5.7 Ligation

For ligation of digested DNA fragments (see 3.5.5) or annealed oligonucleotides, 50 ng vector backbone was mixed with insert DNA in a 1:3 ratio calculated by the following formula:

$$\text{amount}_{\text{insert}}\,[\text{ng}] = \frac{\text{size}_{\text{insert}}\,[\text{kb}]}{\text{size}_{\text{vector backbone}}\,[\text{kb}]} * \text{amount}_{\text{vector backbone}}\,[\text{ng}] * \text{ratio}$$

Ligation was performed using T4 Ligase for 2 h at 22 °C. Composition of the ligation mixtures is described in Table 26.

Table 26: Composition of ligation mixture

Compound	Volume/amount
Plasmid DNA	50 ng
Insert DNA	as calculated
T4 DNA ligase	1 µl
T4 DNA ligase buffer	1x
H_2O	up to 10 µl

After ligation, samples were used for transformation into competent *E. coli* DH5α (see 3.4.3).

3.5.8 shRNA concatamerization

shRNAs were concatamers according to Sun et al. (2006). The shRNAs were cloned into the backbone using XhoI and EcoRI restriction enzymes. SbfI, NsiI and BamHI restriction enzymes were used to concatamerized the shRNAs. The vector backbone was digested using NsiI and BamHI while the insert shRNA was digested using SbfI and BamHI. NsiI and SbfI recognize a similar sequence, thus the overhang generated by SbfI matches with the overhang generated by NsiI. By this, the SbfI and NsiI recognition sequence is destroyed (Fig. 9). This cloning step can be repeated to concatamerized multiple shRNAs.

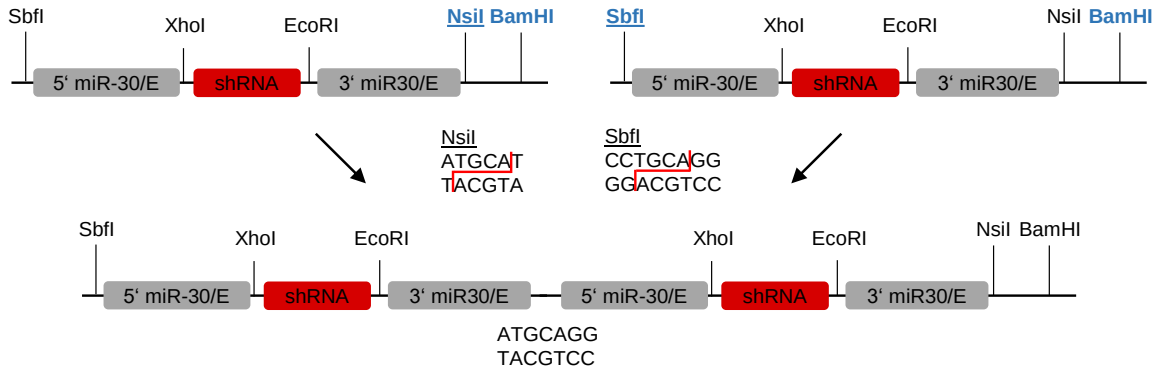

Figure 9: Schematic description of shRNA concatamerization
shRNAs were cloned into the backbone using XhoI and EcoRI restriction enzymes. For shRNA concatamerization the vector backbone was digested using NsiI and BamHI while the insert shRNA was digested using SbfI and BamHI. NsiI and SbfI recognize a similar sequence, thus the overhang generated by SbfI matches with the overhang generated by NsiI. By this, the SbfI and NsiI recognition sequence is destroyed.

3.5.9 Plasmid DNA extraction

For plasmid DNA isolation from *E. coli* DH5α, the NucleoSpin Plasmid Easy Pure or NucleoBond Extra Midi Kit were used according to manufacturer's protocol. DNA concentration was determined using Nanodrop. DNA was stored temporary at -4 °C and long-term at -20 °C.

3.5.10 RNA extraction

RNA was extracted from PDX cell and cell lines using the Qiagen RNeasy Kit according to manufacturer's protocol. RNA concentration was determined using Nanodrop and samples were stored at -20 °C.

3.5.11 Complementary DNA synthesis

For generation of complementary DNA (cDNA), RNA was isolated (see 3.5.10) and reverse transcribed using the QuantiTect Reverse Transcription Kit according to manufacturer's protocol. cDNA was stored at -20 °C.

3.5.12 Quantitative real-time PCR

mRNA expression level was analyzed by quantitative real-time PCR (qRT-PCR) using the Roche LightCycler 480 Probe system according to manufacturer's instructions. The composition listed in Table 27 was prepared.

Table 27: Composition of qRT-PCR

Component	Volume/amount
Master mix	10 µl
Forward primer	0.4 µM
Reverse primer	0.4 µM
Probe	0.2
cDNA	5 µl
H_2O	up to 20 µl

A LightCycler 480 II was used with the settings described in Table 28.

Table 28: Cycler program for qRT-PCR

Temperature	Time	Cycles	Ramp rate
95 °C	10 min	1	
95 °C	10 s		4.4 °C/s
60 °C	30 s	45	2.2 °C/s
72 °C	1 s		4.4 °C/s
40 °C	30 s	1	2.2 °C/s

Relative gene expression levels were normalized to HPRT1 using the $2^{-\Delta\Delta Ct}$ method.

3.5.13 Finger Printing using PCR of mitochondrial DNA

PDX cells were regularly analyzed for their authentication by sequencing distinct areas of mitochondrial DNA and analyzing sample specific nucleotide variants (Hutter et al., 2004). Genomic DNA was isolated using the Qiagen QIAamp DNA Blood Mini Kit according to manufacturers' instructions and used for PCR using the scheme shown in Table 29.

Table 29: Composition of mitochondrial fingerprinting PCR

Component	Volume/amount
Reaction buffer	1x
DNA	300 ng
Forward primer	50 pmol
Reverse primer	50 pmol
dNTPs	10 mM
GoTaq	0.25 µl
H_2O	up to 50 µl

For PCR, the settings described in Table 30 were used.

Table 30: Cycler program for mitochondrial fingerprinting PCR

Temperature	Time	Cycles
95 °C	2 min	1
94 °C	30 s	
60 °C	30 s	35
72 °C	30 s	
72 °C	5 min	1
4 °C	∞	1

PCR products were purified using the MinElute PCR Purification Kit according to manufacturer's instructions and PCR product with a concentration of 100 ng/µl PCR were sent for Sanger sequencing (see 3.6.1). Sequencing results were compared to the original reference sequence from the patient sample.

3.5.14 Protein extraction

For protein extraction, cells were first washed twice with PBS (400 g, 5 min, RT) and then lysed by incubating cells with cell lysis buffer plus PMSF (1:200) for 30 min on ice. Then, cells were centrifuged (13,000 g, 3 min, 4 °C) and the supernatant was transferred in a new tube. Protein lysates were stored at -20 °C.

3.5.15 Simple western

For protein quantification, simple western were performed using the WES system (ProteinSimple, San Jose, CA, USA) according to manufacturers' instruction. Protein concentration of lysates (see 3.5.14) was determined by BCA assay (#7780, New England Biolabs, Frankfurt am Main, Germany) according to manufacturers' protocol. For simple western, a protein concentration of 0.2 mg/ml was used. Results were analyzed using the Compass software 4.0.0.

3.6 Sequencing

3.6.1 Sanger sequencing

Sanger sequencing was performed with GATC Biotech, Konstanz, Germany. 30 – 100 ng/µl DNA were sent for sequencing together with 10 pmol/µl primer.

3.6.2 MACE sequencing

Massive Analysis of cDNA Ends (MACE) is a RNA-Seq variant that generates only a single sequence from each transcript allowing identification of short and rare

transcripts with lower sequencing depth and was performed at GenXPro, Frankfurt am Main, Germany. For this purpose, 50,000 cells were sorted (see 3.3.10) per sample with three biological replicates and sent to GenXPro for total RNA isolation, MACE library preparation and strand-specific sequencing using the HiSeq2500 (Illumina, USA), as previously described (Nold-Petry et al., 2015). First bioinformatic analysis was performed by GenXPro, further investigations were done in collaboration with Alexander Wilhelm (AG Marschalek, Frankfurt am Main).

The bioinformatic analysis was conducted in accordance to the analysis pipeline for MACE libraries by GenXPro GmbH. Distinct Oligo IDs and UMIs on each transcript enabled initial demultiplexing and subsequent removal of PCR-duplicates for alignment of adapter-free sequences with Bowtie 2 to the human reference genome (Genome Reference Consortium Human Build 38 patch release 13, GRCh38.p13). Considering sequencing depth and RNA composition, the sequencing data was normalized with the median of ratios method by DESeq2. Gene set enrichment analysis (GSEA) was carried out to compare the effect of the MLL/AF4 KD in the t(4;11) PDX ALL-707 and ALL-763 with published transcriptomic data from t(4;11) leukemia patients (expression data from Stam et al. (2010); GEO database: GSE19475; significant genes were selected according to Lin et al. (2016): $p \leq 0.05$, FDR≤0.1, fold change ≥2). The GSEA software of UC San Diego and the Broad Institute was used for analysis. Permutation testing was conducted with a gene set specific permutation test, set to 1000 permutations.

3.7 Statistical analysis

GraphPad Prism 7 was used for all statistical analysis if not stated otherwise. Unpaired t-tests with Welch's correction were used for qPCR analysis or to analyze competitive constitutive KD experiments. Unpaired t-test was used to analyze homing assay and paired t-test was used analyzing competitive inducible KD experiments. Therefore, the initial distribution three days after TAM was compared to the final time point. Log-rank (Mantel-Cox) test was used to compare *in vivo* imaging data.

4. Results

MLL translocations are frequent in acute leukemia and result in poor prognosis. MLL/AF4 is the most abundant MLL fusion in acute lymphoblastic leukemia. Many studies exist on the role of MLL/AF4 while only few reports focus on the reciprocal fusion protein AF4/MLL. Research on MLL/AF4 was so far mainly performed using cell lines, which harbor features unknown or rare in patient samples, while few *in vivo* data from mouse models could not efficiently mirror the patient situation. Thus, investigations on the role of those fusion proteins would largely benefit from an *in vivo* mouse model using patient cells.

In this project, a MLL/AF4 rearranged patient-derived xenograft mouse model was used to analyze the essentiality of both fusion proteins for leukemia maintenance *in vivo*.

4.1 Characterization of fusion mRNAs present in t(4;11) cell line and PDX

While all t(4;11) rearranged leukemia samples express MLL/AF4 mRNA, only 50 – 80 % express the reciprocal AF4/MLL mRNA (Agraz-Doblas et al., 2019, Downing et al., 1994, Kowarz et al., 2007, Reichel et al., 2001, Trentin et al., 2009). Furthermore, various breakpoints and alternative splicing are responsible for the existence of different fusion proteins.

First, I wanted to study our samples to understand the complexity of the t(4;11) breakpoint and possible fusion variants in the PDX samples present in our lab. Therefore, eight t(4;11) PDX samples, the t(4;11) SEM cell line and as control the non-MLL rearranged leukemic NALM-6 cell line were analyzed for the expression of the MLL/AF4 and the AF4/MLL fusion mRNA. To this aim, RNA was isolated and reverse transcribed for PCR amplification of either MLL/AF4 or AF4/MLL followed by Sanger sequencing.

SEM cells expressed MLL/AF4 and AF4/MLL mRNA while the non-MLL rearranged leukemic NALM-6 cell line did not express any of these fusion mRNAs as expected. Six out of eight tested PDX samples expressed a reciprocal AF4/MLL mRNA while all t(4;11) PDX samples expressed MLL/AF4 mRNA.

The fusion mRNAs of the SEM cell line and the PDX ALL-706, ALL-707 and ALL-763 were analyzed more in detail for further studies. Therefore, MLL/AF4 and AF4/MLL

PCR products were cloned into the pJET vector and amplified in *E. coli* DH5α. Plasmids were isolated from single colonies and sent for Sanger sequencing to determine fusion variants within each sample.

As a result, the AF4/MLL fusion breakpoint varied between the samples, but no multiple variants could be identified within one sample (Fig. 10a). In detail, the SEM cell line had an AF4/MLL breakpoint between exon 3 of AF4 and exon 11 of MLL. The PDX ALL-706 and ALL-707 had an identical breakpoint between exon 3 of AF4 and exon 10 of MLL (Fig. 10a, c). In contrast, different MLL/AF4 fusion transcripts could be identified in all tested PDX samples and in the SEM cell line (Fig. 10b). The main MLL/AF4 fusion transcript with a frequency of over 80 %, present in all tested samples, had a fusion of exon 9 of MLL and exon 4 of AF4 (Fig. 10b, d). Interestingly, a deletion of the first amino acid of exon 4 of AF4 was missing in the SEM cell line (8.3 %), ALL-706 (4.8 %), ALL-707 (10.0 %) and ALL-763 (10.7 %). Further identified variations were a point mutation at the breakpoint (SEM cell line, 4.2 %), an intronic part of AF4 between the breakpoint (ALL-763, 3.6 %) and a fusion between exon 8 of MLL and exon 4 of AF4 (SEM cell line, 4.2 %, ALL-706, 9.5 %, ALL-763, 3.6 %). As one main MLL/AF4 fusion product was detectable in all samples, it was selected for further studies.

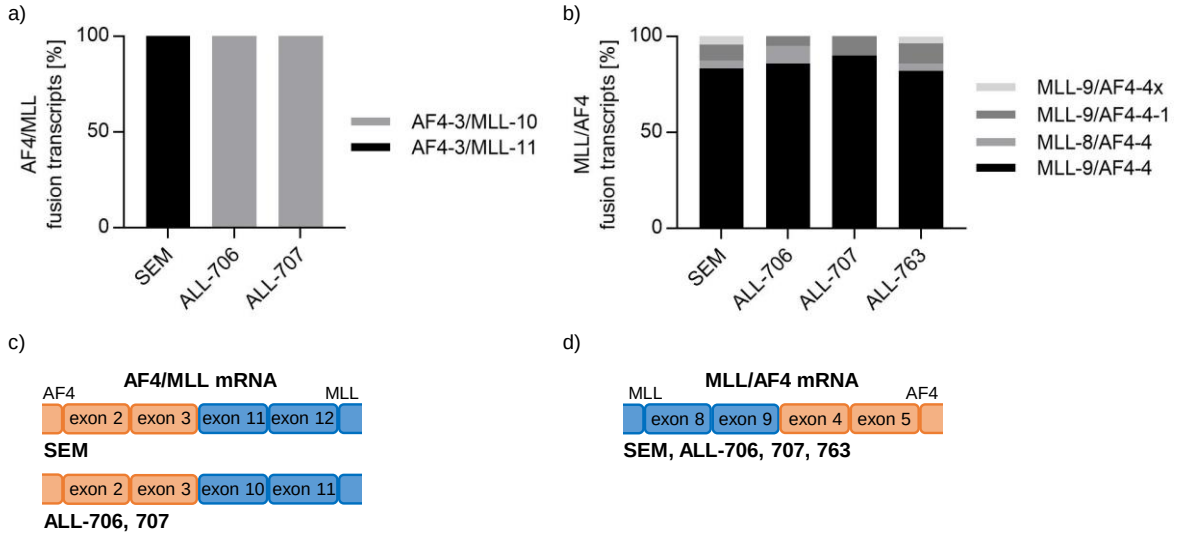

Figure 10: AF4/MLL and MLL/AF4 fusion variants detected in PDX samples and cell lines
RT-PCR of AF4/MLL and MLL/AF4 using SEM cells and PDX ALL-706, ALL-707 and ALL-763. PCR products were separated on agarose gels and cloned into a pJET plasmid. Plasmids were amplified in *E. coli* DH5α and single colonies were sent for Sanger sequencing. a) Sequencing results of AF4/MLL fusion transcripts. Amount of colonies analyzed: SEM n = 7; ALL-706 n = 3; ALL-707 n = 5. b) Sequencing results of MLL/AF4 fusion transcripts. Amount of colonies analyzed: SEM n = 24; ALL-706 n = 21; ALL-707 n = 20; ALL-763 n = 28. c-d) Schematic description of the main fusion product per sample.

Sequencing results and further detailed information on the PDX samples used in this project are summarized in Table 31.

Table 31: PDX sample characteristics
*mRNA expression (analyzed by RT-PCR), **exon number at the genomic breakpoint (exon of MLL/exon of AF4, analyzed by DCAL, Frankfurt, Germany), ***Age at diagnosis.

	707	706	352	389	816	817	763	818	199	265
MLL/AF4*	+	+	+	+	+	+	+	+	-	-
AF4/MLL*	+	+	+	+	+	+	-	-	-	-
Breakpoint**	9/4	9/4	9/4	10/4	11/4	11/6	9/4	10/4	-	-
Age***	1,7	5	67	43	52	74	17	47	8	5
Gender	m	m	m	f	f	f	f	m	f	f

Taken together, the t(4;11) samples analyzed expressed different MLL/AF4 fusion variants while only a part of the samples expressed AF4/MLL mRNA in addition. Thereof, three PDX samples that shared a main MLL/AF4 fusion mRNA were chosen for further studies, from which two samples expressed the AF4/MLL mRNA as well.

4.2 shRNA design targeting t(4;11) mRNA breakpoints

To functionally characterize the role of the fusion proteins in ALL, RNA interference technology was exploited and breakpoint specific shRNAs were designed. Five shRNAs targeting AF4/MLL in ALL-706 and ALL-707 were designed using the SplashRNA algorithm (Pelossof et al., 2017), enabling the design of potent shRNA sequences (Fig. 11a). Here, no cell line model for this specific AF4/MLL mRNA was available. shRNAs targeting the mutual MLL/AF4 breakpoint in the SEM cell line and the PDX samples ALL-706, ALL-707 and ALL-763 were manually designed and previously validated by Birgitta Heckl (Heckl, 2018). The most effective sequence is shown in Fig. 11b.

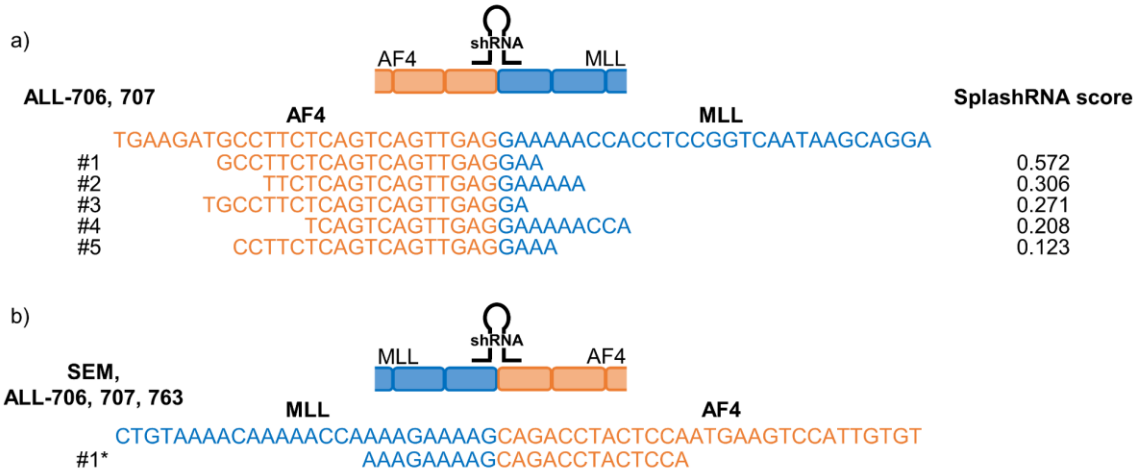

Figure 11: shRNAs targeting the AF4/MLL and MLL/AF4 mRNA breakpoint
a) AF4/MLL shRNAs were designed using the SplashRNA algorithm for PDX ALL-706 and ALL-707 (Pelossof et al., 2017). SplashRNA score determine the shRNA efficiency (>1 = >85 % KD efficiency). b) MLL/AF4 shRNA targeting the fusion in the SEM cell line and in PDX ALL-706, ALL-707 and ALL-763. shRNA was manually designed and previously validated by Birgitta Heckl.

4.3 Silencing of target genes

To test whether the fusion proteins AF4/MLL and MLL/AF4 are essential for ALL, a constitutive and an inducible KD approach were used. With these approaches, the influence of the fusion proteins on leukemia establishment and on leukemia maintenance could be studied. Competitive *in vitro* and *in vivo* assays were performed to enhance sensitivity and reliability. Below, the different experimental settings are described.

4.3.1 Constitutive KD

The constitutive KD system was previously established by Michela Carlet. For this system, the lentiviral pCDH plasmid was modified to obtain the expression of the fluorophore dsRED coupled to the miR-30 cassette under the control of the spleen focus-forming virus (SFFV) promoter. As a result, the previously selected shRNA sequences (embedded into the miR-30 cassette) and dsRED are expressed in equimolar amount, allowing easy identification of the KD population and a relation of the fluorophore expression to the KD strength (Fig. 12a).

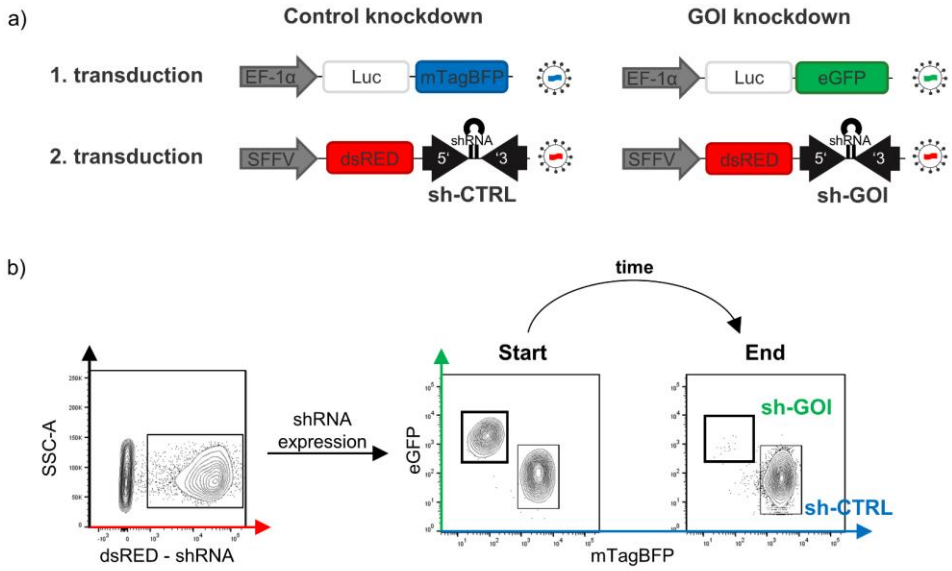

Figure 12: Confirmation of a functional constitutive competitive knockdown system
The constitutive competitive KD system was established by Michela Carlet. a) Constructs for two consecutive lentiviral transductions. First, a fluorophore (mTagBFP or eGFP) combined with a luciferase under the control of EF-1α is transduced to distinguish two cell populations. Second, the fluorophore dsRED and a miR-30 cassette with embedded shRNA sequence (sh-CTRL or sh-GOI) under the SFFV promoter is transduced. b) Gating strategy explained by an experiment with PDX ALL-707 using Renilla shRNA (sh-CTRL) and MLL/AF4 shRNA (sh-GOI) before and 56 days after injection into mice: Living cells were gated on dsRED (shRNA expression) expressing cells. Then, the distribution of dsRed expressing mTagBFP and eGFP positive cells was analyzed. The distribution of the color-coded populations was monitored over time.

To perform competitive experiments, two consecutive transductions are required. First, to distinguish two cell populations, cells are molecularly marked using two different fluorophores, monomeric blue fluorescent protein (mTagBFP) or enhanced GFP (eGFP). The color constructs are expressed under the control of the eukaryotic translation elongation factor 1 alpha (EF-1α) promoter together with a Firefly luciferase for *in vivo* imaging. Second, cells are transduced with the dsRED shRNA expression construct. Here, the mTagBFP positive cells are transduced with a shRNA against Renilla (sh-CTRL) representing the control group, while eGFP positive cells are transduced with a shRNA against the gene of interest (GOI). To perform experiments, the two populations (mTagBFP/sh-CTRL + eGFP/sh-GOI) are mixed 1:1 and the relative proportion is measured over time using flow cytometry. For analysis, living cells with dsRED (shRNA) expression are gated first and then analyzed for their markers' distribution (mTagBFP or eGFP) (Fig. 12b). If the distribution of mTagBFP/sh-CTRL and eGFP/sh-GOI positive cells changes over time and a loss of the eGFP/sh-GOI population is observed the GOI probably has an essential function.

4.3.2 Inducible KD

Studying essential genes for tumor maintenance can be challenging especially *in vivo*, where processes like homing end engraftment can be crucial. However, these steps do not exist in patients already harboring leukemia and might lead to an overestimation of experimental results. To prevent this and to simulate the patient situation where a growing leukemia needs to be treated, an inducible KD system was established by Michela Carlet, Birgitta Heckl and Jenny Vergalli (Fig. 13).

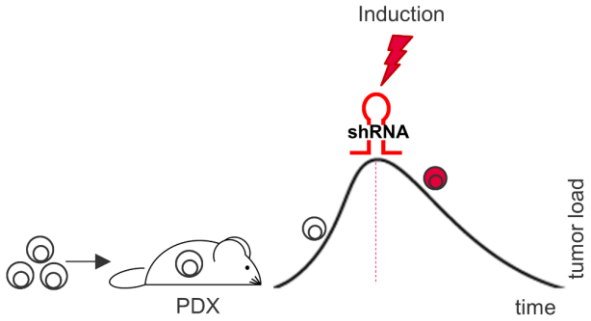

Figure 13: Schematic description of an inducible knockdown *in vivo*
Transgenic PDX acute leukemia cells are injected into NSG mice. The tumor load increases over time until induction of shRNA expression. If the shRNA targets an essential gene, the knockdown leads to a reduction in tumor burden.

With this system, upon injection, transgenic PDX cells can home, engraft and proliferate without any further influences. Moreover, the expression of a shRNA can be induced at any given disease stage and the essential role of the targeted gene in tumor maintenance can be evaluated. If a gene is essential, the KD population will diminish over time.

The inducible KD was generated using a Cre-ER^{T2} loxP system. Thus, a Cre-ER^{T2} vector and a flipping construct were cloned. The TAM inducible Cre-ER^{T2} enzyme is expressed under the control of a SFFV promoter together with a Gaussia luciferase (Luc) for *in vivo* imaging and mCherry for transgenic cell enrichment (Fig. 14a). The flipping construct is expressed under the SFFV promoter as well and consists of two fluorophores, a miR-30 cassette (same as in the constitutive system) and two loxP pairs (Fig. 14b). One marker is in sense orientation (infrared fluorescent protein (iRFP) or mTagBFP) while the second marker (T-sapphire or eGFP) and the miR cassette are in antisense orientation flanked by two loxP pairs. In the absence of TAM, only the first fluorophore (iRFP or mTagBFP) is expressed. Once TAM is administered, two recombination steps are necessary for the constant expression of the second fluorophore and the shRNA expression. In the first step, a reversible inversion takes

place. When the second step occurs, the first fluorophore (iRFP or mTagBFP) is deleted and in the end, the flipping construct consists of a constitutive expressed fluorophore (T-sapphire or eGFP) and a miR cassette expressing a shRNA of choice. To perform competitive experiments and increase the sensitivity of this approach, two independent flipping constructs were developed with different fluorophore combinations, iRFP/T-sapphire and mTagBFP/eGFP (Fig. 14).

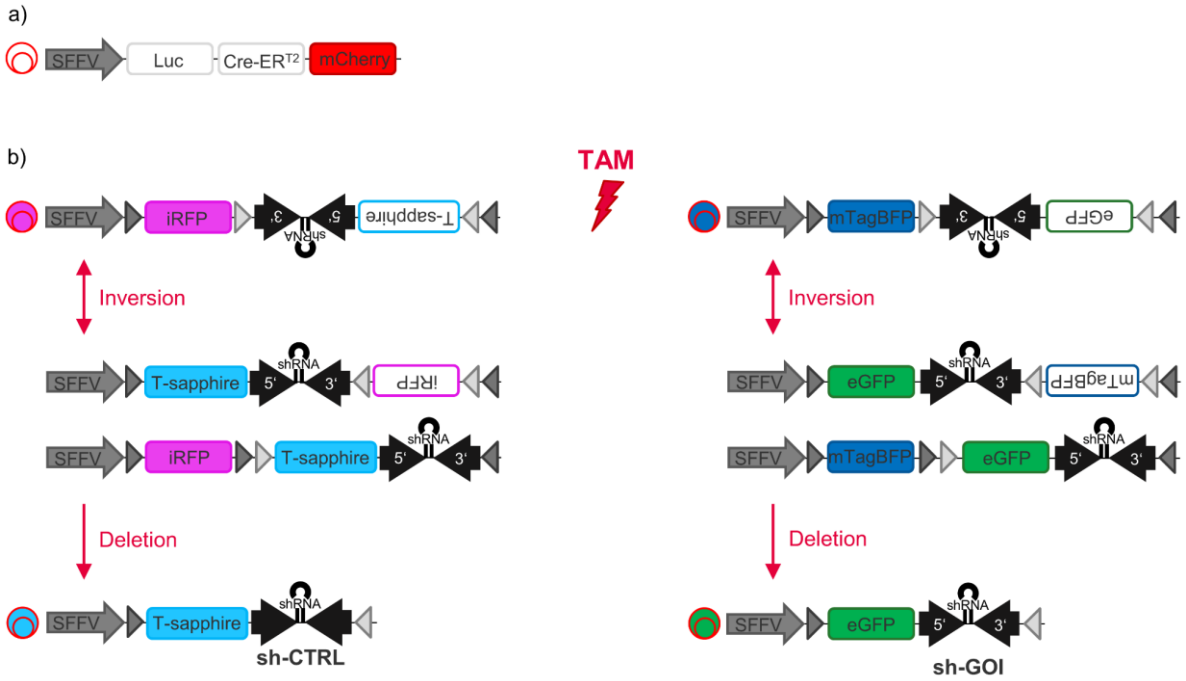

Figure 14: Schematic representation of the inducible knockdown constructs for competitive experiments
The inducible competitive KD system was established by Michela Carlet, Birgitta Heckl and Jenny Vergalli. a) Cre-ER^{T2} expression vector: Cre-ER^{T2}, a Gaussia luciferase (Luc) for *in vivo* imaging and mCherry for cell enrichment (connected via T2A and P2A) are expressed under the control of a SFFV promoter. b) Flipping constructs: The flipping construct consist of two fluorophore, a miR-30 based cassette and two loxP pairs under the control of a SFFV promoter. The first fluorophore (iRFP or mTagBFP) is in sense orientation while the second fluorophore (T-sapphire or eGFP) and the miR cassette are in antisense orientation. Tamoxifen (TAM) leads to fluorophore (T-sapphire or eGFP) and shRNA expression after two steps of recombination: a reversible inversion and a deletion of the first fluorophore (iRFP or mTagBFP). For competitive assays, a control shRNA (sh-CTRL) and a shRNA against the gene of interest (sh-GOI) are cloned each in one of the two flipping constructs.

The gating strategy for analyzing an experiment using the inducible KD is depicted in Figure 15. Briefly, after selecting for viable cells using FSC/SSC, mCherry (Cre-ER^{T2}) positive cells are gated and analyzed for iRFP and T-sapphire (shRNA) expression (Fig. 15a). Without TAM, a neglectable leakiness was observed. Once TAM is administered and recombination takes place, a color switch from iRFP to T-sapphire can be observed. For competitive experiments, a 1:1 mixture of iRFP (sh-CTRL) and mTagBFP (sh-GOI) positive cells is used for *in vitro* experiments or injected into mice

for *in vivo* studies (Fig. 15b). Cells are treated with TAM *in vitro* or *in vivo* and the distribution of recombined shRNA expressing cells (T-sapphire and eGFP) can be quantified at different time points to monitor the KD effect over time.

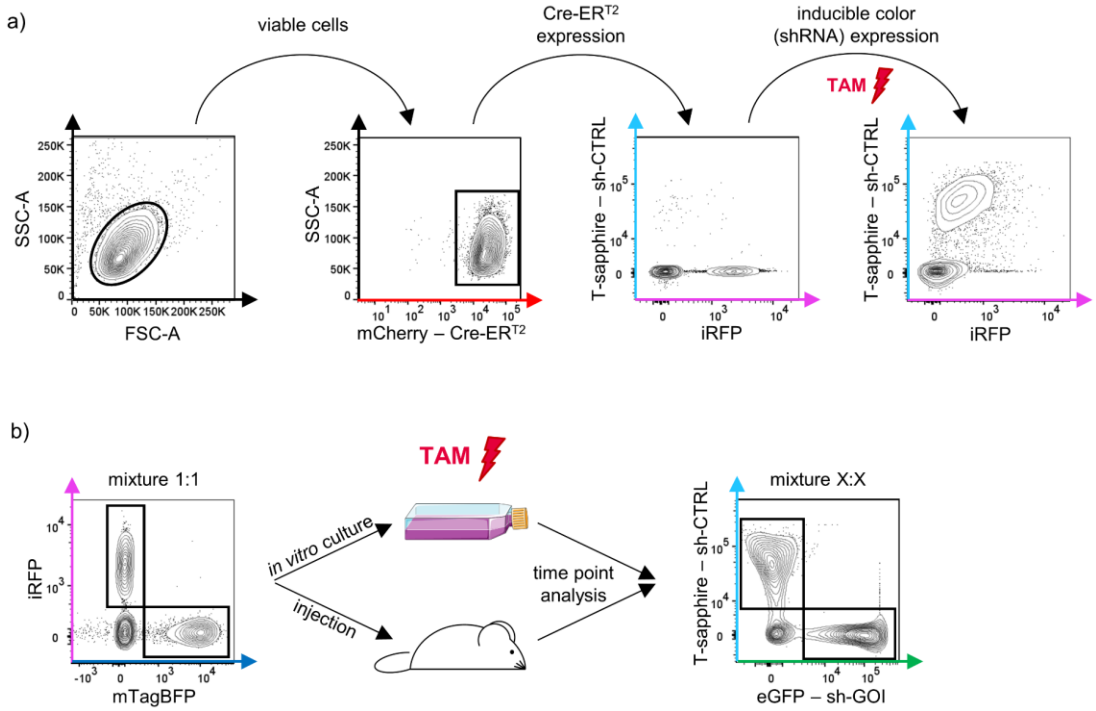

Figure 15: Functional confirmation of the Cre-ER^{T2} inducible knockdown system
The inducible competitive KD system was established by Michela Carlet, Birgitta Heckl and Jenny Vergalli. a) Gating strategy for inducible KD system: Viable NALM-6 cells, selected via FSC/SSC, were gated on mCherry (Cre-ER^{T2}) positive cells and analyzed for the fluorophore iRFP and T-sapphire (sh-CTRL) of the flipping construct. TAM induced recombination led to a loss of iRFP and an increase of T-sapphire expression (3 days after induction). b) For competitive experiments NALM-6 cells were either transduced with the iRFP flipping construct (sh-CTRL) or the mTagBFP flipping construct (sh-GOI, here sh-MLL/AF4) and mixed 1:1. The mixture was used for *in vitro* experiments but could also be injected into mice. After TAM (50 nM) administration, the distribution of recombined cells (T-sapphire and eGFP positive cells) can be measured at different time points using flow cytometry (here 3 days after TAM induction).

Taken together, I applied the Cre-ER^{T2} Flip system established by Michela Carlet, Jenny Vergalli and Birgitta Heckl which allows inducible KD in PDX models *in vivo*, as treatment of mice with TAM induces the KD at any given disease stage.

4.4 Inhibition of AF4/MLL

The role of the fusion protein AF4/MLL is so far poorly investigated and the few existing reports are controversial (Agraz-Doblas et al., 2019, Bueno et al., 2019, Bursen et al., 2004, Gaussmann et al., 2007, Kumar et al., 2011b). The major reason for this are the different model systems used as well as the diverse experimental settings.
Herein, the importance for tumor maintenance of AF4/MLL was analyzed *via* silencing the fusion protein with two different approaches: shRNA mediated KD and expression of a dominant negative Taspase1. Both methods were applied using PDX cells *in vivo*, to be as close as possible to the patients.

4.4.1 AF4/MLL KD

As a first step, AF4/MLL was silenced using shRNAs. To this aim, different shRNAs were designed targeting the specific breakpoint in the PDX samples ALL-706 and ALL-707 (Fig. 11). As the AF4/MLL mRNA of the PDX samples differs from available cells lines, those cannot be used as a control *in vitro*. Thus, the shRNA efficiency was tested using a reporter system.

4.4.1.1 Validation of shRNAs with reporter system

To estimate the KD efficiency of shRNAs, where a cell line model for validation was missing, a retroviral reporter system published by Fellmann et al. (2013) was further developed. In this project, I established a lentiviral shRNA reporter system. Under the control of an EF-1α promoter, the fluorophore dTomato and the respective AF4/MLL breakpoint sequence, located in the 3' UTR of the marker, were expressed (Fig. 16a). Once a shRNA recognizes the sequence located in the 3' UTR, the shRNA binds to it and induces the degradation of the dTomato fluorophore. The drop in fluorophore expression correlates with the shRNA efficiency.
The shRNA potency was determined using the non-MLL rearranged leukemic cell line NALM-6. To generate cells expressing the reporter system, several transductions and sorting steps were carried out. First, cells were transduced with the vector for the reporter system. Second, the Cre-ER^{T2} construct with NGFR as marker for enrichment was transduced and as last, the inducible flipping construct with the AF4/MLL shRNA sequence was transduced (Fig. 16b). After cell recovery, cells were treated with 50 nM TAM to induce recombination and shRNA expression.

The dTomato expression was analyzed in recombined cells one week after TAM application using flow cytometry. All tested shRNAs showed a reduction of the dTomato (reporter) mean fluorescent intensity (MFI) varying from 70 to 90 %, once normalized to unrecombined cells without shRNA expression (Fig. 16c). For further investigations, shRNAs were selected based on the results of the reporter system and on the overlapping regions to AF4 and MLL to avoid unspecific binding to the wild type genes (Fig. 16c, selected shRNAs marked by stars).

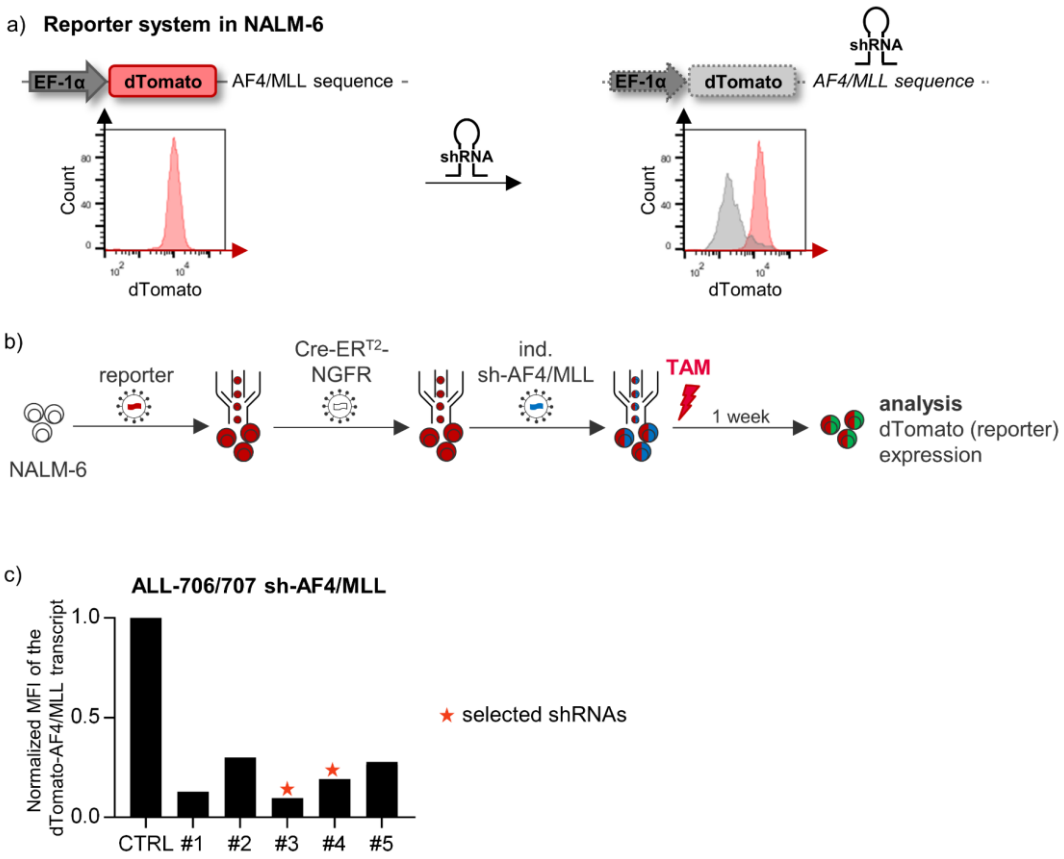

Figure 16: Determination of AF4/MLL shRNA efficiency using a reporter system
a) A retroviral reporter system published by Fellmann et al. (2013) was optimized. Here, the reporter system was cloned in the pCDH vector under the control of an EF-1α promoter expressing the fluorophore dTomato with the respective AF4/MLL sequence located in the 3‘ UTR of the reporter system. Expression of a shRNA targeting the AF4/MLL sequence in the 3‘ UTR of the reporter system reduces the dTomato expression correlating with the efficiency of the shRNA. Representative FACS blots are shown using transgenic NALM-6 cells transduced with the reporter system and an inducible AF4/MLL shRNA before and seven days after shRNA induction using 50 nM TAM. b) Generation of triple transgenic cells using single integrations (<10 % transduction efficiency). NALM-6 cells were transduced with the shRNA reporter system, a Cre-ER^{T2}-NGFR construct and an inducible shRNA flipping construct with the respective AF4/MLL shRNA. After recovering of transduced and sorted cells, cells were treated with 50 nM TAM and reporter expression (dTomato) was analyzed after one week using flow cytometry. c) Mean fluorescence intensity (MFI) of dTomato reporter system normalized to unrecombined cells (CTRL: no shRNA expression, mTagBFP positive cells). #1-5 represent the different AF4/MLL shRNAs tested. The stars mark shRNAs selected for further experiments. The experiment was performed only once.

4.4.1.2 Constitutive competitive AF4/MLL KD in PDX ALL samples *in vivo*

To analyze a putative essential function of AF4/MLL, a competitive growth experiment was performed. In a first step, ALL-707 was transduced with a color construct expressing either mTagBFP or eGFP (constructs are described in Fig. 12a). Transgenic cells were sorted and injected into NSG mice for amplification. As a second step, mTagBFP positive cells were transduced with a dsRed-control shRNA targeting Renilla (sh-CTRL), while eGFP positive cells were transduced with either the same dsRed-control shRNA (sh-CTRL) or a shRNA targeting AF4/MLL (sh-AF4/MLL). For the experiment, two different AF4/MLL shRNAs (#3 and #4) were used which were selected using the shRNA reporter system described before (Fig. 16c). Transgenic cells were sorted and mixed in a 1:1 ratio (sh-CTRL/sh-CTRL or sh-CTRL/sh-AF4/MLL) and injected into NSG mice (Fig. 17a). Growth of the PDX cells was monitored by *in vivo* imaging using a luciferase, which is expressed in the color constructs. Eight weeks after injection, PDX cells were isolated out of the murine BM and analyzed by flow cytometry and qPCR.

At time of injection, the mixtures contained 50 % eGFP positive control or AF4/MLL KD cells. When the distribution of the mixtures were analyzed again eight weeks after injection, the control mixture and the mixtures containing AF4/MLL KD and control cells did not significantly change over time (Fig. 17b). In line with this result, the *in vivo* imaging did not detect any difference in the growth kinetic of the two mixtures compared to the control mixture (Fig. 17c). qPCR analysis showed an AF4/MLL KD efficiency of 51 % and 63 % for shRNA #3 and #4, respectively (Fig. 17d). However, the endogenous MLL and AF4 expression level decreased as well, raising the problem of shRNA specificity. Thus, the shRNA might also target the wildtype sequences of MLL and AF4 mRNA. To analyze the AF4/MLL KD at the protein level, we cooperated with Rolf Marschalek, one of the leading MLL/AF4 experts, but unfortunately, it was not possible to detect AF4/MLL using Western Blot as it was reported before (Kumar et al., 2011b).

In summary, reducing the AF4/MLL fusion mRNA by a factor two or three did not influence the growth of PDX ALL-707 *in vivo*, despite that both AF4 and MLL mRNAs were diminished to similar degrees.

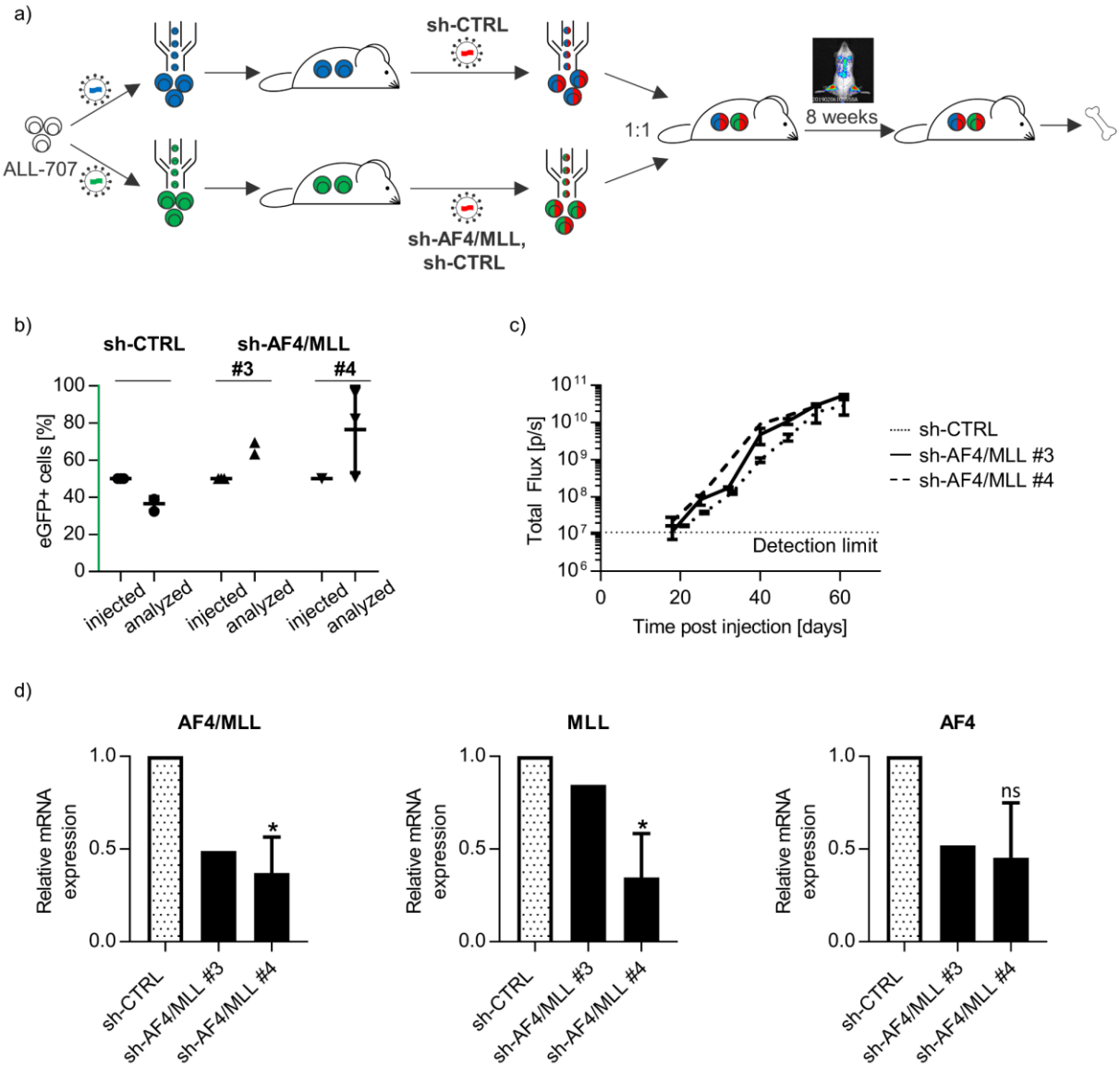

Figure 17: Moderate KD of AF4/MLL, wtMLL and wtAF4 does not impair growth in ALL-707 *in vivo*

a) Experimental setting: First, PDX ALL-707 cells were color marked by transduction with mTagBFP or eGFP, sorted and amplified in NSG mice. Second, cells were transduced with a dsRed-shRNA expression construct and sorted for transgenic cells. mTagBFP positive cells were transduced with a control shRNA targeting Renilla (sh-CTRL) and the eGFP positive cells were transduced either with the same control shRNA or a shRNA targeting the patient specific AF4/MLL breakpoint (sh-AF4/MLL). Cells were mixed 1:1 (mTagBFP/sh-CTRL + eGFP/sh-CTRL or mTagBFP/sh-CTRL + eGFP/sh-AF4/MLL) and injected into NSG mice (4,000 cells/mouse). Cell growth was monitored by *in vivo* imaging using eFirefly luciferase expressed in the color constructs. Eight weeks after injection, PDX cells were isolated out of the murine bone marrow and analyzed using flow cytometry and qPCR. b) Flow cytometry analysis: Percentage of eGFP positive cells out of the whole mixture (eGFP + mTagBFP) is shown. Next to the control mixture, two different AF4/MLL shRNAs (#3 and #4) were used in separate experiments. Control mixture: n = 3 mice, AF4/MLL shRNA #3: n = 2 mice, AF4/MLL shRNA #4: n = 4 mice), mean ± SD. c) Cell growth monitored by *in vivo* imaging. d) qPCR analysis of AF4/MLL, MLL and AF4 (control: 3 biological replicates, AF4/MLL shRNA #3: 2 biological replicates, AF4/MLL shRNA #4: 3 biological replicates). Statistic with unpaired t-test with Welch‘s correction comparing AF4/MLL shRNA #4 and control shRNA, * $p < 0.05$, ns = not significant.

4.4.2 AF4/MLL inhibition with dominant negative Taspase1

As knockdown strength appeared as a major challenge, a second, independent approach was used to study the role of the AF4/MLL fusion. AF4/MLL is cleaved by Taspase1 resulting in a stable fusion protein (Benedikt et al., 2011, Bursen et al., 2004). Therefore, a dominant negative form of Taspase1, dnTASP1, was expressed, to obtain a more potent and general inhibition of AF4/MLL as it has the advantage of targeting all AF4/MLL variants identically.

4.4.2.1 Generation of dnTASP1 expression constructs

The dnTASP1 sequence was provided by Rolf Marschalek (Sabiani et al., 2015) and cloned with a FLAG-tag and the fluorophore iRFP, connected by P2A, in the pCDH vector to allow FACS enrichment and flow cytometry analysis (Fig. 18a). Two different promoter were used, EF-1α (+) and SFFV (++), with a putatively moderate or strong expression, respectively.

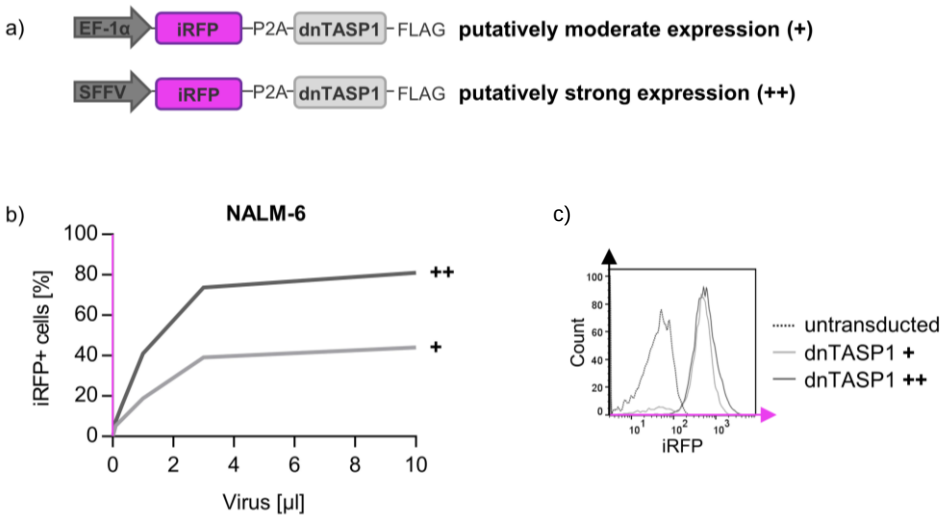

Figure 18: Dominant negative Taspase1 expression constructs
a) The dnTASP1 sequence was provided by Rolf Marschalek (Sabiani et al., 2015). It was cloned with a Flag-tag in the lentiviral pCDH vector together with the fluorophore iRFP, separated by P2A. The construct is expressed under the control of an EF-1α (+) or a SFFV (++) promoter for putatively moderate or strong expression, respectively b) Virus titration in NALM-6 cells. Cells were transduced with different amount of virus and transduction efficiency was analyzed detecting iRFP positive cells with flow cytometry three days after transduction, n = 1. d) iRFP expression of untransduced and transduced NALM-6 cells.

When transducing NALM-6 cells with the two dnTASP1 constructs using the same amount of virus, different transduction efficiencies for the EF-1α and the SFFV promoter were observed three days after transduction (Fig. 18b). 3 µl virus of EF-1α construct led to around 40 % iRFP positive cells while the same amount of virus led to

around 80 % iRFP positive cells when using the construct containing the SFFV promoter. However, the different promoter did not alter the iRFP mean fluorescence intensity in the transduced cells (Fig. 18c).
Thus, two lentiviral constructs expressing dnTASP1 were generated to inhibit the AF4/MLL fusion protein and enable further functional studies.

4.4.2.2 Competitive dnTASP1 expression experiments *in vitro*

The role of AF4/MLL was investigated expressing dnTASP1 in competitive experiments. As control, a new plasmid was cloned expressing iRFP and a control shRNA targeting Renilla under the control of the SFFV promoter (Fig. 19a). Cell lines were first transduced either with a construct expressing mTagBFP or eGFP (Fig. 19b). Then, mTagBFP positive cells were transduced with the iRFP control construct while the eGFP positive cells were transduced with the iRFP dnTASP1 expression construct with EF-1α (+) or SFFV (++) promoter or with the iRFP control construct. Afterwards, cells were mixed 1:1 and cultured *in vitro*. The subpopulations' distribution was analyzed by flow cytometry over time.
The experiment was performed in the t(4;11) SEM cell line and in two non-MLL rearranged leukemic cell lines, CEM and REH, as control. In SEM cells, the distribution of control and dnTASP1 expressing cells remained unchanged over time (Fig. 19c). Expression of dnTASP1 was analyzed by simple western, a capillary protein immunoassay, using a FLAG antibody. Here, a similar dnTASP1 expression level could be shown for both dnTASP1 constructs, with the EF-1α (+) and with the SFFV (++) promoter (Fig. 19d). The control experiments using CEM and REH cells demonstrated a stable distribution of the different cell populations like observed in the SEM cell line (Fig. 19e-f).
All in all, dnTASP1 expression did not influenced the growth of the t(4;11) SEM cells or of the non-MLL rearranged CEM and REH cells regardless which promoter was used.

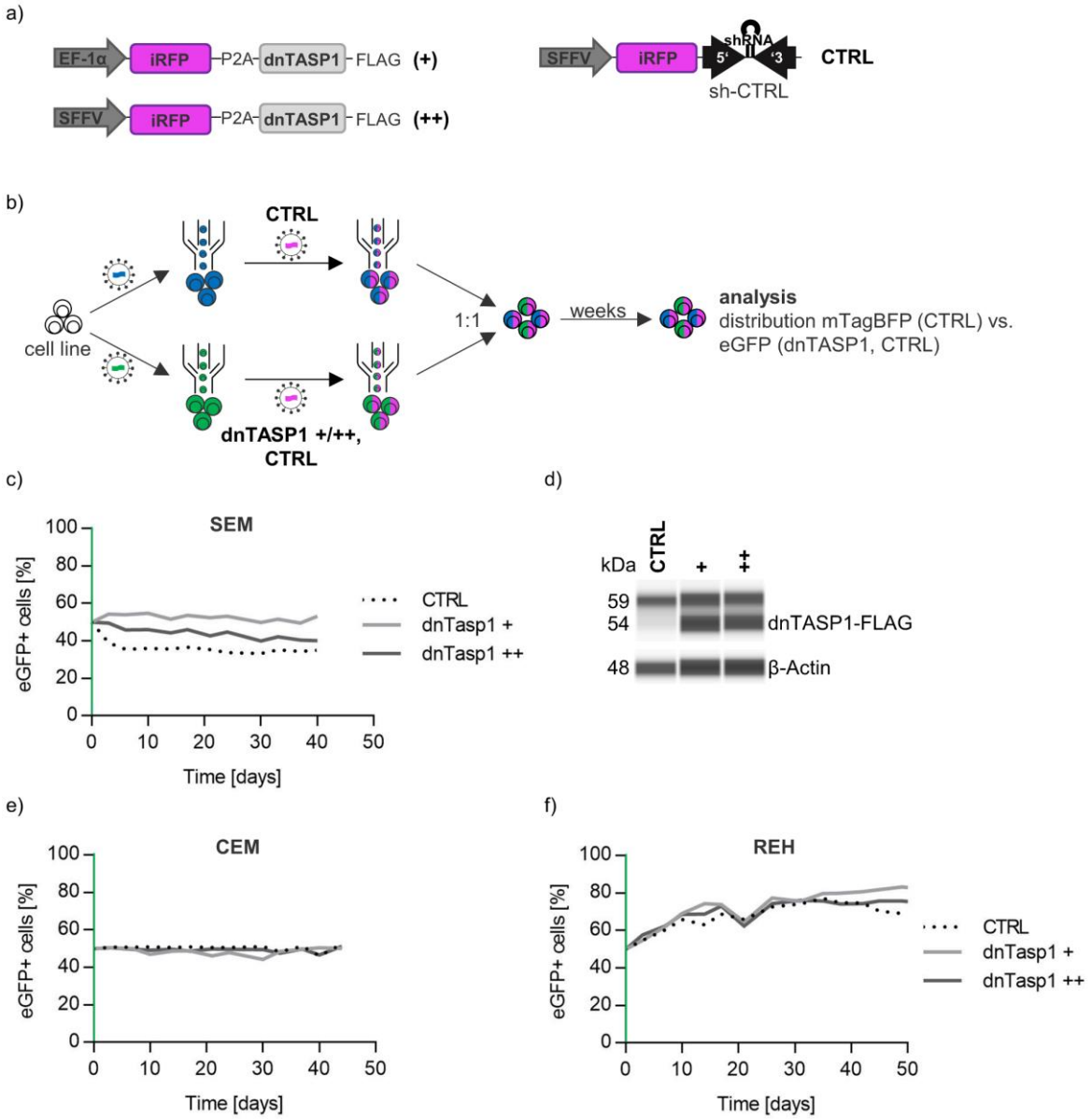

Figure 19: dnTASP1 expression does not impair growth in cell line *in vitro*
a) dnTASP1 was cloned with a FLAG-tag in the lentiviral pCDH vector together with the fluorophore iRFP. The construct is expressed under the control of an EF-1α (+) and a SFFV (++) promoter for moderate or strong expression, respectively. The control vector consists of iRFP and a control shRNA (sh-CTRL) targeting Renilla. b) Experimental setting: First, cells were color marked by transduction with mTagBFP or eGFP, second, cells were transduced with an iRFP dnTaspase1 or shRNA expression construct and sorted, respectively. mTagBFP positive cells were transduced with a control shRNA targeting Renilla (sh-CTRL) and the eGFP positive cells were transduced either with the same control shRNA or with a dnTaspase1 expression construct with moderate (EF-1α, +) or strong (SFFV, ++) promoter. Cells were mixed 1:1 (mTagBFP/sh-CTRL + eGFP/sh-CTRL or mTagBFP/sh-CTRL + eGFP/dnTASP1(+/++)) and the populations' distribution was monitored over time using flow cytometry. c) Results of the t(4;11) SEM cell line: Percentage of eGFP positive cells out of the whole mixture (eGFP + mTagBFP) is shown. Values are normalized to a 1:1 mixture at day 0. Representative data from 2 biological replicates. d) Simple western of SEM cells transduced with control shRNA or dnTaspase1 expression constructs. dnTaspase1 expression was analyzed using a FLAG antibody. β-Actin was used as loading control. A representative blot is shown out of three runs. e-f) Results are shown as described in c) in two non-MLL rearranged leukemia cell lines, e) CEM and f) REH, representative data from 2 biological replicates.

4.4.2.3 Generation of dnTASP1 expressing PDX cells

Despite no effect on the growth kinetic could be identified upon dnTASP1 expression in cell lines, further experiments were performed in PDX cells as these cells are closer related to the patients' cells and might lack interfering alterations required for establishing cell lines. ALL-707 cells were transduced either with the iRFP control shRNA construct or with iRFP dnTASP1 expressed under the moderate EF-1α promoter to avoid unspecific side effects related to overexpression (Fig. 20a). Transgenic cells were sorted and injected into NSG mice for amplification. Eight weeks after injection, PDX cells were isolated out of the murine BM and dnTASP1 expression was analyzed by simple western (Fig. 20b). dnTASP1 was detected using a FLAG antibody in the dnTASP1 transduced cells, while the signal was absent in the control population. Thus, PDX cells expressing dnTASP1 could be generated successfully.

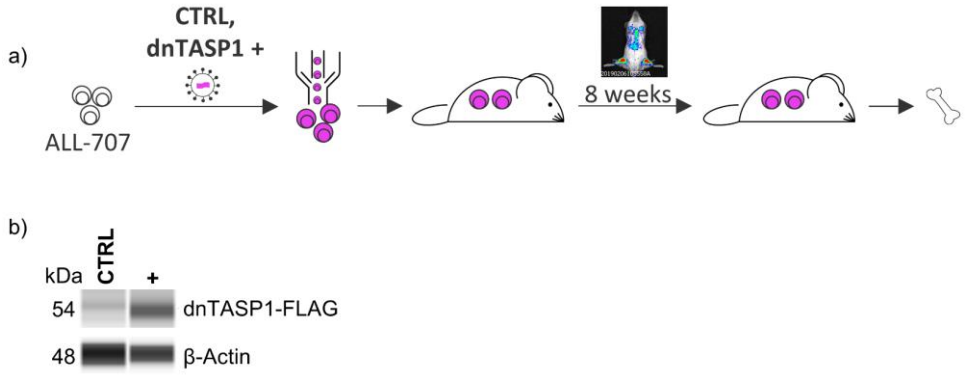

Figure 20: Generation of dnTASP1 expressing PDX cells
a) ALL-707 were either transduced with an iRFP control shRNA construct or with an iRFP dnTASP1 expression construct (constructs see Fig. 19a). Transgenic cells were sorted and injected into NSG mice (4,500 cells/mouse). Eight weeks after injection, PDX cells were isolated out of the murine BM. b) Simple western of control and dnTASP1 (+) transduced ALL-707 cells. dnTASP1 was detected using a FLAG-antibody. β-Actin was used as loading control. A representative blot is shown out of three independent replicates.

4.4.2.4 HOXA expression in dnTASP1 transgenic PDX cells

After generating dnTASP1 transgenic t(4;11) PDX cells, molecular changes due to the transgene expression were investigated. First, expression levels of Homeobox A (HOXA) genes were analyzed. HOXA genes are upregulated in MLL rearranged leukemic cells from ALL patients (Rozovskaia et al., 2001, Armstrong et al., 2002). In the human ALL SEM cell line, HOXA7, HOXA9 and HOXA10 belong to the 226 primary targets of MLL/AF4 (Guenther et al., 2008). Furthermore, different studies showed an impaired leukemogenesy in NOD/SCID mice after knocking down the different HOXA genes in the RS 4;11 cell line (Orlovsky et al., 2011). A recent publication figured out

that HOXA genes are exclusively expressed in patients expressing the reciprocal AF4/MLL protein (Agraz-Doblas et al., 2019).

To test this observation, ten PDX samples with MLL/AF4, MLL/AF4 and AF4/MLL expression or non-MLL rearranged ALL cells were tested for HOXA7, HOXA9 and HOXA10 expression by qPCR (Fig. 21a). Out of ten analyzed PDX samples, only three samples showed a high HOXA expression. These three samples express the reciprocal AF4/MLL mRNA, however, only three out of six PDX samples with AF4/MLL mRNA expression showed this high HOXA expression. Thus, the results only partially confirmed the published data showing a correlation of HOXA and AF4/MLL expression.

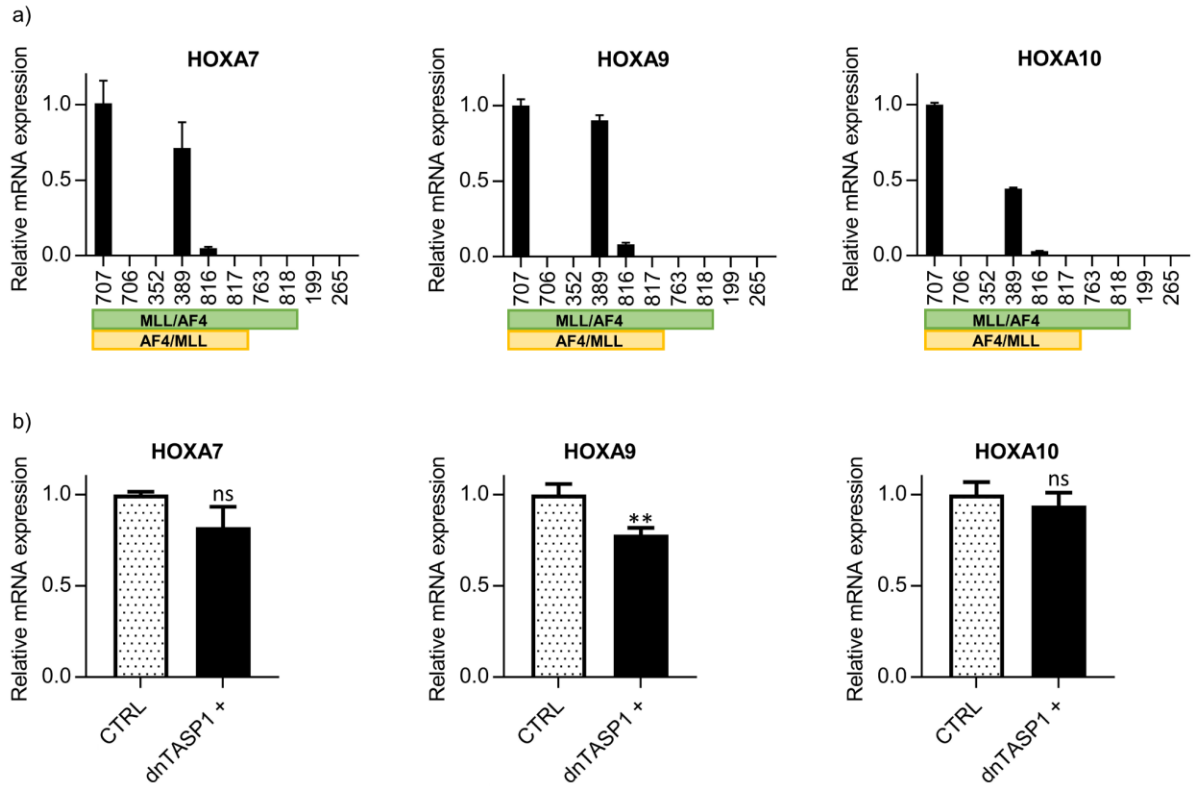

Figure 21: Slightly reduced HOXA expression in dnTASP1 expressing ALL-707 cells
a) HOXA (HOXA7, HOXA9 and HOXA10) expression was analyzed by qPCR of t(4;11) rearranged PDX samples expressing both fusion proteins MLL/AF4 and AF4/MLL (ALL-707, 706, 352, 389, 816 and 817) or expressing only MLL/AF4 (ALL-763 and 818) or of non-MLL rearranged ALL samples (ALL-199 and 265). HPRT1 was used for normalization. n = 3 technical replicates. b) HOXA expression in control and dnTASP1 transduced ALL-707, HPRT1 was used for normalization. n = 3 technical replicates, unpaired t-test, ** $p < 0.01$, ns = not significant.

ALL-707 expressed HOXA7, HOXA9 and HOXA10 on the highest level. The correlation of HOXA and AF4/MLL expression was further investigated comparing ALL-707 with dnTASP1 transgenic ALL-707. The inhibition of AF4/MLL by dnTASP1 led to a downregulation of HOXA7 and HOXA9 of about 20 % while the expression of HOXA10 remained unchanged (Fig. 21b). In conclusion, a correlation between

AF4/MLL and HOXA could be observed, although the effect is minor and might be due to a weak inhibition of AF4/MLL by dnTASP1.

4.4.2.5 Gene expression analysis of dnTASP1 transgenic PDX cells

Next to HOXA gene analysis, further differences in gene expression upon AF4/MLL inhibition by dnTASP1 were investigated. Therefore, RNA was isolated from ALL-707 control and dnTASP1 expressing cells (Fig. 20). Gene expression profiles were studied using Massive Analysis of cDNA Ends (MACE) performed at GenXPro. MACE is a RNA-Seq variant that generates only a single sequence from each transcript allowing identification of short and rare transcripts with lower sequencing depth. First bioinformatic analyses were performed by GenXPro, subsequent investigations were performed in collaboration with Alexander Wilhelm (AG Marschalek, Frankfurt am Main).

The expression profile of control cells was compared to dnTASP1 expressing cells (Fig. 22). Genes with a high fold change were highly expressed in control cells and low expressed in dnTASP1 transgenic cells. Thus, a low fold change correlates with low expression in control cells and high expression in dnTASP1 transgenic cells.

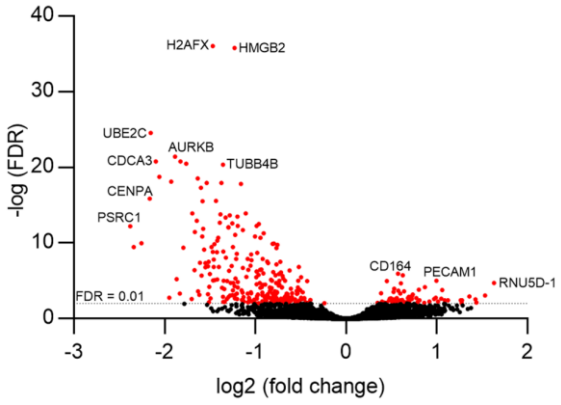

Figure 22: Differential gene expression upon dnTASP1 expression
Volcano blot shows differentially expressed genes of ALL-707 control cells compared to dnTASP1 expressing cells. RNA was isolated from ALL-707 control and dnTASP1 transgenic cells (Fig. 20). Samples were analyzed by MACE seq at GenXPro in cooperation with Alexander Wilhelm (AG Marschalek, Frankfurt am Main). Genes with a high fold change are highly expressed in control cells and low expressed in dnTASP1 transgenic cells. Thus, a low fold change correlates with low expression in control cells and high expression in dnTASP1 transgenic cells. n = 3 biological replicates per sample.

While the expression level of only few genes were reduced (e.g. *RNA U5D Small Nuclear 1* (*RNU5D-1)*, *Platelet endothelial cell adhesion molecule* (*PECAM1*), *Cluster of differentiation 164* (*CD164*)), the expression level of many genes was enriched in dnTASP1 transgenic cells. Among them were genes like *aurora kinase B* (*AURKB*),

Tubulin Beta 4B Class IVb (*TUBB4B*), *Ubiquitin Conjugating Enzyme E2 C* (*UBE2C*), *H2A histone family member X* (H2AFX) and *Centromere Protein A* (*CENPA*) that all play a role in cell cycle. Thus, dnTASP1 expression led to a differential gene expression in ALL-707, especially altering the cell cycle.

4.4.2.6 Function of dnTASP1 transgenic PDX cells *in vivo*

As gene expression data revealed alterations of the cell cycle of dnTASP1 expressing ALL-707 cells, we asked whether the growth of t(4;11) PDX cells is altered *in vivo* even though dnTASP1 expression in cell lines did not show any growth changes *in vitro*. Therefore, ALL-707 control and dnTASP1 expressing cells (constructs see Fig. 19) were injected into NSG mice and cell growth was monitored by *in vivo* imaging.

25 days after injection, first imaging signals above the detection limit of 10^7 p/s could be detected. From this time on, mice were imaged weekly (Fig. 23). The growth kinetics of control and dnTASP1 transgenic PDX cells were similar over time. No significant growth disadvantage or improvement could be observed by dnTASP1 expression. Thus, the alterations found in gene expression data did not affect the cell growth *in vivo* such that it could be observed by imaging.

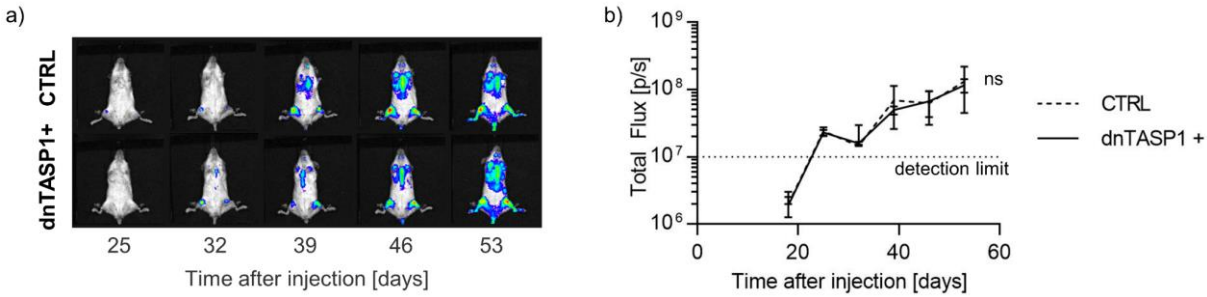

Figure 23: Growth kinetic of dnTASP1 expressing PDX cells *in vivo*
ALL-707 were either transduced with an iRFP control shRNA construct or with an iRFP dnTASP1 (+) expression construct (Fig. 19a). Transgenic cells were sorted and injected into NSG mice (4,500 cells/mouse). Cell growth was monitored by weekly *in vivo* imaging. a) Representative pictures out of four replicates per group per time point. b) Quantification of imaging signals, n = 4. linear regression analysis, ns = not significant.

In conclusion, no AF4/MLL dependent effect on growth could be determined in functional experiments *in vitro* and *in vivo*; however, on gene expression level dnTASP1 expression altered cell cycle in ALL-707 that might be induced due to AF4/MLL inhibition.

4.5 Breakpoint specific MLL/AF4 KD

MLL/AF4 is expressed in all t(4;11) leukemic patients and was studied more intensively in the literature than the reciprocal AF4/MLL fusion protein. So far, an essential function of MLL/AF4 could be shown in cell line experiments *in vitro* or *in vivo* using siRNAs or MLL/AF4 overexpression in non-leukemic cells (Kumar et al., 2011b, Thomas et al., 2005). However, studies showing the essentiality in patient cells are missing as well as information concerning the role of MLL/AF4 for leukemia maintenance. Therefore, the importance of MLL/AF4 was studied in PDX cells *in vivo*.

4.5.1 Constitutive MLL/AF4 KD

To knock down MLL/AF4, a breakpoint specific shRNA was used targeting the MLL/AF4 breakpoint in the SEM cell line as well as in the PDX samples ALL-706, ALL-707 and ALL-763 (see Fig. 11 for shRNA sequence). The MLL/AF4 shRNA specificity was validated by qPCR showing a specific MLL/AF4 KD without affecting the endogenous MLL and AF4 expression (Fig. 24). As also described before for AF4/MLL, the MLL/AF4 fusion protein could not be detected on protein level by western blot.

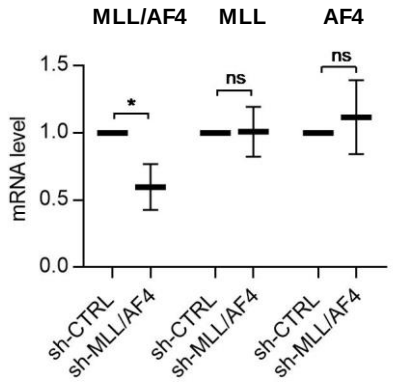

Figure 24: Validation of MLL/AF4 shRNA specificity by qPCR
qPCR of sorted eGFP/sh-CTRL or sh-MLL/AF4 ALL-707 cells from the experiment described in Fig. 34a 28 days after TAM. n = 4 biological replicates, mean ± SD, unpaired t-test with Welch's correction, * $p \leq 0.05$, ns = not significant.

Our former colleague Birgitta Heckl already performed a first competitive *in vivo* experiment, injecting t(4;11) PDX samples which expressed the constitutive MLL/AF4 shRNA or a control shRNA into NSG mice. When she re-isolated the PDX cells ten weeks after injection, she could not detect any PDX cells expressing the MLL/AF4 shRNA suggesting an important function of MLL/AF4 (Heckl, 2018). To prove and

extend her finding, the MLL/AF4 shRNA was used in this project for further studies in cell lines *in vitro* and in PDX cells *in vivo*.

4.5.1.1 MLL/AF4 plays an essential role for SEM cells *in vitro*

The function of MLL/AF4 was first tested in SEM cells that were lentivirally transduced with a dsRED shRNA construct expressing either a control shRNA targeting Renilla (sh-CTRL) or a shRNA targeting MLL/AF4 (sh-MLL/AF4). The distribution of transduced (shRNA and dsRED expression) and non-transduced cells was analyzed by flow cytometry over four weeks (Fig. 25a).

The proportion of dsRED expressing cells increased in the first days after transduction as expected to around 75 % and remained stable in cells expressing the control shRNA one week after transduction (Fig. 25b). In contrast, cells expressing the MLL/AF4 shRNA showed an increase of dsRED expressing cells in the first days similar to the cells expressing the control shRNA, followed by a reduction of MLL/AF4 KD cells and therefore a proportional increase of non-transduced cells. After four weeks, nearly all MLL/AF4 KD cells were depleted and only non-transduced cells could be measured by flow cytometry. This result is in line with published data and proves an essential function of MLL/AF4 in these cells.

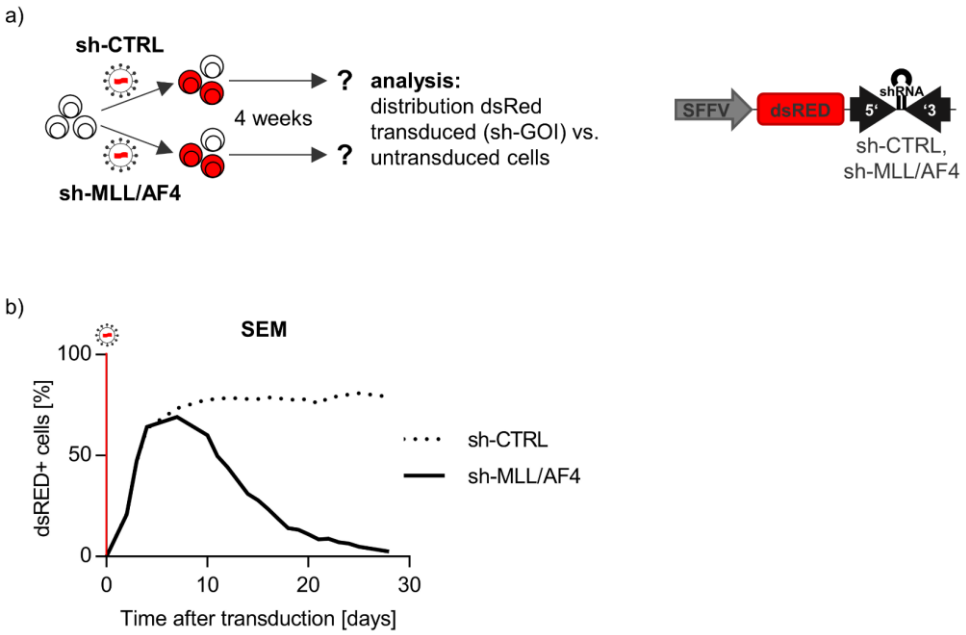

Figure 25: MLL/AF4 KD inhibits growth in SEM cell line
a) Experimental setting: SEM cells were lentivirally transduced with a dsRED-shRNA expression construct containing a shRNA targeting the MLL/AF4 breakpoint (sh-MLL/AF4) or a control shRNA targeting Renilla (sh-CTRL). The distribution of transduced and untransduced cells was monitored over four weeks using flow cytometry. b) Percentage of transduced (dsRED positive) SEM cells over time. Representative result of two independent experiments.

4.5.1.2 Essentiality of MLL/AF4 for ALL PDX cells *in vivo*

As MLL/AF4 KD cells showed a strong phenotype, we asked whether a similar phenotype might be present in PDX cells. To this aim, two different approaches, a non-competitive and a competitive approach, were used.

4.5.1.2.1 Non-competitive MLL/AF4 KD *in vivo*

First, a non-competitive *in vivo* assay was performed to analyze the influence of MLL/AF4 on leukemia growth. Therefore, ALL-707 cells were first color marked with an eGFP-luciferase construct as described previously (Fig. 26a). After amplification in mice, cells were transduced with the dsRED-shRNA construct using either the control shRNA or the shRNA targeting MLL/AF4. eGFP and dsRED double positive cells were sorted and 4,500 cells were injected per mouse. Growth of PDX cells expressing either a control shRNA or the MLL/AF4 shRNA was monitored by *in vivo* imaging. At signs of overt leukemia, PDX cells were isolated out of the murine BM and analyzed by flow cytometry.

Mice injected with MLL/AF4 KD cells needed a longer period until cells could be detected by *in vivo* imaging (Fig. 26b). Afterwards a similar growth kinetic could be observed between the control and MLL/AF4 KD group. Thus, MLL/AF4 KD cells required 54 - 82 days to reach an imaging signal of 10^9 p/s, while control cells reached a comparable imaging signal 40 – 47 days after injection suggesting a slower growth kinetic in the presence of MLL/AF4 inhibition (Fig. 26c). When characterizing PDX cells at overt leukemia, no MLL/AF4 shRNA (dsRED) expressing cells could be detected (Fig. 26d). Only non-transduced cells could be isolated, whose presence might be due to impure sorting, thus leading to the development of leukemia in these mice while all cells with efficient MLL/AF4 KD were depleted. These data prove that PDX ALL-707 cells depend on expression of MLL/AF4 for their growth *in vivo*.

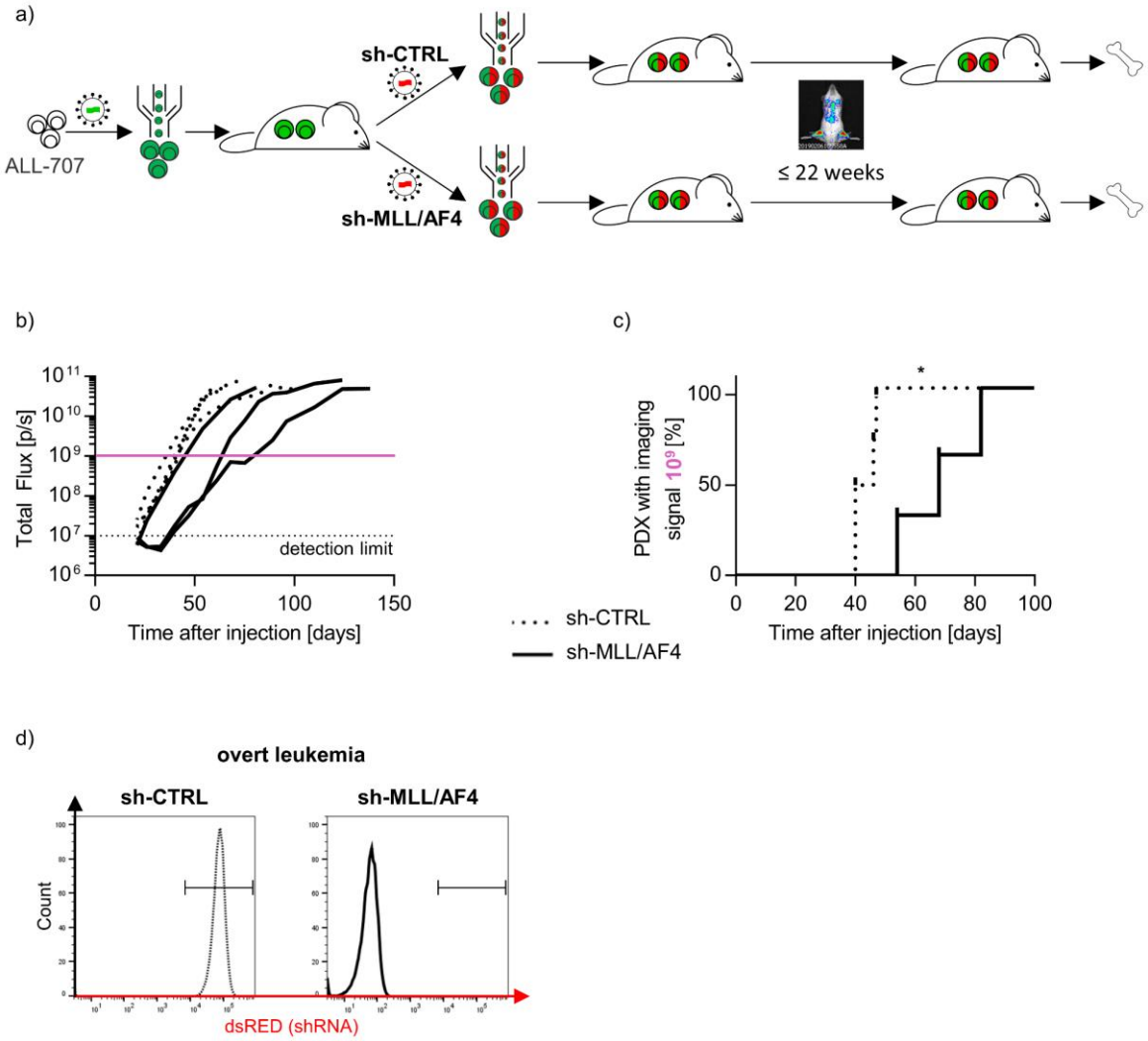

Figure 26: Impaired growth of ALL-707 with MLL/AF4 KD *in vivo*
a) Experimental setting: ALL-707 cells were first transduced with an eGFP-luciferase construct and amplified in NSG mice. Second, cells were transduced with a dsRED-shRNA expression construct using either a control shRNA against Renilla (sh-CTRL) or a shRNA targeting MLL/AF4 (sh-MLL/AF4). 4,500 cells were injected per mouse (sh-CTRL: n = 4, sh-MLL/AF4: n = 3). Growth of leukemic cells was monitored by *in vivo* imaging. At overt leukemia, human cells were isolated out of the murine BM for flow cytometric analysis. b) *In vivo* imaging of ALL-707 control and MLL/AF4 KD cells. Purple line indicates an imaging signal of 10^9 p/s. sh-CTRL: n = 4, sh-MLL/AF4: n = 3. c) Time after injection until an imaging signal of 10^9 p/s was reached per mouse. sh-CTRL: n = 4, sh-MLL/AF4: n = 3, $p < 0.05$, Log-rank (Mantel-Cox) test. d) Flow cytometric analysis of ALL-707 isolated out of the murine BM at overt leukemia. dsRED expression correlating with shRNA expression was analyzed. Representative blot, sh-CTRL: n = 4, sh-MLL/AF4: n = 3.

4.5.1.2.2 Competitive MLL/AF4 KD *in vivo*

To verify that MLL/AF4 plays an essential role for growth of PDX ALL-707 *in vivo*, a second complementary approach was used. A competitive experiment was performed as described before: ALL-707 cells were first color marked with eGFP or mTagBFP and second transduced with a dsRED shRNA expression construct (Fig. 27a). mTagBFP/sh-CTRL and eGFP/sh-MLL/AF4 cells were mixed and 50,000 cells were

injected per mouse. In parallel, a control mixture with mTagBFP/sh-CTRL and eGFP/sh-CTRL cells were injected the same way. The distribution of the different cell populations was analyzed by flow cytometry before injection and eight weeks after injection when signs of overt leukemia occurred.

At time of injection, around 35 % of the cells in the mixtures contained eGFP/sh-CTRL or eGFP/sh-MLL/AF4 cells. When analyzing the cells eight weeks after injection, still around 35 % of the cells in the control mixture contained eGFP/sh-CTRL cells. In comparison, no sh-MLL/AF4 eGFP positive cells could be observed in the mixture at the end of the experiment (Fig. 27b). Thus, the distribution of eGFP control cells remained stable over time, while a significant depletion of MLL/AF4 KD cells could be observed confirming the essential function of the fusion protein.

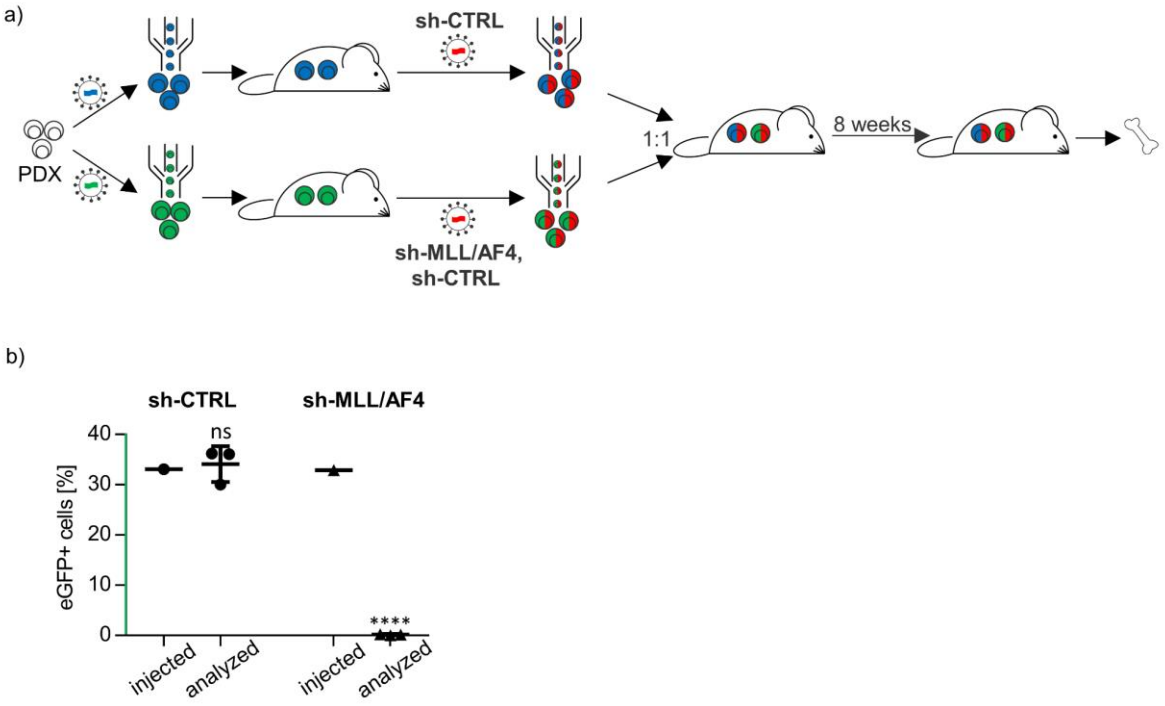

Figure 27: Competitive growth experiment *in vivo* shows disadvantage of ALL-707 cells with MLL/AF4 KD

a) Experimental setting: First, PDX ALL-707 cells were color marked by transduction with mTagBFP or eGFP color constructs and sorted and amplified in NSG mice. Second, cells were transduced with dsRed-shRNA expression constructs and sorted for transgenic cells. mTagBFP positive cells were transduced with a control shRNA targeting Renilla (sh-CTRL) and eGFP positive cells were transduced either with the same control shRNA or a shRNA targeting the MLL/AF4 breakpoint. Cells were mixed 1:1 (mTagBFP/sh-CTRL + eGFP/sh-CTRL or mTagBFP/sh-CTRL + eGFP/sh-MLL/AF4) and injected into NSG mice (50,000 cells/mouse). Eight weeks after injection, PDX cells were isolated out of the murine BM and analyzed using flow cytometry. b) Results of the ALL-707 *in vivo* experiment: Percentage of eGFP positive cells out of the whole mixture (eGFP + mTagBFP) is depicted. n = 3 biological replicates per group, mean ± SD, unpaired t-test with Welch‘s correction, **** $p < 0.0001$, ns = not significant.

In conclusion, a constitutive MLL/AF4 KD results in a depletion of KD cells in the SEM cell line *in vitro* as well as in PDX cells *in vivo*. However, with this experimental setting, no MLL/AF4 KD cells could be re-isolated from these mice to prove that they were able to engraft in mice and no further analyses could be performed with these cells.

4.5.2 Inducible MLL/AF4 KD

While the constitutive inhibition of MLL/AF4 resulted in the impaired growth of ALL PDX cells, it still remained unclear whether processes like homing and engraftment are crucial for the growth of MLL/AF4 KD cells. Nevertheless, these steps are not clinically relevant as patients enter the clinic with an established leukemia, which needs to be treated. Therefore, we next asked whether MLL/AF4 is still required in an established leukemia. To answer this question, an inducible KD system was used and further optimized (Fig. 13, 14).

4.5.2.1 Improving KD efficiency with the inducible KD system

The former colleague Birgitta Heckl successfully performed an inducible MLL/AF4 KD experiment in SEM cell lines *in vitro* showing a time depended reduction of MLL/AF4 KD cells (Heckl, 2018) that is in line with the results described before using the constitutive KD system *in vitro* and *in vivo* (Fig. 25 - 27). When she performed the inducible MLL/AF4 KD experiment in PDX cells *in vivo*, the mixture of MLL/AF4 KD and control cells remained unchanged over time, indicating that the KD induced did not alter the growth of the cells *in vivo*. Because of the opposite results observed *in vitro* and *in vivo*, we hypothesized that the KD strength might have been insufficient in the PDX samples.

For the inducible *in vitro* experiment, SEM cells were transduced with a high transduction efficiency leading to multiple copies of the constructs in the genome. In contrast, for PDX cells only a low transduction efficiency resulting in single integrations was technically feasible. When SEM cells were transduced with a low transduction efficiency similar to PDX, MLL/AF4 KD cells were only marginally reduced. This phenotype might be explained by the low transduction efficiency resulting in low shRNA expression and thus by a weak KD.

To increase KD strength and as it was technically unfeasible to increase the transduction efficiency of PDX cells (data not shown), shRNAs were concatamerized to increase shRNA expression and KD efficiency in PDX cells (Fig. 28) (Sun et al.,

2006). The inducible shRNA expression cassette was concatamerized up to four shRNA copies in a row. In addition, the miR-30 cassette was replaced by a miR-E cassette, which was described to allow a more efficient KD (Fellmann et al., 2013). Both, the mTagBFP flipping construct as well as the iRFP control flipping construct were concatamerized the same way.

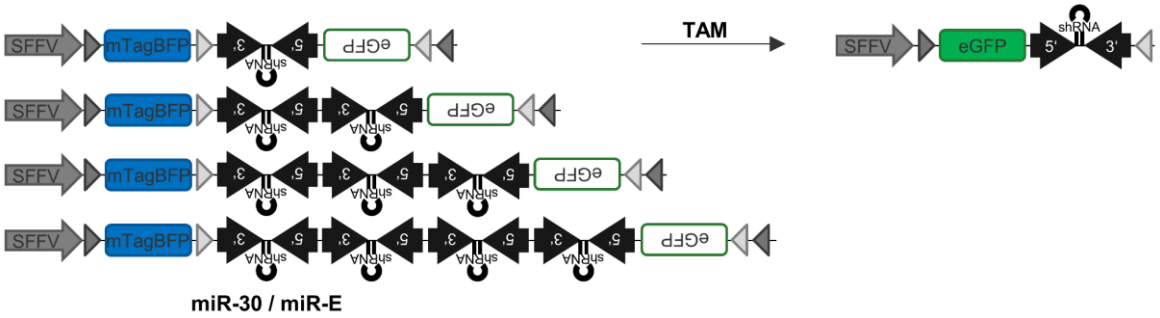

Figure 28: shRNA concatamerization in inducible flipping construct
Illustration of concatamerized mTagBFP flipping constructs. shRNAs in the iRFP flipping construct (described in Fig. 14) were concatamerized the same way. shRNA cassette was concatamerized resulting in one to four copies in a row. All constructs were cloned with miR-30 and miR-E cassette respectively.

4.5.2.2 Inducible MLL/AF4 KD *in vitro*

Especially when working with shRNA sequences of difficult design, as for example for the MLL/AF4 breakpoint, where the putative target sequence for a KD is very limited as it has to cover the mRNA breakpoint and where no algorithm could be used to select potent and specific shRNAs, an improvement like concatamerization or a stronger miR cassette could be beneficial. Therefore, MLL/AF4 shRNAs and control shRNAs were concatamerized with miR-30 and miR-E cassette as 1, 2 and 4mer shRNA constructs (Fig. 29a). SEM cells were used for initial testing and were transduced first with Cre-ER^{T2}-mCherry and second with the different concatamers with transduction efficiencies below 10 % to obtain single integrations (Fig. 29b). After sorting and cell recovery, 50 nM TAM was added to induce recombination and shRNA expression. The distribution of non-recombined (mTagBFP) and recombined (eGFP) cells was analyzed over 20 days by flow cytometry.

In all control populations, around 80 % of cells showed a recombination followed by a color switch from mTagBFP to eGFP after three days (Fig. 29c). Afterwards, the distribution of recombined and non-recombined control cells stayed stable over time, while expression of MLL/AF4 shRNA constructs showed different results. At 72 h, the recombination efficiency in the different cell populations was tested, which was similar

for control and MLL/AF4 constructs. The distribution of recombined and non-recombined cells were nearly unchanged in cells transduced with a construct containing a single MLL/AF4 shRNA embedded in the miR-30 cassette over time. Cells with a MLL/AF4 2 or 4mer using the miR-30 cassette showed a weak but significant depletion of recombined cells over time. A similar effect was observed in cells with a MLL/AF4 1mer in a miR-E backbone. The effect was significantly increased by expression of the MLL/AF4 2 and 4mer using the miR-E cassette. For the MLL/AF4 4mer, we could not observe a recombination efficiency of 80 % as for the other constructs, as depletion of MLL/AF4 KD cells started already earlier than 72 h. Thus, the concatamerization of miR-E cassettes resulted in a stronger KD efficiency, leading to increased depletion of MLL/AF4 KD cells.

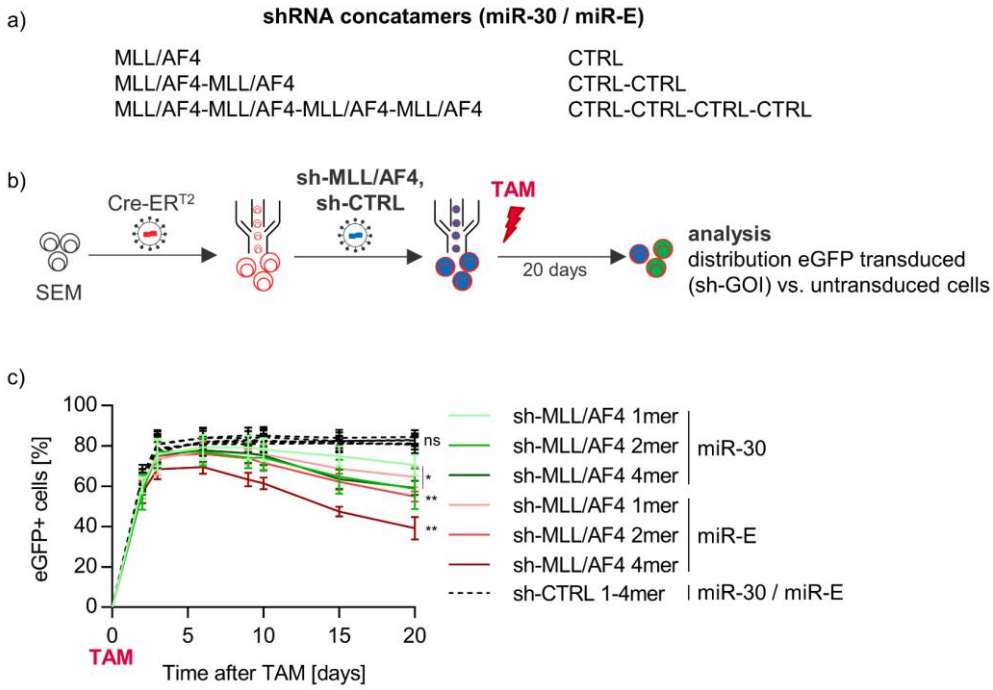

Figure 29: Concatamerization of MLL/AF4 shRNA combined with miR-E cassette increase growth inhibition of MLLA/F4 KD cells
a) shRNAs targeting MLL/AF4 or Renilla (CTRL) were concatamerized in the mTagBFP flipping construct (described in Fig. 14) resulting 1, 2 and 4mers. For all constructs, shRNAs were embedded in the miR-30 and the miR-E cassette, respectively. b) Experimental setting: SEM cells were transduced with Cre-ER^{T2}-mCherry and the flipping constructs with transduction efficiencies below 10 % to obtain single integrations. After sorting and cell recovery, cells were treated with 50 nM TAM to induce recombination and shRNA expression. The distribution of recombined (eGFP, shRNA expression) and non-recombined (mTagBFP, no shRNA expression) cells was analyzed over 20 days by flow cytometry. c) Percentage of eGFP positive cells out of all mTagBFP and eGFP positive cells is shown. For clarity, all control constructs are depicted as black dotted line as they all behave the same. n = 3 biological replicates, mean ± SD, paired t-test of the different shRNA constructs compared to the respective sh-CTRL construct, ns = not significant, * $p \leq 0.05$, ** $p \leq 0.01$.

After characterization of the optimized KD system, competitive *in vitro* assays were performed. The experiments were done in the t(4;11) SEM cell line as well as in two

non-MLL rearranged cell lines, NALM-6 and REH. First, cells were transduced with Cre-ER^{T2}-mCherry (Fig. 30a). Second, cells were transduced with the different concatamers with MLL/AF4 or control shRNA with a transduction efficiency below 10 % to obtain single integrations. For each construct, a control construct was cloned in the iRFP/T-sapphire vector with the same number of shRNA copies and the same miR-cassette. mTagBFP and iRFP positive cells were mixed 1:1 and treated with 50 nM TAM. As a readout, the distribution of recombined eGFP and T-sapphire positive cells was analyzed over 20 days by flow cytometry.

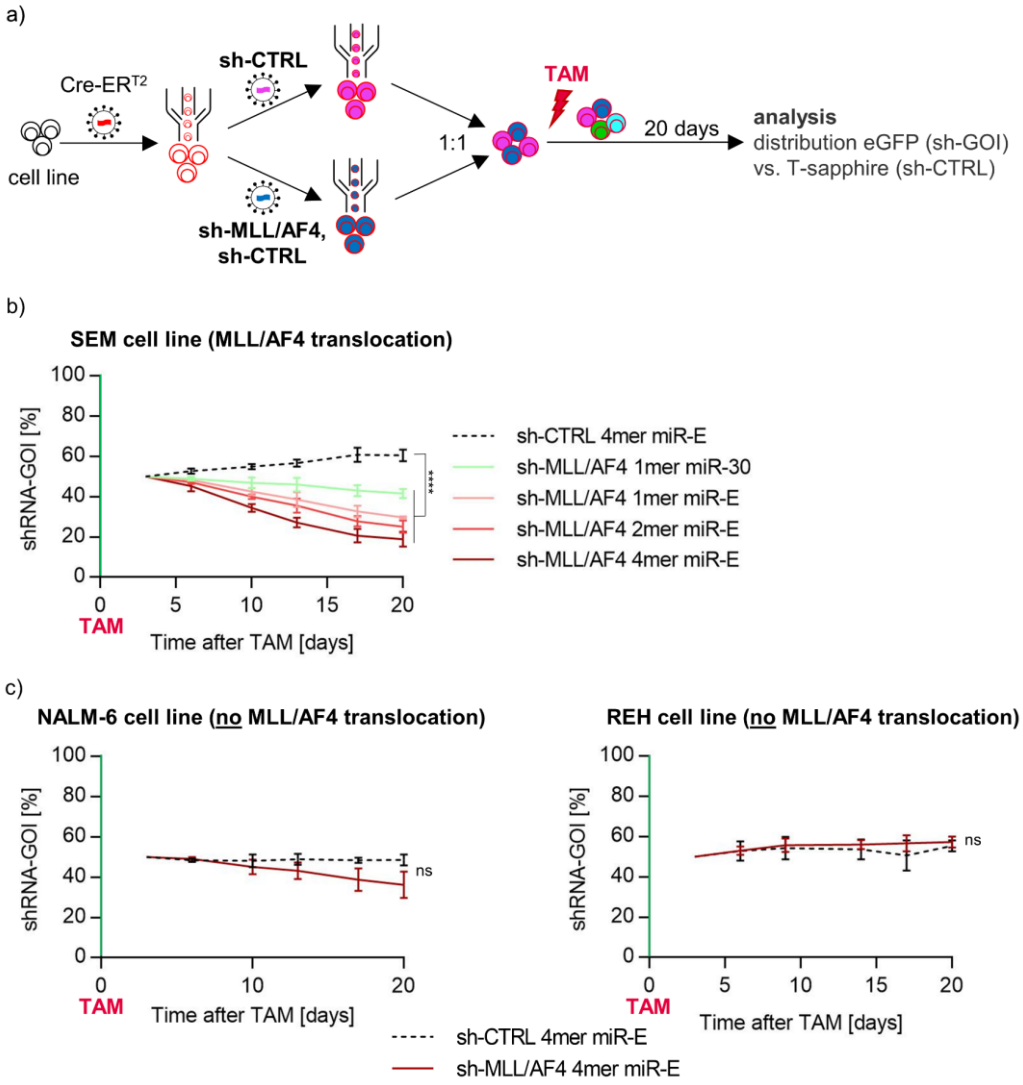

Figure 30: Inducible MLL/AF4 KD impairs growth in t(4;11) SEM cell line but not in non-MLL rearranged leukemic cell lines

a) Experimental setting: Cells were transduced with Cre-ER^{T2}-mCherry and the mTagBFP/sh-GOI and iRFP/sh-CTRL flipping constructs with transduction efficiencies below 10 % to obtain single integrations. After sorting and cell recovery, cells were mixed 1:1 and treated with 50 nM TAM to induce recombination and shRNA expression. The distribution of recombined eGFP/sh-GOI and T-sapphire/sh-CTRL cells was analyzed over 20 days by flow cytometry. b) Results of the t(4;11) SEM cell line: Percentage of eGFP positive cells out of all recombined cells (eGFP + T-sapphire) is shown. n = 3 biological replicates, mean ± SD, paired t-test of the different sh-MLL/AF4 constructs compared to sh-CTRL, **** $p \leq 0.0001$. c) Results of the non-MLL rearranged cell lines NALM-6 and REH are depicted as described in b). n = 3 biological replicates, mean ± SD, paired t-test, ns = not significant.

The mixture of control cells remained stable over time. In contrast, depletion of MLL/AF4 led to a significant reduction of the cell population (Fig. 30b). 20 days after TAM, 40 % eGFP positive cells could be detected expressing a MLL/AF4 1mer embedded in a miR-30 cassette, while only 30 % eGFP positive cells could be seen when using the miR-E cassette. Thus, the depletion of MLL/AF4 KD cells increased by using the miR-E cassette instead of the miR-30 cassette. Further, concatamerization of the MLL/AF4 shRNAs led to an increased depletion. While for the MLL/AF4 1mer (miR-E cassette) 30 % eGFP positive cells could be detected after 20 days, only 25 or 19 % eGFP expressing cells could be shown for cells transduced with a MLL/AF4 2 or 4mer, respectively. For the control experiments using the non-MLL rearranged cell lines, the most effective constructs with four shRNA copies and miR-E cassette were used. Here, the control mixture as well as the MLL/AF4/control mixture was stable over time (Fig. 30c). Only a small but not significant decrease of MLL/AF4 shRNA expressing NALM-6 cells was observed.

Thus, a MLL/AF4 dependent depletion could be shown using an improved inducible KD system in the t(4;11) SEM cell line while using a low transduction efficiency for the shRNA constructs.

4.5.2.3 Homing of MLL/AF4 KD PDX cells *in vivo*

As PDX MLL/AF4 KD cells could not be isolated at the end of an *in vivo* experiment using the constitutive KD system (Fig. 26 & 27), it remained to be determined if the cells were vanished the first days after injection or if the cells could engraft and were depleted over time.

The experiments with the constitutive KD system were technically complex for the MLL rearranged PDX samples as they are characterized by very low transduction efficiencies. In contrast, using the inducible KD system, transgenic cells could be easily amplified in mice to perform different experiments. Therefore, the homing capacity of these cells was investigated. ALL-707 cells were transduced with the Cre-ER^{T2}-mCherry construct and amplified in mice (Fig. 31a). Subsequently, cells were transduced with the mTagBFP/sh-MLL/AF4, mTagBFP/sh-CTRL or iRFP/sh-CTRL construct and amplified in mice. All constructs consisted of four shRNA copies embedded in a miR-E cassette. After amplification, transgenic cells were mixed 1:1 using cells with MLL/AF4 shRNA and control shRNA (mTagBFP/sh-MLLAF4 + iRFP/sh-CTRL) or a mixture of control cells (mTagBFP/sh-CTRL + iRFP/sh-CTRL).

Cells were treated with 150 nM TAM *in vitro* and injected 10 days later in mice (2 x 10^6 cells/mouse). Three days after injection, human cells were isolated out of the murine BM and the distribution of recombined cells was analyzed by flow cytometry. After re-isolation of the PDX cells, around 50 % of the cells expressed eGFP, independent if the cells expressed the control shRNA or the shRNA targeting MLL/AF4 in addition (Fig. 31b). Thus, the MLL/AF4 KD cells did not had a disadvantage in homing.

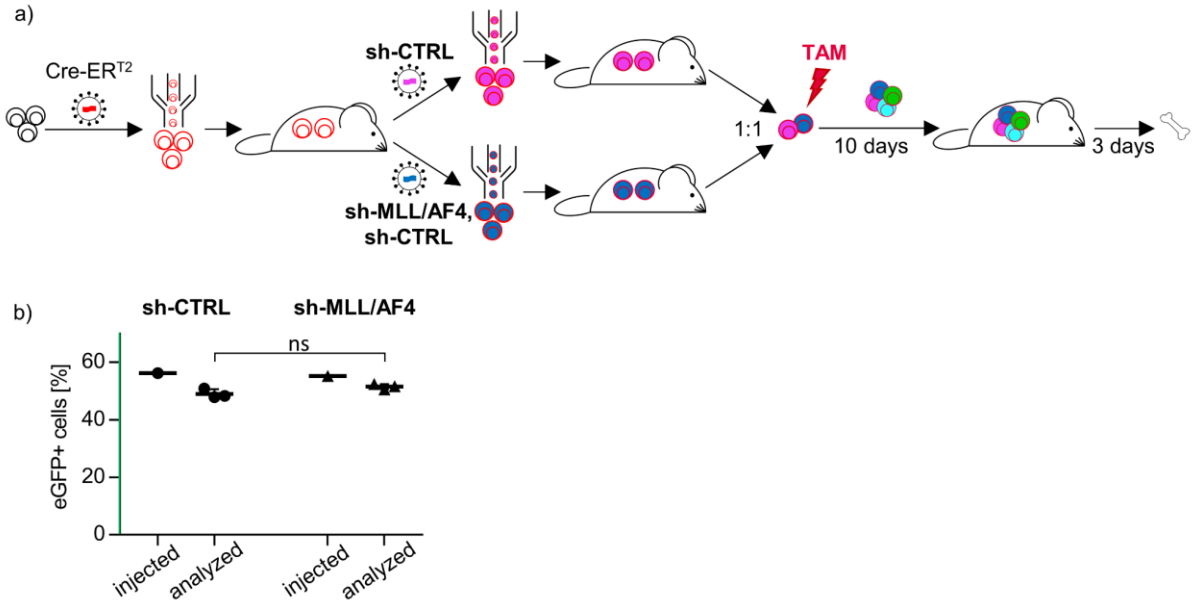

Figure 31: Inhibition of MLL/AF4 does not impair homing of ALL-707 cells
a) Experimental setting: ALL-707 cells were transduced with Cre-ER^{T2}-mCherry, sorted and amplified in mice. Then, cells were transduced with the mTagBFP/sh-GOI and iRFP/sh-CTRL flipping constructs (4 shRNA copies embedded in miR-E), sorted and amplified in mice again. Transgenic cells were mixed 1:1 using cells with MLL/AF4 shRNA and control shRNA (mTagBFP/sh-MLLAF4 + iRFP/sh-CTRL) or only control cells (mTagBFP/sh-CTRL + iRFP/sh-CTRL) were mixed. Cells were treated with 150 nM TAM *in vitro* and injected 10 days after treatment into mice (2 x 10^6 cells/mouse, n = 3 per group). Three days after injection, human cells were isolated out of the murine bone marrow and the distribution of recombined cells was analyzed by flow cytometry. b) Percentage of eGFP positive cells out of all recombined cells (eGFP + T-sapphire) is shown. One injection mixture per group, three mice per group at analysis time point, mean ± SD, unpaired t-test, ns = not significant.

These data indicate that the effect seen with the constitutive system was due to a growth disadvantage and not due to an impaired homing.

4.5.2.4 Competitive inducible MLL/AF4 KD *in vivo*

The result of the homing assay suggested that the depletion of MLL/AF4 KD cells, observed using the constitutive KD-system *in vivo*, occurred rather later, over a longer period of time than during the first days. Thus, the hypothesis was tested with different PDX samples *in vivo* and further investigated by gene expression analysis.

4.5.2.4.1 Competitive inducible MLL/AF4 KD in a non-MLL rearranged PDX sample *in vivo*

First, the inducible KD system was validated in PDX *in vivo* using the non-MLL rearranged PDX sample ALL-265. Therefore, PDX cells were stepwise transduced with Cre-ER^{T2}-mCherry and the flipping constructs targeting MLL/AF4 or Renilla as control (Fig. 32a). After sorting and amplification of cells in mice, mTagBFP/sh-MLL/AF4 and iRFP/sh-CTRL cells were mixed 1:1 as well as mTagBFP/sh-CTRL + iRFP/sh-CTRL cells. 300,000 cells were injected in six mice per group. One week after injection, mice were treated with 50 mg/kg TAM orally. Afterwards, cells were analyzed at different time points to monitor the variation of populations' distribution over time. The first animals were analyzed three days after TAM for the distribution of recombined shRNA expressing cells by flow cytometry. This early time point after TAM administration showed the initial distribution of the cells and is used as reference (time 0) for further time points. 18 days after TAM, human cells were analyzed out of a BM aspiration. In the presence of full-blown leukemia, cells were isolated out of the murine BM and analyzed as the final time point.

Three days after TAM application, around 30 % eGFP positive cells out of all recombined cells could be detected in the control group as well as in the MLL/AF4 KD group. When analyzing the distribution of eGFP and T-sapphire expressing cells over time, no significant changes could be detected within both groups (Fig. 32b). Thus, no effect could be observed in the non-MLL rearranged ALL-265 cells, showing the specificity and reliability of this technique.

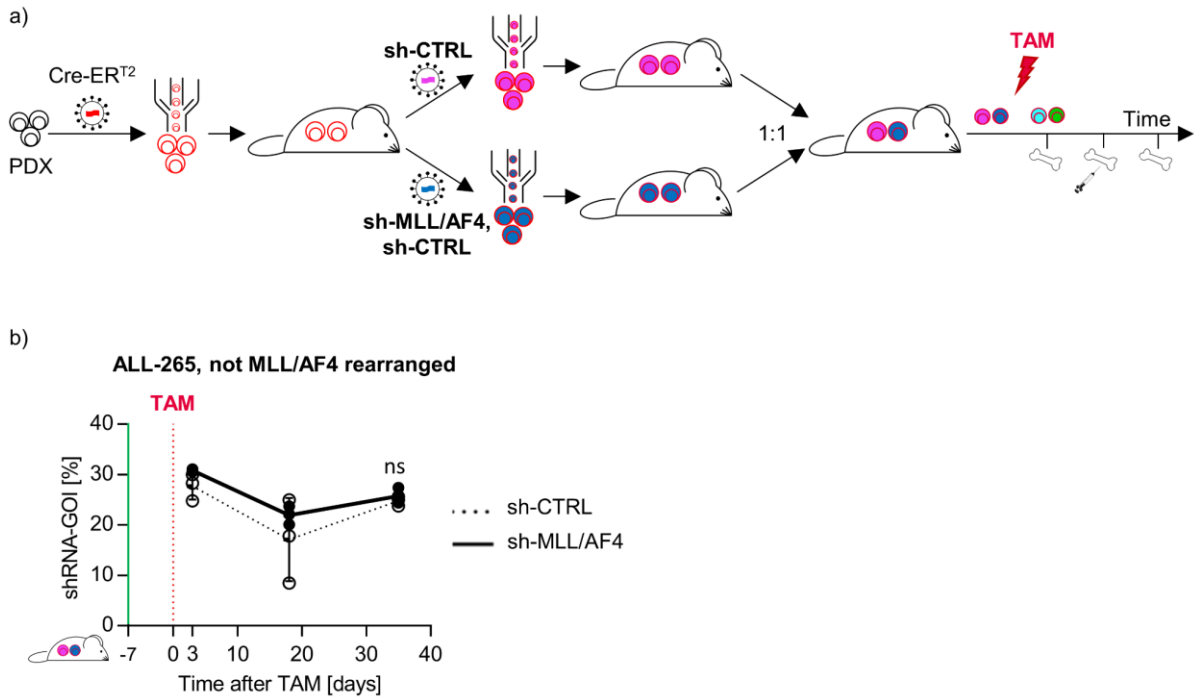

Figure 32: Inducible MLL/AF4 KD in non-MLL rearranged PDX does not impair growth *in vivo*
a) Experimental setting: Non-MLL rearranged ALL-265 cells were transduced with Cre-ER^{T2}-mCherry, sorted and amplified in mice. Then, cells were transduced with the mTagBFP/sh-GOI and iRFP/sh-CTRL flipping constructs (4 shRNA copies embedded in miR-E), sorted and amplified in mice again. Transgenic cells were mixed 1:1 using cells with MLL/AF4 shRNA and control shRNA (mTagBFP/sh-MLLAF4 + iRFP/sh-CTR) or only control cells (mTagBFP/sh-CTRL + iRFP/sh-CTRL) were mixed. 300,000 cells were injected per mouse (n = 6 per group). One week after injection, mice were treated with 50 mg/kg TAM by oral gavage to induce recombination and shRNA expression. Cells were analyzed at different time points to monitor the populations' distribution over time. Therefore, cells were isolated out of all bones of a mice or a BM aspiration was performed (marked by a syringe). b) Results of the non-MLL rearranged ALL-265: Cells were analyzed 3, 18 (BM aspiration) and 35 days after TAM for the distribution of recombined cells by flow cytometry. Percentage of eGFP positive cells out of all recombined cells (eGFP + T-sapphire) is shown. n = 3 mice per group per time point, mean ± SD, Two-way ANOVA, ns = not significant.

4.5.2.4.2 Gene expression analysis of MLL/AF4 KD PDX cells

With the inducible KD system, it was technically feasible to re-isolate injected MLL/AF4 KD PDX cells out of the murine BM. For the first time, it was possible to investigate a MLL/AF4 KD in PDX cells in more detail. To analyze the gene expression profile, ALL-707 and ALL-763, transgenic for the inducible eGFP MLL/AF4 or the control shRNA construct, were injected into NSG mice. One week after injection, mice were treated twice with 100 mg/kg TAM and cells were isolated out of the murine BM 28 or 33 days after TAM for ALL-707 and ALL-763, respectively. eGFP positive MLL/AF4 KD or control cells were purified and sent for MACE seq to GenXPro. Here, bioinformatic analysis were initially performed by GenXPro with further investigations being done in collaboration with Alexander Wilhelm (AG Marschalek, Frankfurt am Main).

Stam et al. (2010) analyzed 73 ALL infants with t(4;11), t(11;19) or t(9;11) translocation or without MLL rearrangement. There, a distinct gene expression pattern in MLL-rearranged leukemia patients could be shown. Here, the MACE seq data were compared to the Stam et al. (2010) data set comparing PDX control and MLL/AF4 KD samples with t(4;11) translocated and non-translocated ALL patient expression data. For both PDX samples, ALL-707 and ALL-763, a correlation of control cells to t(4;11) ALL patient data and a correlation of MLL/AF4 KD cells to non-MLL rearranged ALL patient data could be observed by gene set enrichment analysis (Fig. 33a-b). Even though similar results were detected for ALL-707 and ALL-763 in gene set enrichment analysis, the individual highly differential expressed genes between control and MLL/AF4 KD cells differed (Fig. 33c-d). Genes depicted in the volcano blot with a high fold change were highly expressed in control cells and low expressed in MLL/AF4 KD cells. Thus, a low fold change correlates with low expression in control cells and high expression in MLL/AF4 KD cells. Interestingly, all highly differential expressed genes in ALL-707 could also be found differentially expressed in ALL-763. In contrast, none of the described highly differentially expressed genes in ALL-763 were found in ALL-707 the same way. In ALL-707, e.g. the transforming growth factor (TGF)-beta mediated SMAD signaling, that is also known as a tumor suppressor regulating proliferation, apoptosis and differentiation, is upregulated upon MLL/AF4 KD as well as apoptotic members like *p63* or the *BCL2 Binding Component 3* (*BBC3*). In addition, *Ribosomal Protein S6 Kinases* (*RSK*) and genes involved in *Vascular Endothelial Growth Factor Receptor 2* (*VEGFR2*) mediated cell proliferation (*Phospholipase C Gamma 1* (PLCG1), *Sphingosine Kinase 1* (*SPHK1*), *Pyruvate Dehydrogenase Kinase 1* (*PDK1*)) are downregulated in MLL/AF4 KD cells. In ALL-763, the SMAD signaling and genes regulating apoptosis (*Apoptosis-inducing factor 2* (*AIFM2*), *BBC3*, *Tumor Protein P53 Inducible Nuclear Protein 1* (*TP53INP1*)) are upregulated as well upon MLL/AF4 KD. Further, *human leucocyte antigen* (*HLA*) genes were upregulated in MLL/AF4 KD cells. Genes involved in cell cycle (*BRCA1 Interacting Protein C-Terminal Helicase 1* (*BRIP1*), *Minichromosome Maintenance Complex Component* (*MCM3,4,6,10*), *Cyclin Dependent Kinase 2* (*CDK2*), *Cell Division Cycle 6* (*CDC6*), *DNA Polymerase Epsilon 2* (*POLE2*)) were downregulated in MLL/AF4 KD cells.

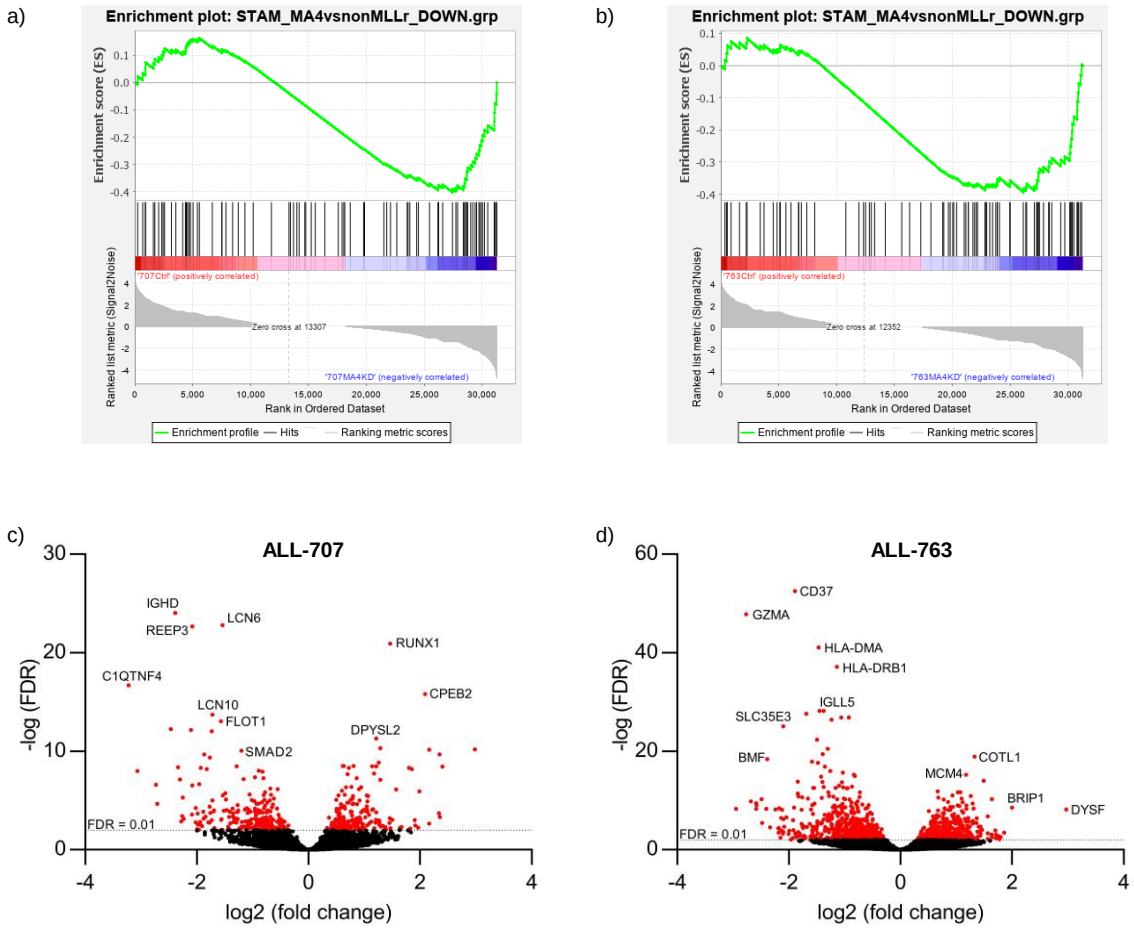

Figure 33: Gene expression analysis reveals similarity to non-MLL rearranged leukemia patients' expression data upon MLL/AF4 KD

a) Gene set enrichment analysis (GSEA) of ALL-707 MLL/AF4 KD and control cells. ALL-707 transgenic for Cre-ER^{T2}-mCherry and the mTagBFP/sh-GOI flipping constructs (4 shRNA copies embedded in miR-E) were injected into mice (300,000 cells/mouse, n=3 per group). One week after injection, mice were treated twice with 100 mg/kg TAM by oral gavage to induce recombination and shRNA expression. ALL-707 cells were isolated 28 days after TAM and sorted for eGFP/sh-GOI expression. Samples were analyzed by MACE seq at GenXPro and in cooperation with Alexander Wilhelm (AG Marschalek, Frankfurt am Main). For GSEA, results were compared with RNA seq data from Stam et al. (2010). NES = -1.37, p = 0.031. b) GSEA as described in a) using ALL-763 cells 33 days after TAM. NES = -1.38, p = 0.036. c) Volcano blot shows differentially expressed genes of ALL-707 control cells compared to MLL/AF4 KD cells. Data obtained from MACE seq described in a). Genes with a high fold change are highly expressed in control cells and low expressed in MLL/AF4 KD cells. Thus, a low fold change correlates with low expression in control cells and high expression in MLL/AF4 KD cells. n = 3 biological replicates per sample. d) Volcano blot shows differentially expressed genes of ALL-763 control cells compared to MLL/AF4 KD cells as depicted in c). Data obtained from MACE seq described in b).

In summary, inhibition of MLL/AF4 changed the expression profile patient specific to profiles observed in non-MLL rearranged ALL patients and similar pathways were up- and downregulated upon MLL/AF4 KD.

4.5.2.4.3 Competitive inducible MLL/AF4 KD in t(4;11) rearranged PDX samples *in vivo*

As major changes in gene expression were overserved upon MLL/AF4 KD in PDX cells, the MLL/AF4 rearranged PDX samples ALL-707 and ALL-763 were used for competitive inducible MLL/AF4 silencing (Fig. 34). The experiment was performed as described for the non-MLL rearranged PDX ALL-265 (see chapter 4.5.2.4.1); to induce recombination 100 mg/kg TAM was applied twice. For ALL-707, cells were analyzed 3, 13, 21 and 28 days after TAM administration.

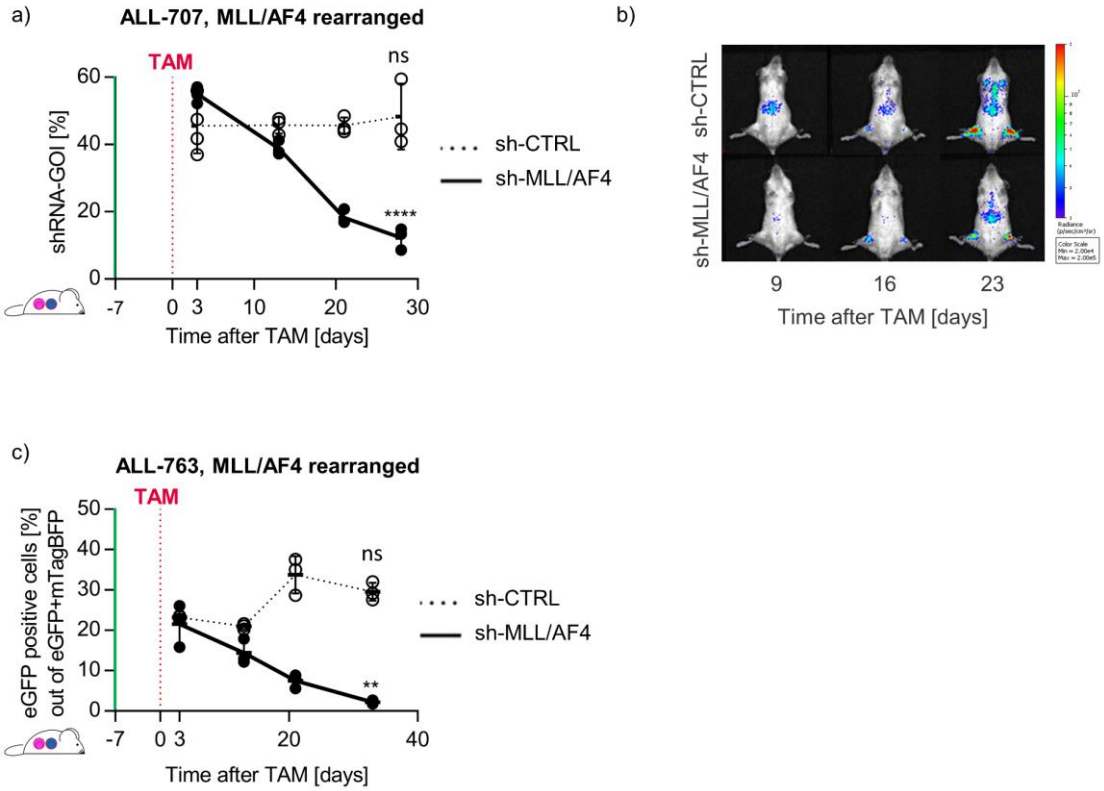

Figure 34: Inducible MLL/AF4 KD impairs growth in MLL rearranged PDX cells *in vivo*

a) Experiment was performed as described in Fig. 32a. Adaption: One week after injection, mice were treated twice with 100 mg/kg TAM by oral gavage to induce recombination and shRNA expression. Cells were analyzed 3 (n = 4), 13 (n = 3), 21 (n = 3) and 28 (n = 3) days after TAM administration to monitor the distribution of recombined cells by flow cytometry over time. Percentage of eGFP positive cells out of all recombined cells (eGFP + T-sapphire) is shown. Mean ± SD, Two-way ANOVA, **** $p \leq 0.0001$; ns = not significant. b) *In vivo* imaging of experiment described in a). Representative pictures out of three replicates per time point. c) Experiment was performed as described in Fig. 32a. Adaption: One week after injection, mice were treated twice with 100 mg/kg TAM by oral gavage to induce recombination and shRNA expression. Cells were analyzed 3 (n = 3), 13 (n = 3), 21 (n = 3) and 33 (n = 3) days after TAM administration to monitor distribution of recombined cells by flow cytometry over time. Percentage of eGFP positive cells out of non-recombined mTagBFP and recombined eGFP positive cells is shown. Mean ± SD, Two-way ANOVA, ** $p \leq 0.01$, ns = not significant.

Three days after TAM administration, around 46 % eGFP control cells and 55 % eGFP MLL/AF4 KD out of all recombined cells could be detected in the different mixtures

(Fig. 34a). While the distribution of recombined cells stayed unchanged in the control mixture, the MLL/AF4 KD cells were depleted significantly over time. At the final time point, 28 days after TAM application, only 12 % eGFP MLL/AF4 KD cells remained. Mice were imaged during the experiment to monitor the growth of human cells. The depletion of MLL/AF4 KD cells could already be observed by *in vivo* imaging by a reduced growth kinetic of the MLL/AF4 KD/control mixture compared to the control/control mixture (Fig. 34b). For ALL-763, cells were analyzed 3, 13, 21 and 33 days after TAM. In this case, the iRFP/sh-CTRL population got lost in both mixtures; therefore, the analysis was performed in a different way analyzing the distribution of non-recombined mTagBFP versus recombined eGFP positive cells. The control cells were nearly unchanged over time while a strong depletion of MLL/AF4 KD cells was detected (Fig. 34d). Thus, for both PDX samples a time depended depletion of MLL/AF4 KD cells was observed showing an essential function of MLL/AF4 for leukemia maintenance.

In conclusion, for AF4/MLL no essential function for leukemia growth could be determined in different functional assays after partial AF4/MLL inhibition; however, an altered gene expression could be identified upon dnTASP1 expression. In contrast, MLL/AF4 does not impair processes like homing and engraftment, but the fusion protein is essential for tumor maintenance shown in multiple experiments *in vitro* and *in vivo*.

5. Discussion

Childhood ALL has in general a good prognosis, however, for specific subtypes, the percentage of successfully treated patients drastically declines (Brenner and Spix, 2003, Pulte et al., 2008). Among them, chromosomal translocations are frequently detected in acute leukemia and lead to a poor outcome. One predominant translocated gene is *KMT2A* encoding MLL, for which more than 135 MLL fusion partners were identified with different frequencies (Meyer et al., 2018). In ALL, the main MLL fusion partner is AF4 with survival rates of only 10 – 30 % in patients carrying the translocation (Isoyama et al., 2002, Meyer et al., 2018, Pui et al., 2002). As the treatment of such an aggressive form of leukemia remains challenging, further investigations are definitely required. Many studies focused on the role of the MLL/AF4 fusion protein, hypothesizing an important and maybe essential function of this fusion protein for leukemia development (Chen et al., 2006, Krivtsov et al., 2008, Secker et al., 2019, Thomas et al., 2005). However, as other studies could not confirm this observation but showed opposite results, the role of MLL/AF4 in ALL still remains controversial (Bursen et al., 2010). Compared to the numerous studies on MLL/AF4, only few groups focused on the reciprocal AF4/MLL fusion protein, which is not always expressed in t(4;11) leukemia patients (Agraz-Doblas et al., 2019, Kowarz et al., 2007, Trentin et al., 2009). In this case, as well, controversial results were published ranging from an important to neglectable function of AF4/MLL (Bueno et al., 2019, Bursen et al., 2010, Gaussmann et al., 2007, Kumar et al., 2011b).

In this project, the role of the two fusion proteins for leukemia maintenance was further investigated with a focus on mimicking the clinical situation of patients with an established leukemia who require treatment.

5.1 t(4;11) breakpoint characterization

MLL/AF4 translocations and their reciprocal products represent a challenge for treatment of leukemia patients. As the presence of different rearrangement-dependent fusion proteins can be detected in the same patient, it is important to carefully characterize ALL cells.

Therefore, to start this project, different PDX samples and the SEM cell line with t(4;11) translocation were analyzed regarding their expressed MLL/AF4 and AF4/MLL fusion transcripts. As expected, 8/8 t(4;11) rearranged PDX expressed MLL/AF4 while only

6/8 (75%) expressed the reciprocal AF4/MLL fusion in addition. Our observation is in line with published data that showed an expression of MLL/AF4 in all t(4;11) leukemia patients but an expression of AF4/MLL in only 50 – 80 % of the cases (Agraz-Doblas et al., 2019, Kowarz et al., 2007, Trentin et al., 2009). In those cases, AF4/MLL expression could not be detected even at the genomic level and instead, cryptic and three-way translocations were found (Downing et al., 1994, Kowarz et al., 2007, Reichel et al., 2001). The t(4;11) PDX samples used here, differ regarding the age at diagnosis, the MLL/AF4 breakpoint and the gender and expression of AF4/MLL did not correlate with any of these patient characteristics (Heckl, 2018). Recently, Agraz-Doblas et al. (2019) reported a positive correlation between AF4/MLL and HOXA expression in t(4;11) infants. In our group of samples, I could partially confirm this observation, when analyzing the expression of HOXA7, HOXA9 and HOXA10. In my hands, PDX samples without AF4/MLL expression did not show any HOXA expression that is in line with the reported results from Agraz-Doblas et al. (2019). However, in only 3/6 PDX samples expressing AF4/MLL also a HOXA expression could be detected. Again, no correlation of this observation to any of the above mentioned patient characteristics were found.

I further characterized the samples and found a fusion between exon 9 of MLL and exon 4 of AF4 on genomic level in ALL-706, 707, 763 and in the SEM cell line. Accordingly, the main MLL/AF4 mRNA fusion transcript detected in these cells was a fusion of exon 9 of MLL and exon 4 of AF4. However, when analyzing the breakpoint mRNA sequences in more detail, different splicing forms for MLL/AF4 were identified. These heterogeneous mRNA transcripts arise from alternative MLL splice sites that lead to fusion of different MLL exons to the AF4 BCR (Borkhardt et al., 1994, Divoky et al., 2000, Domer et al., 1993). In the SEM cell line and the ALL-706 and ALL-763, a fusion of MLL exon 8 to AF4 exon 4 was identified. In exon 8, a cryptic splice site was described allowing alternative splicing. Fusions with the MLL exon 8 often lead to frameshift because this exon ends after the first nucleotide of a triplet resulting in new stop codons and an early termination (Divoky et al., 2000). Further, in all samples analyzed, fusions between exon 9 of MLL and exon 4 of AF4 were observed with a deletion of the first amino acid of exon 4 of AF4 or with a point mutation at the fusion site in the SEM cells, complicating the targeting of the breakpoint. Nevertheless, with more than 80 % frequency, a main MLL/AF4 fusion transcript was present in the studied cells. For AF4/MLL, no multiple mRNA transcripts could be detected either in

the SEM cell line or in ALL-706 or ALL-707. This is in contrast to published data for the SEM cell line that reported a second AF4/MLL mRNA fusion transcript with exon 3 of AF4 fused to exon 12 to MLL (Marschalek et al., 1995). It might be that more fusion transcripts need to be sequenced to detect this further variant. Nevertheless, the AF4/MLL fusion transcript differs between the SEM cell line and the PDX samples analyzed. Thus, due to the complex profile of the PDX samples and in order to silence AF4/MLL in PDX *in vivo*, patient specific shRNAs were designed and validated in an adapted reporter system, as a cell line model is missing in this case.

Taken together, the presence of the various breakpoints and splicing variants within the same patient cells represents a challenge for a putative targeted treatment of t(4;11) patients. Nevertheless, a single MLL/AF4 variant is very frequent across different patients´ tumors and was studied here.

5.2 Breakpoint specific targeting using shRNAs

Translocations are ideal therapeutic targets as they are not present in healthy cells. Thus, by targeting the t(4;11) breakpoint, only leukemic cells are attacked while normal tissue should not be affected avoiding treatment-induced undesired effects. Identification of specific shRNAs targeting the t(4;11) fusions might be of clinical interest as a new option to treat leukemia patients.

In this project, I focused on the design of potent and specific shRNAs to target the AF4/MLL breakpoint in ALL-706 and ALL-707. To this aim, the SplashRNA algorithm was used, a sequential learning algorithm trained by largescale miR-30 and miR-E data sets predicting potent miRNA-based shRNAs (Pelossof et al., 2017). There, the goal is to reach SplashRNA scores above 1 that correlates with KD efficiencies above 85 %. Nevertheless, when designing shRNAs against the fusion, the tool presents its limitation, as the SplashRNA scores for the designed breakpoint specific shRNAs targeting AF4/MLL were all very low, ranging between 0.123 and 0.572 for ALL-706 and ALL-707. Also when comparing the designed shRNAs to guidelines published for manual shRNA design, many characteristics were not fulfilled like an AT-rich region from position 3 - 7, at position 9 and 12 as well from 17 - 19 or GC-rich regions at position 11 or from 14 - 16. (Bofill-De Ros and Gu, 2016, Li et al., 2007).

As no cell line model was available with the same AF4/MLL fusion transcript of ALL-706 and ALL-707, an optimized reporter system was used to test the KD efficiency. The shRNA reporter system was originally published by Fellmann et al. (2013) as retroviral

reporter and was here optimized for lentiviral transductions. The efficiency did not correlate with the estimated scores, but the efficiency was above 70 % for all tested shRNAs, despite calculated scores below 0.5. Unfortunately, all tested AF4/MLL shRNAs were unspecific, targeting the endogenous AF4 and MLL as well. Nevertheless, as AF4/MLL was partially inhibited, I hypothesize that possible biological effects could be studied even under this suboptimal condition. On the contrary, a highly specific sequence against MLL/AF4 was used for further investigations.

5.3 Experimental settings for gene inhibition

Targeted inhibition using shRNAs better mimics the partial inhibition induced by drugs rather than complete knockouts mediated by Clustered Regularly Interspaced Short Palindromic Repeats (CRISPR)/Cas9 approaches (Hulton et al., 2020). KD experiments were performed using two different experimental settings, with constitutive and with inducible expressed shRNAs. With the constitutive expression of shRNAs, targets are inhibited directly and due the stable integration, targets with a long half-life can be easily inhibited as well (Harborth et al., 2003). Beside many advantages of this system, one limitation is the impossibility to study essential genes. After transduction of SEM cells with the shRNA targeting MLL/AF4, cells started to die. Thus, for example competitive assays, requiring a stressful sorting step, were not possible. An additional drawback of the constitutive system while studying essential genes is that shRNA transduced cells cannot be amplified. The t(4;11) rearranged PDX are difficult to transduce with transduction efficiencies far below 10 % (Heckl, 2018). Thus, cells need to be enriched and amplified in NSG mice in order to have enough cells to perform experiments. Consequently, only few cells could be injected for *in vivo* experiments prohibiting engraftment controls and analyzing cells over time. Another major point is the overestimation of the results due to homing or engraftment deficiencies upon transplantation into mice. Because of all these reasons Michela Carlet, Birgitta Heckl and Jenny Vergalli developed a competitive inducible KD system for PDX *in vivo (Carlet et al., 2021)*. This system is based on Cre-loxP using two differently mutated loxP sites (Oberdoerffer et al., 2003). Stern et al. (2008) combined this system with shRNA expression, called FLIP cassette. Based on this system, an inducible KD system with five different fluorophores was generated in our lab (Carlet et al., 2021) enabling proper analysis of lethal targets. In the absence of KD induction, transgenic cells can be easily amplified for experiments. Moreover, it mimics the clinical

situation, where patients with a certain stage of leukemia are diagnosed before treatment. Thus, mimicking this situation, the KD can be induced at defined points of leukemic burden *in vivo* without being affected by critical parameters like homing and engraftment.

For ideal controlling, competitive experiments were performed. Different fluorophore combinations enabled the distinction between control and target KD cells in the same mouse. Therefore, control and KD cells were used in the same approach for *in vitro* experiments or injected together into the same mouse increasing sensitivity of each experiment, thus already small changes can be detected easily. Moreover, the experimental quality was enhanced by the presence of control and KD cells in the same mouse as all cells are handled and treated the same way. Furthermore, regarding animal welfare, also fewer mice are needed for *in vivo* experiments. Thus, the competitive KD systems are valuable and robust approaches for *in vitro* and *in vivo* experiments.

An additional challenge I had, while trying to strongly silence the fusion proteins, relied in the low transduction efficiency achieved in translocated PDX samples, accompanied by limited possibility in the shRNA design. It is known that single shRNA genomic copies have a reduced potency and that a weak shRNA design reduces drastically the KD efficiency (Fellmann et al., 2011). I encountered both problems when targeting the t(4;11) breakpoint in t(4;11) rearranged PDX cells. As already mentioned, the t(4;11) rearranged PDX samples used in this study were characterized by extremely low transduction efficiencies, below 1 % for the inducible KD system. Even after trying different strategies to enhance the transduction efficiency, no multiple integrations could be detected (data not shown). In addition, designing shRNAs against a specific fusion did not yield potent shRNAs. Thus, to increase the KD efficiency the inducible KD system was optimized by using a more efficient miR-30 based backbone and by concatamerizing shRNAs as described by Fellmann et al. (2013) and Sun et al. (2006). Both, the miR-E backbone and concatamerizing the MLL/AF4 shRNA increased the MLL/AF4 depended lethality that is in line with published data (Choi et al., 2015, Aagaard et al., 2008, Chung et al., 2012, Liu et al., 2008).

Next to comparing the KD efficiencies, also control experiments were performed concatamerizing control shRNAs targeting Renilla. Here, 1, 2 and 4 shRNA copies were concatamerized and tested for toxicity. No impact on growth or cell viability was observed upon transduction of the control concatamers suggesting that the RNAi

machinery was not saturated with these constructs as it was published when using strong Pol III promoters (Boudreau et al., 2009, Grimm et al., 2006).
In summary, concatamerization of shRNAs and the miR-E cassette increased the effect upon MLL/AF4 KD without observing any side effect from control shRNAs. Thus enabling investigations on MLL/AF4 KD cells *in vivo*.

5.4 AF4/MLL is not essential for leukemia maintenance

As the reciprocal AF4/MLL fusion protein is not expressed in all t(4;11) rearranged leukemia patients, I asked whether the fusion protein is important for leukemia development and maintenance (Agraz-Doblas et al., 2019, Kowarz et al., 2007, Trentin et al., 2009). So far, single AF4/MLL expression experiments or in combination with MLL/AF4 expression were performed showing increased resistance against apoptotic triggers and enhanced cell cycling capacity (Bueno et al., 2019, Gaussmann et al., 2007). Bursen et al. (2010) reported that LSPCs expressing AF4/MLL were capable of causing ALL in mice. However, Kumar et al. (2011b) performed AF4/MLL KD experiments using siRNAs *in vitro* showing no changes in proliferation, cell cycle or apoptosis. Of note, Rolf Marschalek, one of the leading MLL/AF4 experts, commented on this publication e.g. by criticizing the experimental setting using transient siRNAs that would not be able to downregulate the very stable AF4/MLL on protein level (Marschalek, 2011). Thus, the results observed in cell lines *in vitro* and from transduced LSPCs in mice and the weak points of the experiments performed by Kumar et al. (2011b) were decisive for the design of experiments described in this project.
Here, the stable AF4/MLL fusion protein was inhibited using either shRNAs or a dominant negative Taspase1. The constitutive shRNA expression led to a constant downregulation of AF4/MLL mRNA that should also effect the protein level. Unfortunately, also in cooperation with our collaboration partner Rolf Marschalek, no reliable AF4/MLL western blots detecting the fusion protein could be performed as it was reported before (Kumar et al., 2011a). Therefore, only qPCR data validated the shRNA mediated KD leading to an intermediate unspecific silencing. Although the endogenous MLL and AF4 were additionally partially silenced, no growth aberrations could be observed; finally reproducing the results reported by Kumar et al. (2011b), despite our stable and persistent KD approach.

Next to targeting AF4/MLL with shRNAs, a dnTASP1 was used provided by Rolf Marschalek (Sabiani et al., 2015). Dominant negative proteins are widely used especially for proteins assembling into multimers to be active (Sheppard, 1994, Barren and Artemyev, 2007, Voellmy, 2005, Gao et al., 2002). They compete with wildtype proteins for multimers or for the direct targets, thus inhibiting the function of the wildtype protein. Major disadvantages of dominant negative proteins are that they mostly have more than a single target and that overexpression of a new protein could have harmful side effects (Prelich, 2012). For Taspase1, only MLL, MLL4, TFIIA and AF4/MLL are confirmed targets (Bursen et al., 2004, Hsieh et al., 2003b, Zhou et al., 2006). Further, Taspase1 plays an important role in the mouse embryonic development, but a deletion at later time points has no discernible toxicities (Chen et al., 2012, Takeda et al., 2006). Big advantage for the use of dnTASP1 relies in its capacity to inhibit all AF4/MLL variants regardless of the breakpoint or splicing variants. AF4/MLL inhibition by dnTASP1 could not be validated by western blot and qPCR would be useless here as the inhibition occurs post-translationally. However, the expression of dnTASP1 could be visualized on protein level using its FLAG-tag. Similar to the result obtained using shRNAs, no growth defects upon dnTASP1 mediated AF4/MLL inhibition was detected. Next, HOXA expression was analyzed after AF4/MLL inhibition. Here, HOXA9 expression was significantly reduced while for HOXA7 and HOXA10 only a minor reduction was observed. Agraz-Doblas et al. (2019) published a positive correlation of AF4/MLL and HOXA (HOXA5, HOXA7, HOXA9, HOXA10 etc.) expression in t(4;11) infant B-cell precursor ALL. When Trentin et al. (2009) compared HOXA (HOXA5, HOXA9, HOXA10) and AF4/MLL expression, no correlation were found. There, only 8/12 patients with AF4/MLL expressed HOXA genes. In this study, three infant patients expressed AF4/MLL of which only one expressed HOXA genes in addition. Thus, the different results cannot be explained by the age of the patients. Further, Stam et al. (2010) showed the existence of subgroups in t(4;11) infant ALL patients regarding HOXA (HOXA3, HOXA5, HOXA7, HOXA9, HOXA10) expression. Importantly, they found a correlation between the lack of AF4/MLL expression and a high risk of disease relapse. This is in line with recently published data by Agraz-Doblas et al. (2019) discovering a prolonged overall survival of t(4;11) infant ALL patients expressing AF4/MLL and HOXA genes. Low HOXA expression was observed to correlate with an overexpression of Iroquois-class homeodomain protein IRX-1 or IRX-2 (Kang et al., 2012, Trentin et al., 2009). IRX proteins regulate Early Growth Response

(EGR) expression that control p21 and induces quiescence that might lead to treatment resistance (Guzman, 2015, Kühn et al., 2016).

Gene expression analysis revealed dnTASP1 dependent alterations in cell cycle. The dnTASP1 target TFIIA is transcriptionally active also without cleavage and not hampered by Taspase1 inhibition (Zhou et al., 2006). In addition, uncleaved MLL is still active but with reduced activity (Takeda et al., 2006). For MLL4 only little is known about the Taspase1 dependent cleavage. Nevertheless, cyclins are targets of MLL and MLL4 and in Taspase1 deficient mice, cyclins were downregulated due to reduced histone methyl transferase activity of uncleaved MLL and proliferation of MEFs was impaired, while deletion of Taspase1 in 7-week-old mice led to no discernible toxicities (Chen et al., 2012, Takeda et al., 2006). Thus, follow up studies are necessary to explore if the altered cell cycle depend on AF4/MLL inhibition or if it is a site effect of inhibiting MLL and MLL4 in addition.

In conclusion, AF4/MLL expression is favorable for the leukemic patients' outcome and correlates with HOXA expression. The partial molecular inhibition induced in the present work did not show an essential function of AF4/MLL for tumor maintenance, however, it still might be that the inhibition was just not strong enough.

5.5 MLL/AF4 is required for leukemia growth

MLL/AF4 is expressed in all t(4;11) rearranged leukemic patients and an important function for the fusion protein was described in cell lines *in vitro* before. Nevertheless, different model systems led to different results and patient cells were never studied (Chen et al., 2006, Krivtsov et al., 2008, Secker et al., 2019, Thomas et al., 2005, Bursen et al., 2010). The reasons responsible for these different results depend on the limited knowledge about the cell of origin where the translocation arises, if and how the cells interact with the bone marrow environment and the different molecular approaches used (Ottersbach et al., 2018, Milne, 2017). Here, a t(4;11) PDX mouse model was used as perfect model system to study the function of MLL/AF4 for tumor maintenance as it is the model currently closest to the clinical situation of the patient.

In this project, I used a shRNA in order to target MLL/AF4. Breakpoint specific KD could be achieved enabling the study of MLL/AF4 under ideal settings. As also described for AF4/MLL, detection of the MLL/AF4 fusion protein by western blot is challenging and could not be performed; instead, MLL/AF4 inhibition was confirmed by qPCR. First data that Birgitta Heckl produced using the constitutive KD system could

be reproduced *in vitro* and *in vivo* showing a loss of cells upon MLL/AF4 KD (Heckl, 2018). When she performed experiments using the inducible KD system *in vivo*, no changes in cell growth were observed upon MLL/AF4 KD. When I reproduced her experimental settings using low transduction efficiencies in the SEM cell line *in vitro*, cells weren't altered upon MLL/AF4 KD as well. Probably, single genomic integrations of the inducible KD system were not enough to perform a strong KD as described by Fellmann et al. (2011). Therefore, the system was improved using a stronger miR-30 based backbone and shRNA concatamers. Then, also with low transduction efficiencies leading to single integrations, a MLL/AF4 KD could be achieved and a time dependent loss of MLL/AF4 KD cells could be observed in the SEM cell line *in vitro* as well as in PDX samples *in vivo*. This observation was independent from the AF4/MLL expression in the cells; thus, expression of AF4/MLL does not influence the importance of MLL/AF4 on leukemia maintenance. With this system, it could be shown that MLL/AF4 is not essential for homing and engraftment in mice but an inhibition of the fusion protein impaired the growth of the cells. Thus, an essential function of MLL/AF4 for leukemia maintenance could be described.

This result is in line with published data of Krivtsov et al. (2008) who created a mouse model with conditional expression of Mll/AF4 that induced B-ALL. It also fits with the study of Secker et al. (2019) who generated MLL/AF4 rearranged cells from umbilical cord blood cells using CRISPR/Cas9 that had phenotypcial, morphological and molecular features similar to t(4;11) patients. However, the result from my study contrasts with the published data of Bursen et al. (2010) who transplanted MLL/AF4 transduced LSPCs into mice. There, no disease was developed over a period of 13 month. Bursen and colleagues claimed that the titer of the MLL/AF4 containing retrovirus was low such that only few transgenic cells could be injected into mice that might have influenced the result of this experiment (Bursen et al., 2010). Otherwise, it might be that the AF4/MLL fusion protein is essential for the leukemia onset, even though the conditional expression of Mll/AF4 by Krivtsov et al. (2008) induced B-ALL in mice without the presence of the AF4/MLL fusion protein. The model systems used in these studies are suitable to understand and simulate the leukemia onset. To study the importance of the fusion proteins for tumor maintenance, the PDX mouse model system is the most suitable system mimicking the clinical situation of patients with an established leukemia; whether additional factors are needed for leukemia onset needs to be investigated further.

For t(4;11) patients, specific MLL/AF4 signatures were published that could be compared to PDX with and without MLL/AF4 KD, in order to validate the approach. Here, a MLL/AF4 signature correlating to leukemic patients with and without t(4;11) translocation was shown. Sequencing data detected similar amounts of genes up and down regulated for both PDX samples. This equilibrium of deregulated genes was already observed in a study analyzing a siRNA mediated MLL/AF4 KD in the SEM cell line (Harman et al., 2020). There, especially RUNX1, a direct target of MLL/AF4, was shown to be responsible for the regulation of multiple indirect target genes of MLL/AF4 (Harman et al., 2020, Wilkinson et al., 2013). In this study, in both PDX samples, a downregulation of RUNX1 was shown upon MLL/AF4 KD leading to altered expression of multiple target genes. Even though the highly differential expressed genes differed between the samples, altered pathways were common in both samples showing mainly changes in proliferation, differentiation and apoptosis. However, a direct regulation of BCL-2 by MLL/AF4 could not be confirmed as published by Benito et al. (2015).

Thus, an essential function of MLL/AF4 for tumor maintenance could be shown in a perfect controlled inducible KD system in PDX *in vivo* that was supported by sequencing data demonstrating expression profiles similar to the one observed in non-MLL rearranged leukemic cells.

According to these results, MLL/AF4 might be a potential therapeutic target using RNAi. RNAi-based drugs are promising and are tested in different clinical trials (Kleinman et al., 2008, DeVincenzo et al., 2010, Davis et al., 2010, Gottlieb et al., 2016, Setten et al., 2019). Sequences have been modified and chemical modifications were introduced in order to attenuate the immune system detecting dsRNA and to enhance nuclease resistance (Bramsen et al., 2009, Robbins et al., 2007). Besides administering naked chemical modified siRNAs, delivery systems were developed like nanoparticle-based delivery systems showing a successful delivery of siRNAs in multiple trials (Yuan et al., 2014, Coelho et al., 2013, Fitzgerald et al., 2014). Lipid nanoparticles consist of neutral and cationic lipids that are important for encapsulation of siRNAs as they interact with the negatively charged cell membrane and mediate the cellular uptake binding to the low density lipoprotein receptor (LDL) that is commonly expressed on leukemic cells (He et al., 2014, Jyotsana et al., 2018). Jyotsana et al. (2018) reported that lipid nanoparticles are able to target leukemic cells leading to a prolonged survival of mice when targeting the leukemic TCF3-PBX1 fusion in PDX *in vivo* with encapsulated siRNAs. Two years ago, the first RNAi-based drug called

patisiran was approved for treatment of hereditary transthyretin amyloidosis (hATTR), recently, the second RNAi-based drug called givosiran was approved to treat acute hepatic porphyria (AHP) and also permission of further RNAi-based drugs looks promising (Scott, 2020, Setten et al., 2019).

Taken together, targeting MLL/AF4 in t(4;11) leukemia patients might be effective using RNAi-based drugs improving the current therapy.

5.6 Conclusion and Outlook

In this study, different molecular approaches were established to investigate the function of the fusion proteins MLL/AF4 and AF4/MLL. Patient specific shRNAs were designed and validated, allowing targeting the individual fusions and an inducible KD system was improved leading to effective inhibition upon shRNA induction also in PDX cells *in vivo*. As AF4/MLL was difficult to target by shRNAs, a dnTASP1 was used in addition to inhibit the stable fusion protein. The partial inhibition of AF4/MLL in both methods did not reveal an essential function of AF4/MLL in an established leukemia. In contrast, a loss of cells upon MLL/AF4 KD could be shown over time in PDX cells *in vivo*. Thus, I conclude that targeting MLL/AF4 might be a promising therapeutic solution.

The investigation of the AF4/MLL fusion protein is part of a DFG project (MA 1876/13-1) in cooperation with Alexander Wilhelm and Rolf Marschalek. While here the importance of AF4/MLL for leukemia maintenance was investigated, they are studying the role of AF4/MLL for leukemia establishment. The inhibition of AF4/MLL should be improved to finally verify if there is any essential function of the fusion protein on leukemia maintenance. However, first experimental results of Alexander Wilhelm suggest an important role of the fusion protein for leukemia establishment by chromatin activation and requires further investigation (Marschalek, 2019).

As first RNAi-based drugs were approved and an *in vivo* experiment with encapsulated siRNAs targeting a fusion in leukemic PDX cells prolonged the survival of mice, MLL/AF4 might also be a promising target for RNAi based therapy at least in those patients having the same breakpoint.

6. References

Aagaard, L. A., Zhang, J., von Eije, K. J., Li, H., Saetrom, P., Amarzguioui, M. & Rossi, J. J. 2008. Engineering and optimization of the miR-106b cluster for ectopic expression of multiplexed anti-HIV RNAs. *Gene Ther,* 15**,** 1536-49.

Agraz-Doblas, A., Bueno, C., Bashford-Rogers, R., Roy, A., Schneider, P., Bardini, M., Ballerini, P., Cazzaniga, G., Moreno, T., Revilla, C., Gut, M., Valsecchi, M. G., Roberts, I., Pieters, R., De Lorenzo, P., Varela, I., Menendez, P. & Stam, R. W. 2019. Unraveling the cellular origin and clinical prognostic markers of infant B-cell acute lymphoblastic leukemia using genome-wide analysis. *Haematologica,* 104**,** 1176-1188.

Ait-ali, T., Rands, C. & Harberd, N. P. 2003. Flexible control of plant architecture and yield via switchable expression of Arabidopsis gai. *Plant Biotechnol J,* 1**,** 337-43.

Andersson, A. K., Ma, J., Wang, J., Chen, X., Gedman, A. L., Dang, J., Nakitandwe, J., Holmfeldt, L., Parker, M., Easton, J., Huether, R., Kriwacki, R., Rusch, M., Wu, G., Li, Y., Mulder, H., Raimondi, S., Pounds, S., Kang, G., Shi, L., Becksfort, J., Gupta, P., Payne-Turner, D., Vadodaria, B., Boggs, K., Yergeau, D., Manne, J., Song, G., Edmonson, M., Nagahawatte, P., Wei, L., Cheng, C., Pei, D., Sutton, R., Venn, N. C., Chetcuti, A., Rush, A., Catchpoole, D., Heldrup, J., Fioretos, T., Lu, C., Ding, L., Pui, C. H., Shurtleff, S., Mullighan, C. G., Mardis, E. R., Wilson, R. K., Gruber, T. A., Zhang, J. & Downing, J. R. 2015. The landscape of somatic mutations in infant MLL-rearranged acute lymphoblastic leukemias. *Nat Genet,* 47**,** 330-7.

Armstrong, S. A., Staunton, J. E., Silverman, L. B., Pieters, R., den Boer, M. L., Minden, M. D., Sallan, S. E., Lander, E. S., Golub, T. R. & Korsmeyer, S. J. 2002. MLL translocations specify a distinct gene expression profile that distinguishes a unique leukemia. *Nat Genet,* 30**,** 41-7.

Barren, B. & Artemyev, N. O. 2007. Mechanisms of dominant negative G-protein alpha subunits. *J Neurosci Res,* 85**,** 3505-14.

Barrett, A. J., Rawlings, N. D. & O'Brien, E. A. 2001. The MEROPS database as a protease information system. *J Struct Biol,* 134**,** 95-102.

Barrett, D. M., Seif, A. E., Carpenito, C., Teachey, D. T., Fish, J. D., June, C. H., Grupp, S. A. & Reid, G. S. 2011. Noninvasive bioluminescent imaging of primary patient acute lymphoblastic leukemia: a strategy for preclinical modeling. *Blood,* 118**,** e112-7.

Bartel, D. P. 2004. MicroRNAs: genomics, biogenesis, mechanism, and function. *Cell,* 116**,** 281-97.

Benedikt, A., Baltruschat, S., Scholz, B., Bursen, A., Arrey, T. N., Meyer, B., Varagnolo, L., Müller, A. M., Karas, M., Dingermann, T. & Marschalek, R. 2011. The leukemogenic AF4-MLL fusion protein causes P-TEFb kinase activation and altered epigenetic signatures. *Leukemia,* 25**,** 135-44.

Benito, J. M., Godfrey, L., Kojima, K., Hogdal, L., Wunderlich, M., Geng, H., Marzo, I., Harutyunyan, K. G., Golfman, L., North, P., Kerry, J., Ballabio, E., Chonghaile, T. N., Gonzalo, O., Qiu, Y., Jeremias, I., Debose, L., O'Brien, E., Ma, H., Zhou, P., Jacamo, R., Park, E., Coombes, K. R., Zhang, N., Thomas, D. A., O'Brien, S., Kantarjian, H. M., Leverson, J. D., Kornblau, S. M., Andreeff, M., Müschen, M., Zweidler-McKay, P. A., Mulloy, J. C., Letai, A., Milne, T. A. & Konopleva, M. 2015. MLL-Rearranged Acute Lymphoblastic Leukemias Activate BCL-2

through H3K79 Methylation and Are Sensitive to the BCL-2-Specific Antagonist ABT-199. *Cell Rep,* 13**,** 2715-27.

Bennett, J. H. 1845. Case of hypertrophy of the spleen and liver in which death took place from suppuration of the blood. *Edinburgh Medical and Surgical Journal,* 64**,** 413–423.

Bier, C., Knauer, S. K., Klapthor, A., Schweitzer, A., Rekik, A., Krämer, O. H., Marschalek, R. & Stauber, R. H. 2011. Cell-based analysis of structure-function activity of threonine aspartase 1. *J Biol Chem,* 286**,** 3007-17.

Birke, M., Schreiner, S., García-Cuéllar, M. P., Mahr, K., Titgemeyer, F. & Slany, R. K. 2002. The MT domain of the proto-oncoprotein MLL binds to CpG-containing DNA and discriminates against methylation. *Nucleic Acids Res,* 30**,** 958-65.

Bitoun, E., Oliver, P. L. & Davies, K. E. 2007. The mixed-lineage leukemia fusion partner AF4 stimulates RNA polymerase II transcriptional elongation and mediates coordinated chromatin remodeling. *Hum Mol Genet,* 16**,** 92-106.

Bofill-De Ros, X. & Gu, S. 2016. Guidelines for the optimal design of miRNA-based shRNAs. *Methods,* 103**,** 157-66.

Bomken, S., Buechler, L., Rehe, K., Ponthan, F., Elder, A., Blair, H., Bacon, C. M., Vormoor, J. & Heidenreich, O. 2013. Lentiviral marking of patient-derived acute lymphoblastic leukaemic cells allows in vivo tracking of disease progression. *Leukemia,* 27**,** 718-21.

Borkhardt, A., Repp, R., Haupt, E., Brettreich, S., Buchen, U., Gossen, R. & Lampert, F. 1994. Molecular analysis of MLL-1/AF4 recombination in infant acute lymphoblastic leukemia. *Leukemia,* 8**,** 549-53.

Bosma, G. C., Custer, R. P. & Bosma, M. J. 1983. A severe combined immunodeficiency mutation in the mouse. *Nature,* 301**,** 527-30.

Boudreau, R. L., Martins, I. & Davidson, B. L. 2009. Artificial microRNAs as siRNA shuttles: improved safety as compared to shRNAs in vitro and in vivo. *Mol Ther,* 17**,** 169-75.

Bramsen, J. B., Laursen, M. B., Nielsen, A. F., Hansen, T. B., Bus, C., Langkjaer, N., Babu, B. R., Højland, T., Abramov, M., Van Aerschot, A., Odadzic, D., Smicius, R., Haas, J., Andree, C., Barman, J., Wenska, M., Srivastava, P., Zhou, C., Honcharenko, D., Hess, S., Müller, E., Bobkov, G. V., Mikhailov, S. N., Fava, E., Meyer, T. F., Chattopadhyaya, J., Zerial, M., Engels, J. W., Herdewijn, P., Wengel, J. & Kjems, J. 2009. A large-scale chemical modification screen identifies design rules to generate siRNAs with high activity, high stability and low toxicity. *Nucleic Acids Res,* 37**,** 2867-81.

Brenner, H. & Spix, C. 2003. Combining cohort and period methods for retrospective time trend analyses of long-term cancer patient survival rates. *Br J Cancer,* 89**,** 1260-5.

Brummelkamp, T. R., Bernards, R. & Agami, R. 2002. A system for stable expression of short interfering RNAs in mammalian cells. *Science,* 296**,** 550-3.

Bueno, C., Calero-Nieto, F. J., Wang, X., Valdés-Mas, R., Gutiérrez-Agüera, F., Roca-Ho, H., Ayllon, V., Real, P. J., Arambilet, D., Espinosa, L., Torres-Ruiz, R., Agraz-Doblas, A., Varela, I., de Boer, J., Bigas, A., Gottgens, B., Marschalek, R. & Menendez, P. 2019. Enhanced hemato-endothelial specification during human embryonic differentiation through developmental cooperation between AF4-MLL and MLL-AF4 fusions. *Haematologica,* 104**,** 1189-1201.

Bursen, A., Moritz, S., Gaussmann, A., Moritz, S., Dingermann, T. & Marschalek, R. 2004. Interaction of AF4 wild-type and AF4.MLL fusion protein with SIAH proteins: indication for t(4;11) pathobiology? *Oncogene,* 23**,** 6237-49.

Bursen, A., Schwabe, K., Rüster, B., Henschler, R., Ruthardt, M., Dingermann, T. & Marschalek, R. 2010. The AF4.MLL fusion protein is capable of inducing ALL in mice without requirement of MLL.AF4. *Blood,* 115**,** 3570-9.

Carlet, M., Völse, K., Vergalli, J., Becker, M., Herold, T., Arner, A., Senft, D., Jurinovic, V., Liu, W. H., Gao, Y., Dill, V., Fehse, B., Baldus, C. D., Bastian, L., Lenk, L., Schewe, D. M., Bagnoli, J. W., Vick, B., Schmid, J. P., Wilhelm, A., Marschalek, R., Jost, P. J., Miething, C., Riecken, K., Schmidt-Supprian, M., Binder, V. & Jeremias, I. 2021. In vivo inducible reverse genetics in patients' tumors to identify individual therapeutic targets. *Nat Commun,* 12**,** 2020.05.02.073577.

Cassidy, J. W., Caldas, C. & Bruna, A. 2015. Maintaining Tumor Heterogeneity in Patient-Derived Tumor Xenografts. *Cancer Res,* 75**,** 2963-8.

Chen, C. S., Hilden, J. M., Frestedt, J., Domer, P. H., Moore, R., Korsmeyer, S. J. & Kersey, J. H. 1993. The chromosome 4q21 gene (AF-4/FEL) is widely expressed in normal tissues and shows breakpoint diversity in t(4;11)(q21;q23) acute leukemia. *Blood,* 82**,** 1080-5.

Chen, D. Y., Lee, Y., Van Tine, B. A., Searleman, A. C., Westergard, T. D., Liu, H., Tu, H. C., Takeda, S., Dong, Y., Piwnica-Worms, D. R., Oh, K. J., Korsmeyer, S. J., Hermone, A., Gussio, R., Shoemaker, R. H., Cheng, E. H. & Hsieh, J. J. 2012. A pharmacologic inhibitor of the protease Taspase1 effectively inhibits breast and brain tumor growth. *Cancer Res,* 72**,** 736-46.

Chen, D. Y., Liu, H., Takeda, S., Tu, H. C., Sasagawa, S., Van Tine, B. A., Lu, D., Cheng, E. H. & Hsieh, J. J. 2010. Taspase1 functions as a non-oncogene addiction protease that coordinates cancer cell proliferation and apoptosis. *Cancer Res,* 70**,** 5358-67.

Chen, W., Li, Q., Hudson, W. A., Kumar, A., Kirchhof, N. & Kersey, J. H. 2006. A murine Mll-AF4 knock-in model results in lymphoid and myeloid deregulation and hematologic malignancy. *Blood,* 108**,** 669-77.

Chiaretti, S., Zini, G. & Bassan, R. 2014. Diagnosis and subclassification of acute lymphoblastic leukemia. *Mediterr J Hematol Infect Dis,* 6**,** e2014073.

Choi, J. G., Bharaj, P., Abraham, S., Ma, H., Yi, G., Ye, C., Dang, Y., Manjunath, N., Wu, H. & Shankar, P. 2015. Multiplexing seven miRNA-Based shRNAs to suppress HIV replication. *Mol Ther,* 23**,** 310-20.

Chung, J., Zhang, J., Li, H., Ouellet, D. L., DiGiusto, D. L. & Rossi, J. J. 2012. Endogenous MCM7 microRNA cluster as a novel platform to multiplex small interfering and nucleolar RNAs for combinational HIV-1 gene therapy. *Hum Gene Ther,* 23**,** 1200-8.

Coelho, T., Adams, D., Silva, A., Lozeron, P., Hawkins, P. N., Mant, T., Perez, J., Chiesa, J., Warrington, S., Tranter, E., Munisamy, M., Falzone, R., Harrop, J., Cehelsky, J., Bettencourt, B. R., Geissler, M., Butler, J. S., Sehgal, A., Meyers, R. E., Chen, Q., Borland, T., Hutabarat, R. M., Clausen, V. A., Alvarez, R., Fitzgerald, K., Gamba-Vitalo, C., Nochur, S. V., Vaishnaw, A. K., Sah, D. W., Gollob, J. A. & Suhr, O. B. 2013. Safety and efficacy of RNAi therapy for transthyretin amyloidosis. *N Engl J Med,* 369**,** 819-29.

Cullen, B. R. 2004. Transcription and processing of human microRNA precursors. *Mol Cell,* 16**,** 861-5.

Cullen, B. R. 2005. RNAi the natural way. *Nat Genet,* 37**,** 1163-5.

Daley, G., Van Etten, R. & Baltimore, D. 1990. Induction of chronic myelogenous leukemia in mice by the P210bcr/abl gene of the Philadelphia chromosome. *Science,* 247**,** 824-830.

Davis, M. E., Zuckerman, J. E., Choi, C. H., Seligson, D., Tolcher, A., Alabi, C. A., Yen, Y., Heidel, J. D. & Ribas, A. 2010. Evidence of RNAi in humans from

systemically administered siRNA via targeted nanoparticles. *Nature,* 464**,** 1067-70.

DeVincenzo, J., Lambkin-Williams, R., Wilkinson, T., Cehelsky, J., Nochur, S., Walsh, E., Meyers, R., Gollob, J. & Vaishnaw, A. 2010. A randomized, double-blind, placebo-controlled study of an RNAi-based therapy directed against respiratory syncytial virus. *Proc Natl Acad Sci U S A,* 107**,** 8800-5.

Dickins, R. A., Hemann, M. T., Zilfou, J. T., Simpson, D. R., Ibarra, I., Hannon, G. J. & Lowe, S. W. 2005. Probing tumor phenotypes using stable and regulated synthetic microRNA precursors. *Nat Genet,* 37**,** 1289-95.

Divoky, V., Trka, J. M., Watzinger, F. & Lion, T. 2000. Cryptic splice site activation during RNA processing of MLL/AF4 chimeric transcripts in infants with t(4;11) positive ALL. *Gene,* 247**,** 111-8.

Domer, P. H., Fakharzadeh, S. S., Chen, C. S., Jockel, J., Johansen, L., Silverman, G. A., Kersey, J. H. & Korsmeyer, S. J. 1993. Acute mixed-lineage leukemia t(4;11)(q21;q23) generates an MLL-AF4 fusion product. *Proceedings of the National Academy of Sciences,* 90**,** 7884-7888.

Downing, J. R., Head, D. R., Raimondi, S. C., Carroll, A. J., Curcio-Brint, A. M., Motroni, T. A., Hulshof, M. G., Pullen, D. J. & Domer, P. H. 1994. The der(11)-encoded MLL/AF-4 fusion transcript is consistently detected in t(4;11)(q21;q23)-containing acute lymphoblastic leukemia. *Blood,* 83**,** 330-5.

Dull, T., Zufferey, R., Kelly, M., Mandel, R. J., Nguyen, M., Trono, D. & Naldini, L. 1998. A third-generation lentivirus vector with a conditional packaging system. *J Virol,* 72**,** 8463-71.

Ebinger, S., Özdemir, E. Z., Ziegenhain, C., Tiedt, S., Castro Alves, C., Grunert, M., Dworzak, M., Lutz, C., Turati, V. A., Enver, T., Horny, H. P., Sotlar, K., Parekh, S., Spiekermann, K., Hiddemann, W., Schepers, A., Polzer, B., Kirsch, S., Hoffmann, M., Knapp, B., Hasenauer, J., Pfeifer, H., Panzer-Grümayer, R., Enard, W., Gires, O. & Jeremias, I. 2016. Characterization of Rare, Dormant, and Therapy-Resistant Cells in Acute Lymphoblastic Leukemia. *Cancer Cell,* 30**,** 849-862.

Elbashir, S. M., Lendeckel, W. & Tuschl, T. 2001. RNA interference is mediated by 21- and 22-nucleotide RNAs. *Genes Dev,* 15**,** 188-200.

Ernst, P., Fisher, J. K., Avery, W., Wade, S., Foy, D. & Korsmeyer, S. J. 2004. Definitive hematopoiesis requires the mixed-lineage leukemia gene. *Dev Cell,* 6**,** 437-43.

Ernst, P., Wang, J., Huang, M., Goodman, R. H. & Korsmeyer, S. J. 2001. MLL and CREB bind cooperatively to the nuclear coactivator CREB-binding protein. *Mol Cell Biol,* 21**,** 2249-58.

Esparza, S. D. & Sakamoto, K. M. 2005. Topics in pediatric leukemia--acute lymphoblastic leukemia. *MedGenMed,* 7**,** 23.

Fair, K., Anderson, M., Bulanova, E., Mi, H., Tropschug, M. & Diaz, M. O. 2001. Protein Interactions of the MLL PHD Fingers Modulate MLL Target Gene Regulation in Human Cells. *Molecular and Cellular Biology,* 21**,** 3589-3597.

Feil, R., Brocard, J., Mascrez, B., LeMeur, M., Metzger, D. & Chambon, P. 1996. Ligand-activated site-specific recombination in mice. *Proc Natl Acad Sci U S A,* 93**,** 10887-90.

Feil, R., Wagner, J., Metzger, D. & Chambon, P. 1997. Regulation of Cre recombinase activity by mutated estrogen receptor ligand-binding domains. *Biochem Biophys Res Commun,* 237**,** 752-7.

Fellmann, C., Hoffmann, T., Sridhar, V., Hopfgartner, B., Muhar, M., Roth, M., Lai, D. Y., Barbosa, I. A., Kwon, J. S., Guan, Y., Sinha, N. & Zuber, J. 2013. An

optimized microRNA backbone for effective single-copy RNAi. *Cell Rep,* 5**,** 1704-13.

Fellmann, C., Zuber, J., McJunkin, K., Chang, K., Malone, C. D., Dickins, R. A., Xu, Q., Hengartner, M. O., Elledge, S. J., Hannon, G. J. & Lowe, S. W. 2011. Functional identification of optimized RNAi triggers using a massively parallel sensor assay. *Mol Cell,* 41**,** 733-46.

Fire, A., Xu, S., Montgomery, M. K., Kostas, S. A., Driver, S. E. & Mello, C. C. 1998. Potent and specific genetic interference by double-stranded RNA in Caenorhabditis elegans. *Nature,* 391**,** 806-11.

Fitzgerald, K., Frank-Kamenetsky, M., Shulga-Morskaya, S., Liebow, A., Bettencourt, B. R., Sutherland, J. E., Hutabarat, R. M., Clausen, V. A., Karsten, V., Cehelsky, J., Nochur, S. V., Kotelianski, V., Horton, J., Mant, T., Chiesa, J., Ritter, J., Munisamy, M., Vaishnaw, A. K., Gollob, J. A. & Simon, A. 2014. Effect of an RNA interference drug on the synthesis of proprotein convertase subtilisin/kexin type 9 (PCSK9) and the concentration of serum LDL cholesterol in healthy volunteers: a randomised, single-blind, placebo-controlled, phase 1 trial. *Lancet,* 383**,** 60-68.

Flanagan, S. P. 1966. 'Nude', a new hairless gene with pleiotropic effects in the mouse. *Genet Res,* 8**,** 295-309.

Ford, A. M., Ridge, S. A., Cabrera, M. E., Mahmoud, H., Steel, C. M., Chan, L. C. & Greaves, M. 1993. In utero rearrangements in the trithorax-related oncogene in infant leukaemias. *Nature,* 363**,** 358-60.

Frestedt, J. L., Hilden, J. M., Moore, R. O. & Kersey, J. H. 1996. Differential expression of AF4/FEL mRNA in human tissues. *Genet Anal,* 12**,** 147-9.

Gao, G., Guo, X. & Goff, S. P. 2002. Inhibition of retroviral RNA production by ZAP, a CCCH-type zinc finger protein. *Science,* 297**,** 1703-6.

Gatz, C., Frohberg, C. & Wendenburg, R. 1992. Stringent repression and homogeneous de-repression by tetracycline of a modified CaMV 35S promoter in intact transgenic tobacco plants. *Plant J,* 2**,** 397-404.

Gaussmann, A., Wenger, T., Eberle, I., Bursen, A., Bracharz, S., Herr, I., Dingermann, T. & Marschalek, R. 2007. Combined effects of the two reciprocal t(4;11) fusion proteins MLL.AF4 and AF4.MLL confer resistance to apoptosis, cell cycling capacity and growth transformation. *Oncogene,* 26**,** 3352-63.

Gökbuget, N., Stanze, D., Beck, J., Diedrich, H., Horst, H.-A., Hüttmann, A., Kobbe, G., Kreuzer, K.-A., Leimer, L., Reichle, A., Schaich, M., Schwartz, S., Serve, H., Starck, M., Stelljes, M., Stuhlmann, R., Viardot, A., Wendelin, K., Freund, M., Hoelzer, D. & Leukemia, o. b. o. t. G. M. S. G. f. A. A. L. 2012. Outcome of relapsed adult lymphoblastic leukemia depends on response to salvage chemotherapy, prognostic factors, and performance of stem cell transplantation. *Blood,* 120**,** 2032-2041.

Gottlieb, J., Zamora, M. R., Hodges, T., Musk, A. W., Sommerwerk, U., Dilling, D., Arcasoy, S., DeVincenzo, J., Karsten, V., Shah, S., Bettencourt, B. R., Cehelsky, J., Nochur, S., Gollob, J., Vaishnaw, A., Simon, A. R. & Glanville, A. R. 2016. ALN-RSV01 for prevention of bronchiolitis obliterans syndrome after respiratory syncytial virus infection in lung transplant recipients. *J Heart Lung Transplant,* 35**,** 213-21.

Greaves, M. F. & Wiemels, J. 2003. Origins of chromosome translocations in childhood leukaemia. *Nat Rev Cancer,* 3**,** 639-49.

Grimm, D., Streetz, K. L., Jopling, C. L., Storm, T. A., Pandey, K., Davis, C. R., Marion, P., Salazar, F. & Kay, M. A. 2006. Fatality in mice due to oversaturation of cellular microRNA/short hairpin RNA pathways. *Nature,* 441**,** 537-41.

Gu, Y., Nakamura, T., Alder, H., Prasad, R., Canaani, O., Cimino, G., Croce, C. M. & Canaani, E. 1992. The t(4;11) chromosome translocation of human acute leukemias fuses the ALL-1 gene, related to Drosophila trithorax, to the AF-4 gene. *Cell,* 71**,** 701-8.

Guenther, M. G., Lawton, L. N., Rozovskaia, T., Frampton, G. M., Levine, S. S., Volkert, T. L., Croce, C. M., Nakamura, T., Canaani, E. & Young, R. A. 2008. Aberrant chromatin at genes encoding stem cell regulators in human mixed-lineage leukemia. *Genes Dev,* 22**,** 3403-8.

Guo, F., Gopaul, D. N. & van Duyne, G. D. 1997. Structure of Cre recombinase complexed with DNA in a site-specific recombination synapse. *Nature,* 389**,** 40-6.

Guzman, M. L. 2015. CDK6 is a regulator of stem cells "Egr" to wake up. *Blood,* 125**,** 7-9.

Harborth, J., Elbashir, S. M., Vandenburgh, K., Manninga, H., Scaringe, S. A., Weber, K. & Tuschl, T. 2003. Sequence, chemical, and structural variation of small interfering RNAs and short hairpin RNAs and the effect on mammalian gene silencing. *Antisense Nucleic Acid Drug Dev,* 13**,** 83-105.

Harman, J. R., Thorne, R., Jamilly, M., Tapia, M., Crump, N. T., Rice, S., Beveridge, R., Morrissey, E., de Bruijn, M. F. T. R., Roberts, I., Roy, A., Fulga, T. A. & Milne, T. A. 2020. Phenotypic analysis of an MLL-AF4 gene regulatory network reveals indirect CASP9 repression as a mode of inducing apoptosis resistance. *bioRxiv***,** 2020.06.30.179796.

He, W., Bennett, M. J., Luistro, L., Carvajal, D., Nevins, T., Smith, M., Tyagi, G., Cai, J., Wei, X., Lin, T. A., Heimbrook, D. C., Packman, K. & Boylan, J. F. 2014. Discovery of siRNA lipid nanoparticles to transfect suspension leukemia cells and provide in vivo delivery capability. *Mol Ther,* 22**,** 359-370.

Heckl, B. C. 2018. *The molecular function of MLL/AF4 for patient derived acute leukemias growing in mice.* Dissertation, Technische Universität München.

Hess, J. L., Yu, B. D., Li, B., Hanson, R. & Korsmeyer, S. J. 1997. Defects in Yolk Sac Hematopoiesis in Mll-Null Embryos. *Blood,* 90**,** 1799-1806.

Hoess, R. H., Ziese, M. & Sternberg, N. 1982. P1 site-specific recombination: nucleotide sequence of the recombining sites. *Proc Natl Acad Sci U S A,* 79**,** 3398-402.

Hope, K. J., Jin, L. & Dick, J. E. 2004. Acute myeloid leukemia originates from a hierarchy of leukemic stem cell classes that differ in self-renewal capacity. *Nat Immunol,* 5**,** 738-43.

Hsieh, J. J.-D., Ernst, P., Erdjument-Bromage, H., Tempst, P. & Korsmeyer, S. J. 2003a. Proteolytic Cleavage of MLL Generates a Complex of N- and C-Terminal Fragments That Confers Protein Stability and Subnuclear Localization. *Molecular and Cellular Biology,* 23**,** 186-194.

Hsieh, J. J., Cheng, E. H. & Korsmeyer, S. J. 2003b. Taspase1: a threonine aspartase required for cleavage of MLL and proper HOX gene expression. *Cell,* 115**,** 293-303.

Hulton, C. H., Costa, E. A., Shah, N. S., Quintanal-Villalonga, A., Heller, G., de Stanchina, E., Rudin, C. M. & Poirier, J. T. 2020. Direct genome editing of patient-derived xenografts using CRISPR-Cas9 enables rapid in vivo functional genomics. *Nature Cancer,* 1**,** 359-369.

Hutter, G., Nickenig, C., Garritsen, H., Hellenkamp, F., Hoerning, A., Hiddemann, W. & Dreyling, M. 2004. Use of polymorphisms in the noncoding region of the human mitochondrial genome to identify potential contamination of human leukemia-lymphoma cell lines. *Hematol J,* 5**,** 61-8.

Iacobucci, I. & Mullighan, C. G. 2017. Genetic Basis of Acute Lymphoblastic Leukemia. *Journal of Clinical Oncology,* 35**,** 975-983.

Isaacs, A. M., Oliver, P. L., Jones, E. L., Jeans, A., Potter, A., Hovik, B. H., Nolan, P. M., Vizor, L., Glenister, P., Simon, A. K., Gray, I. C., Spurr, N. K., Brown, S. D., Hunter, A. J. & Davies, K. E. 2003. A mutation in Af4 is predicted to cause cerebellar ataxia and cataracts in the robotic mouse. *J Neurosci,* 23**,** 1631-7.

Isnard, P., Coré, N., Naquet, P. & Djabali, M. 2000. Altered lymphoid development in mice deficient for the mAF4 proto-oncogene. *Blood,* 96**,** 705-10.

Isnard, P., Depetris, D., Mattei, M. G., Ferrier, P. & Djabali, M. 1998. cDNA cloning, expression and chromosomal localization of the murine AF-4 gene involved in human leukemia. *Mamm Genome,* 9**,** 1065-8.

Isoyama, K., Eguchi, M., Hibi, S., Kinukawa, N., Ohkawa, H., Kawasaki, H., Kosaka, Y., Oda, T., Oda, M., Okamura, T., Nishimura, S., Hayashi, Y., Mori, T., Imaizumi, M., Mizutani, S., Tsukimoto, I., Kamada, N. & Ishii, E. 2002. Risk-directed treatment of infant acute lymphoblastic leukaemia based on early assessment of MLL gene status: results of the Japan Infant Leukaemia Study (MLL96). *Br J Haematol,* 118**,** 999-1010.

Jones, L., Richmond, J., Evans, K., Carol, H., Jing, D., Kurmasheva, R. T., Billups, C. A., Houghton, P. J., Smith, M. A. & Lock, R. B. 2017. Bioluminescence Imaging Enhances Analysis of Drug Responses in a Patient-Derived Xenograft Model of Pediatric ALL. *Clin Cancer Res,* 23**,** 3744-3755.

Jyotsana, N., Sharma, A., Chaturvedi, A., Scherr, M., Kuchenbauer, F., Sajti, L., Barchanski, A., Lindner, R., Noyan, F., Sühs, K. W., Grote-Koska, D., Brand, K., Vornlocher, H. P., Stanulla, M., Bornhauser, B., Bourquin, J. P., Eder, M., Thol, F., Ganser, A., Humphries, R. K., Ramsay, E., Cullis, P. & Heuser, M. 2018. RNA interference efficiently targets human leukemia driven by a fusion oncogene in vivo. *Leukemia,* 32**,** 224-226.

Kamel-Reid, S., Letarte, M., Sirard, C., Doedens, M., Grunberger, T., Fulop, G., Freedman, M. H., Phillips, R. A. & Dick, J. E. 1989. A model of human acute lymphoblastic leukemia in immune-deficient SCID mice. *Science,* 246**,** 1597-600.

Kang, H., Wilson, C. S., Harvey, R. C., Chen, I. M., Murphy, M. H., Atlas, S. R., Bedrick, E. J., Devidas, M., Carroll, A. J., Robinson, B. W., Stam, R. W., Valsecchi, M. G., Pieters, R., Heerema, N. A., Hilden, J. M., Felix, C. A., Reaman, G. H., Camitta, B., Winick, N., Carroll, W. L., Dreyer, Z. E., Hunger, S. P. & Willman, C. L. 2012. Gene expression profiles predictive of outcome and age in infant acute lymphoblastic leukemia: a Children's Oncology Group study. *Blood,* 119**,** 1872-81.

Kawagoe, H., Humphries, R. K., Blair, A., Sutherland, H. J. & Hogge, D. E. 1999. Expression of HOX genes, HOX cofactors, and MLL in phenotypically and functionally defined subpopulations of leukemic and normal human hematopoietic cells. *Leukemia,* 13**,** 687-98.

Kikutani, H. & Makino, S. 1992. The murine autoimmune diabetes model: NOD and related strains. *Adv Immunol,* 51**,** 285-322.

Kleinman, M. E., Yamada, K., Takeda, A., Chandrasekaran, V., Nozaki, M., Baffi, J. Z., Albuquerque, R. J., Yamasaki, S., Itaya, M., Pan, Y., Appukuttan, B., Gibbs, D., Yang, Z., Karikó, K., Ambati, B. K., Wilgus, T. A., DiPietro, L. A., Sakurai, E., Zhang, K., Smith, J. R., Taylor, E. W. & Ambati, J. 2008. Sequence- and target-independent angiogenesis suppression by siRNA via TLR3. *Nature,* 452**,** 591-7.

Kowarz, E., Burmeister, T., Lo Nigro, L., Jansen, M. W., Delabesse, E., Klingebiel, T., Dingermann, T., Meyer, C. & Marschalek, R. 2007. Complex MLL rearrangements in t(4;11) leukemia patients with absent AF4.MLL fusion allele. *Leukemia,* 21**,** 1232-8.

Krämer, O. H., Stauber, R. H., Bug, G., Hartkamp, J. & Knauer, S. K. 2013. SIAH proteins: critical roles in leukemogenesis. *Leukemia,* 27**,** 792-802.

Krivtsov, A. V., Feng, Z., Lemieux, M. E., Faber, J., Vempati, S., Sinha, A. U., Xia, X., Jesneck, J., Bracken, A. P., Silverman, L. B., Kutok, J. L., Kung, A. L. & Armstrong, S. A. 2008. H3K79 methylation profiles define murine and human MLL-AF4 leukemias. *Cancer Cell,* 14**,** 355-68.

Kühn, A., Löscher, D. & Marschalek, R. 2016. The IRX1/HOXA connection: insights into a novel t(4;11)- specific cancer mechanism. *Oncotarget,* 7**,** 35341-52.

Kumar, A. R., Yao, Q., Li, Q., Sam, T. A. & Kersey, J. H. 2011a. Authors' comments: t(4;11) leukemias display addiction to MLL-AF4 but not to AF4-MLL. *Leuk Res,* 35**,** 697.

Kumar, A. R., Yao, Q., Li, Q., Sam, T. A. & Kersey, J. H. 2011b. t(4;11) leukemias display addiction to MLL-AF4 but not to AF4-MLL. *Leuk Res,* 35**,** 305-9.

Lagos-Quintana, M., Rauhut, R., Lendeckel, W. & Tuschl, T. 2001. Identification of novel genes coding for small expressed RNAs. *Science,* 294**,** 853-8.

Lee, E. M., Bachmann, P. S. & Lock, R. B. 2007. Xenograft models for the preclinical evaluation of new therapies in acute leukemia. *Leuk Lymphoma,* 48**,** 659-68.

Lee, R. C., Feinbaum, R. L. & Ambros, V. 1993. The C. elegans heterochronic gene lin-4 encodes small RNAs with antisense complementarity to lin-14. *Cell,* 75**,** 843-54.

Lee, Y., Ahn, C., Han, J., Choi, H., Kim, J., Yim, J., Lee, J., Provost, P., Rådmark, O., Kim, S. & Kim, V. N. 2003. The nuclear RNase III Drosha initiates microRNA processing. *Nature,* 425**,** 415-9.

Lee, Y., Jeon, K., Lee, J. T., Kim, S. & Kim, V. N. 2002. MicroRNA maturation: stepwise processing and subcellular localization. *Embo j,* 21**,** 4663-70.

Leroy, B., Girard, L., Hollestelle, A., Minna, J. D., Gazdar, A. F. & Soussi, T. 2014. Analysis of TP53 mutation status in human cancer cell lines: a reassessment. *Hum Mutat,* 35**,** 756-65.

Li, L., Lin, X., Khvorova, A., Fesik, S. W. & Shen, Y. 2007. Defining the optimal parameters for hairpin-based knockdown constructs. *Rna,* 13**,** 1765-74.

Liao, Y. & Tang, L. 2016. Inducible RNAi system and its application in novel therapeutics. *Crit Rev Biotechnol,* 36**,** 630-8.

Libura, J., Slater, D. J., Felix, C. A. & Richardson, C. 2005. Therapy-related acute myeloid leukemia-like MLL rearrangements are induced by etoposide in primary human CD34+ cells and remain stable after clonal expansion. *Blood,* 105**,** 2124-31.

Liem, N. L., Papa, R. A., Milross, C. G., Schmid, M. A., Tajbakhsh, M., Choi, S., Ramirez, C. D., Rice, A. M., Haber, M., Norris, M. D., MacKenzie, K. L. & Lock, R. B. 2004. Characterization of childhood acute lymphoblastic leukemia xenograft models for the preclinical evaluation of new therapies. *Blood,* 103**,** 3905-14.

Lin, C., Smith, E. R., Takahashi, H., Lai, K. C., Martin-Brown, S., Florens, L., Washburn, M. P., Conaway, J. W., Conaway, R. C. & Shilatifard, A. 2010. AFF4, a component of the ELL/P-TEFb elongation complex and a shared subunit of MLL chimeras, can link transcription elongation to leukemia. *Mol Cell,* 37**,** 429-37.

Lin, S., Luo, R. T., Ptasinska, A., Kerry, J., Assi, S. A., Wunderlich, M., Imamura, T., Kaberlein, J. J., Rayes, A., Althoff, M. J., Anastasi, J., O'Brien, M. M., Meetei, A. R., Milne, T. A., Bonifer, C., Mulloy, J. C. & Thirman, M. J. 2016. Instructive Role of MLL-Fusion Proteins Revealed by a Model of t(4;11) Pro-B Acute Lymphoblastic Leukemia. *Cancer Cell,* 30**,** 737-749.

Liu, W. H., Mrozek-Gorska, P., Wirth, A. K., Herold, T., Schwarzkopf, L., Pich, D., Völse, K., Melo-Narváez, M. C., Carlet, M., Hammerschmidt, W. & Jeremias, I. 2020. Inducible transgene expression in PDX models in vivo identifies KLF4 as a therapeutic target for B-ALL. *Biomark Res,* 8**,** 46.

Liu, Y. P., Haasnoot, J., ter Brake, O., Berkhout, B. & Konstantinova, P. 2008. Inhibition of HIV-1 by multiple siRNAs expressed from a single microRNA polycistron. *Nucleic Acids Res,* 36**,** 2811-24.

Lund, E., Güttinger, S., Calado, A., Dahlberg, J. E. & Kutay, U. 2004. Nuclear export of microRNA precursors. *Science,* 303**,** 95-8.

Ma, Q., Alder, H., Nelson, K. K., Chatterjee, D., Gu, Y., Nakamura, T., Canaani, E., Croce, C. M., Siracusa, L. D. & Buchberg, A. M. 1993. Analysis of the murine All-1 gene reveals conserved domains with human ALL-1 and identifies a motif shared with DNA methyltransferases. *Proc Natl Acad Sci U S A,* 90**,** 6350-4.

Makino, S., Kunimoto, K., Muraoka, Y., Mizushima, Y., Katagiri, K. & Tochino, Y. 1980. Breeding of a non-obese, diabetic strain of mice. *Jikken Dobutsu,* 29**,** 1-13.

Marschalek, R. 2011. It takes two-to-leukemia: about addictions and requirements. *Leuk Res,* 35**,** 424-5.

Marschalek, R. 2019. Another piece of the puzzle added to understand t(4;11) leukemia better. *Haematologica,* 104**,** 1098-1100.

Marschalek, R., Greil, J., Löchner, K., Nilson, I., Siegler, G., Zweckbronner, I., Beck, J. D. & Fey, G. H. 1995. Molecular analysis of the chromosomal breakpoint and fusion transcripts in the acute lymphoblastic SEM cell line with chromosomal translocation t(4;11). *Br J Haematol,* 90**,** 308-20.

Marschalek, R., Nilson, I., Löchner, K., Greim, R., Siegler, G., Greil, J., Beck, J. D. & Fey, G. H. 1997. The structure of the human ALL-1/MLL/HRX gene. *Leuk Lymphoma,* 27**,** 417-28.

Martinez, J., Patkaniowska, A., Urlaub, H., Lührmann, R. & Tuschl, T. 2002. Single-stranded antisense siRNAs guide target RNA cleavage in RNAi. *Cell,* 110**,** 563-74.

Mattioni, T., Louvion, J. F. & Picard, D. 1994. Regulation of protein activities by fusion to steroid binding domains. *Methods Cell Biol,* 43 Pt A**,** 335-52.

Mbangkollo, D., Burnett, R., McCabe, N., Thirman, M., Gill, H., Yu, H., Rowley, J. D. & Diaz, M. O. 1995. The human MLL gene: nucleotide sequence, homology to the Drosophila trx zinc-finger domain, and alternative splicing. *DNA Cell Biol,* 14**,** 475-83.

McDermott, S. P., Eppert, K., Lechman, E. R., Doedens, M. & Dick, J. E. 2010. Comparison of human cord blood engraftment between immunocompromised mouse strains. *Blood,* 116**,** 193-200.

Mett, V. L., Lochhead, L. P. & Reynolds, P. H. 1993. Copper-controllable gene expression system for whole plants. *Proc Natl Acad Sci U S A,* 90**,** 4567-71.

Metzger, D., Clifford, J., Chiba, H. & Chambon, P. 1995. Conditional site-specific recombination in mammalian cells using a ligand-dependent chimeric Cre recombinase. *Proc Natl Acad Sci U S A,* 92**,** 6991-5.

Meyer, C., Burmeister, T., Gröger, D., Tsaur, G., Fechina, L., Renneville, A., Sutton, R., Venn, N. C., Emerenciano, M., Pombo-de-Oliveira, M. S., Barbieri Blunck, C., Almeida Lopes, B., Zuna, J., Trka, J., Ballerini, P., Lapillonne, H., De

Braekeleer, M., Cazzaniga, G., Corral Abascal, L., van der Velden, V. H. J., Delabesse, E., Park, T. S., Oh, S. H., Silva, M. L. M., Lund-Aho, T., Juvonen, V., Moore, A. S., Heidenreich, O., Vormoor, J., Zerkalenkova, E., Olshanskaya, Y., Bueno, C., Menendez, P., Teigler-Schlegel, A., Zur Stadt, U., Lentes, J., Göhring, G., Kustanovich, A., Aleinikova, O., Schäfer, B. W., Kubetzko, S., Madsen, H. O., Gruhn, B., Duarte, X., Gameiro, P., Lippert, E., Bidet, A., Cayuela, J. M., Clappier, E., Alonso, C. N., Zwaan, C. M., van den Heuvel-Eibrink, M. M., Izraeli, S., Trakhtenbrot, L., Archer, P., Hancock, J., Möricke, A., Alten, J., Schrappe, M., Stanulla, M., Strehl, S., Attarbaschi, A., Dworzak, M., Haas, O. A., Panzer-Grümayer, R., Sedék, L., Szczepański, T., Caye, A., Suarez, L., Cavé, H. & Marschalek, R. 2018. The MLL recombinome of acute leukemias in 2017. *Leukemia,* 32**,** 273-284.

Meyer, C., Hofmann, J., Burmeister, T., Gröger, D., Park, T. S., Emerenciano, M., Pombo de Oliveira, M., Renneville, A., Villarese, P., Macintyre, E., Cavé, H., Clappier, E., Mass-Malo, K., Zuna, J., Trka, J., De Braekeleer, E., De Braekeleer, M., Oh, S. H., Tsaur, G., Fechina, L., van der Velden, V. H., van Dongen, J. J., Delabesse, E., Binato, R., Silva, M. L., Kustanovich, A., Aleinikova, O., Harris, M. H., Lund-Aho, T., Juvonen, V., Heidenreich, O., Vormoor, J., Choi, W. W., Jarosova, M., Kolenova, A., Bueno, C., Menendez, P., Wehner, S., Eckert, C., Talmant, P., Tondeur, S., Lippert, E., Launay, E., Henry, C., Ballerini, P., Lapillone, H., Callanan, M. B., Cayuela, J. M., Herbaux, C., Cazzaniga, G., Kakadiya, P. M., Bohlander, S., Ahlmann, M., Choi, J. R., Gameiro, P., Lee, D. S., Krauter, J., Cornillet-Lefebvre, P., Te Kronnie, G., Schäfer, B. W., Kubetzko, S., Alonso, C. N., zur Stadt, U., Sutton, R., Venn, N. C., Izraeli, S., Trakhtenbrot, L., Madsen, H. O., Archer, P., Hancock, J., Cerveira, N., Teixeira, M. R., Lo Nigro, L., Möricke, A., Stanulla, M., Schrappe, M., Sedék, L., Szczepański, T., Zwaan, C. M., Coenen, E. A., van den Heuvel-Eibrink, M. M., Strehl, S., Dworzak, M., Panzer-Grümayer, R., Dingermann, T., Klingebiel, T. & Marschalek, R. 2013. The MLL recombinome of acute leukemias in 2013. *Leukemia,* 27**,** 2165-76.

Meyer, C., Kowarz, E., Schneider, B., Oehm, C., Klingebiel, T., Dingermann, T. & Marschalek, R. 2006. Genomic DNA of leukemic patients: target for clinical diagnosis of MLL rearrangements. *Biotechnol J,* 1**,** 656-63.

Milne, T. A. 2017. Mouse models of MLL leukemia: recapitulating the human disease. *Blood,* 129**,** 2217-2223.

Milne, T. A., Briggs, S. D., Brock, H. W., Martin, M. E., Gibbs, D., Allis, C. D. & Hess, J. L. 2002. MLL targets SET domain methyltransferase activity to Hox gene promoters. *Mol Cell,* 10**,** 1107-17.

Mullighan, C. G., Goorha, S., Radtke, I., Miller, C. B., Coustan-Smith, E., Dalton, J. D., Girtman, K., Mathew, S., Ma, J., Pounds, S. B., Su, X., Pui, C. H., Relling, M. V., Evans, W. E., Shurtleff, S. A. & Downing, J. R. 2007. Genome-wide analysis of genetic alterations in acute lymphoblastic leukaemia. *Nature,* 446**,** 758-64.

Nakamura, T., Mori, T., Tada, S., Krajewski, W., Rozovskaia, T., Wassell, R., Dubois, G., Mazo, A., Croce, C. M. & Canaani, E. 2002. ALL-1 is a histone methyltransferase that assembles a supercomplex of proteins involved in transcriptional regulation. *Mol Cell,* 10**,** 1119-28.

Nilson, I., Löchner, K., Siegler, G., Greil, J., Beck, J. D., Fey, G. H. & Marschalek, R. 1996. Exon/intron structure of the human ALL-1 (MLL) gene involved in translocations to chromosomal region 11q23 and acute leukaemias. *Br J Haematol,* 93**,** 966-72.

Nilson, I., Reichel, M., Ennas, M. G., Greim, R., Knörr, C., Siegler, G., Greil, J., Fey, G. H. & Marschalek, R. 1997. Exon/intron structure of the human AF-4 gene, a member of the AF-4/LAF-4/FMR-2 gene family coding for a nuclear protein with structural alterations in acute leukaemia. *Br J Haematol,* 98**,** 157-69.

Nold-Petry, C. A., Lo, C. Y., Rudloff, I., Elgass, K. D., Li, S., Gantier, M. P., Lotz-Havla, A. S., Gersting, S. W., Cho, S. X., Lao, J. C., Ellisdon, A. M., Rotter, B., Azam, T., Mangan, N. E., Rossello, F. J., Whisstock, J. C., Bufler, P., Garlanda, C., Mantovani, A., Dinarello, C. A. & Nold, M. F. 2015. IL-37 requires the receptors IL-18Rα and IL-1R8 (SIGIRR) to carry out its multifaceted anti-inflammatory program upon innate signal transduction. *Nat Immunol,* 16**,** 354-65.

Notarangelo, L. D., Giliani, S., Mazza, C., Mella, P., Savoldi, G., Rodriguez-Pérez, C., Mazzolari, E., Fiorini, M., Duse, M., Plebani, A., Ugazio, A. G., Vihinen, M., Candotti, F. & Schumacher, R. F. 2000. Of genes and phenotypes: the immunological and molecular spectrum of combined immune deficiency. Defects of the gamma(c)-JAK3 signaling pathway as a model. *Immunol Rev,* 178**,** 39-48.

Oberdoerffer, P., Otipoby, K. L., Maruyama, M. & Rajewsky, K. 2003. Unidirectional Cre-mediated genetic inversion in mice using the mutant loxP pair lox66/lox71. *Nucleic Acids Res,* 31**,** e140.

Ohler, U., Yekta, S., Lim, L. P., Bartel, D. P. & Burge, C. B. 2004. Patterns of flanking sequence conservation and a characteristic upstream motif for microRNA gene identification. *Rna,* 10**,** 1309-22.

Ono, R., Nosaka, T. & Hayashi, Y. 2005. Roles of a trithorax group gene, MLL, in hematopoiesis. *Int J Hematol,* 81**,** 288-93.

Ordóñez, G. R., Puente, X. S., Quesada, V. & López-Otín, C. 2009. Proteolytic systems: constructing degradomes. *Methods Mol Biol,* 539**,** 33-47.

Orlovsky, K., Kalinkovich, A., Rozovskaia, T., Shezen, E., Itkin, T., Alder, H., Ozer, H. G., Carramusa, L., Avigdor, A., Volinia, S., Buchberg, A., Mazo, A., Kollet, O., Largman, C., Croce, C. M., Nakamura, T., Lapidot, T. & Canaani, E. 2011. Down-regulation of homeobox genes MEIS1 and HOXA in MLL-rearranged acute leukemia impairs engraftment and reduces proliferation. *Proc Natl Acad Sci U S A,* 108**,** 7956-61.

Ottersbach, K., Sanjuan-Pla, A., Torres-Ruíz, R., Bueno, C., Velasco-Hernández, T. & Menendez, P. 2018. The "Never-Ending" Mouse Models for MLL-Rearranged Acute Leukemia Are Still Teaching Us. *Hemasphere,* 2**,** e57.

Paddison, P. J., Caudy, A. A., Bernstein, E., Hannon, G. J. & Conklin, D. S. 2002. Short hairpin RNAs (shRNAs) induce sequence-specific silencing in mammalian cells. *Genes Dev,* 16**,** 948-58.

Patel, B., Dey, A., Castleton, A. Z., Schwab, C., Samuel, E., Sivakumaran, J., Beaton, B., Zareian, N., Zhang, C. Y., Rai, L., Enver, T., Moorman, A. V. & Fielding, A. K. 2014. Mouse xenograft modeling of human adult acute lymphoblastic leukemia provides mechanistic insights into adult LIC biology. *Blood,* 124**,** 96-105.

Paulsson, K., Lilljebjörn, H., Biloglav, A., Olsson, L., Rissler, M., Castor, A., Barbany, G., Fogelstrand, L., Nordgren, A., Sjögren, H., Fioretos, T. & Johansson, B. 2015. The genomic landscape of high hyperdiploid childhood acute lymphoblastic leukemia. *Nat Genet,* 47**,** 672-6.

Pelossof, R., Fairchild, L., Huang, C. H., Widmer, C., Sreedharan, V. T., Sinha, N., Lai, D. Y., Guan, Y., Premsrirut, P. K., Tschaharganeh, D. F., Hoffmann, T., Thapar, V., Xiang, Q., Garippa, R. J., Rätsch, G., Zuber, J., Lowe, S. W., Leslie, C. S. &

Fellmann, C. 2017. Prediction of potent shRNAs with a sequential classification algorithm. *Nat Biotechnol,* 35**,** 350-353.

Pieters, R., Schrappe, M., De Lorenzo, P., Hann, I., De Rossi, G., Felice, M., Hovi, L., LeBlanc, T., Szczepanski, T., Ferster, A., Janka, G., Rubnitz, J., Silverman, L., Stary, J., Campbell, M., Li, C. K., Mann, G., Suppiah, R., Biondi, A., Vora, A. & Valsecchi, M. G. 2007. A treatment protocol for infants younger than 1 year with acute lymphoblastic leukaemia (Interfant-99): an observational study and a multicentre randomised trial. *Lancet,* 370**,** 240-250.

Piller, G. 2001. Leukaemia - a brief historical review from ancient times to 1950. *Br J Haematol,* 112**,** 282-92.

Prasad, R., Yano, T., Sorio, C., Nakamura, T., Rallapalli, R., Gu, Y., Leshkowitz, D., Croce, C. M. & Canaani, E. 1995. Domains with transcriptional regulatory activity within the ALL1 and AF4 proteins involved in acute leukemia. *Proceedings of the National Academy of Sciences,* 92**,** 12160-12164.

Prelich, G. 2012. Gene overexpression: uses, mechanisms, and interpretation. *Genetics,* 190**,** 841-54.

Prieto, C., Marschalek, R., Kühn, A., Bursen, A., Bueno, C. & Menéndez, P. 2017. The AF4-MLL fusion transiently augments multilineage hematopoietic engraftment but is not sufficient to initiate leukemia in cord blood CD34(+) cells. *Oncotarget,* 8**,** 81936-81941.

Pui, C. H., Gaynon, P. S., Boyett, J. M., Chessells, J. M., Baruchel, A., Kamps, W., Silverman, L. B., Biondi, A., Harms, D. O., Vilmer, E., Schrappe, M. & Camitta, B. 2002. Outcome of treatment in childhood acute lymphoblastic leukaemia with rearrangements of the 11q23 chromosomal region. *Lancet,* 359**,** 1909-15.

Pulte, D., Gondos, A. & Brenner, H. 2008. Trends in 5- and 10-year survival after diagnosis with childhood hematologic malignancies in the United States, 1990-2004. *J Natl Cancer Inst,* 100**,** 1301-9.

Rabinovich, B. A., Ye, Y., Etto, T., Chen, J. Q., Levitsky, H. I., Overwijk, W. W., Cooper, L. J., Gelovani, J. & Hwu, P. 2008. Visualizing fewer than 10 mouse T cells with an enhanced firefly luciferase in immunocompetent mouse models of cancer. *Proc Natl Acad Sci U S A,* 105**,** 14342-6.

Reichel, M., Gillert, E., Angermüller, S., Hensel, J. P., Heidel, F., Lode, M., Leis, T., Biondi, A., Haas, O. A., Strehl, S., Panzer-Grümayer, E. R., Griesinger, F., Beck, J. D., Greil, J., Fey, G. H., Uckun, F. M. & Marschalek, R. 2001. Biased distribution of chromosomal breakpoints involving the MLL gene in infants versus children and adults with t(4;11) ALL. *Oncogene,* 20**,** 2900-7.

Richardson, C. & Jasin, M. 2000. Frequent chromosomal translocations induced by DNA double-strand breaks. *Nature,* 405**,** 697-700.

Robbins, M., Judge, A., Liang, L., McClintock, K., Yaworski, E. & MacLachlan, I. 2007. 2'-O-methyl-modified RNAs act as TLR7 antagonists. *Mol Ther,* 15**,** 1663-9.

Rössler, T. & Marschalek, R. 2013. An alternative splice process renders the MLL protein either into a transcriptional activator or repressor. *Pharmazie,* 68**,** 601-7.

Rozovskaia, T., Feinstein, E., Mor, O., Foa, R., Blechman, J., Nakamura, T., Croce, C. M., Cimino, G. & Canaani, E. 2001. Upregulation of Meis1 and HoxA9 in acute lymphocytic leukemias with the t(4 : 11) abnormality. *Oncogene,* 20**,** 874-8.

Rozovskaia, T., Rozenblatt-Rosen, O., Sedkov, Y., Burakov, D., Yano, T., Nakamura, T., Petruck, S., Ben-Simchon, L., Croce, C. M., Mazo, A. & Canaani, E. 2000. Self-association of the SET domains of human ALL-1 and of Drosophila TRITHORAX and ASH1 proteins. *Oncogene,* 19**,** 351-7.

Sabiani, S., Geppert, T., Engelbrecht, C., Kowarz, E., Schneider, G. & Marschalek, R. 2015. Unraveling the Activation Mechanism of Taspase1 which Controls the Oncogenic AF4-MLL Fusion Protein. *EBioMedicine,* 2**,** 386-95.

Scott, L. J. 2020. Givosiran: First Approval. *Drugs,* 80**,** 335-339.

Secker, K. A., Keppeler, H., Duerr-Stoerzer, S., Schmid, H., Schneidawind, D., Hentrich, T., Schulze-Hentrich, J. M., Mankel, B., Fend, F. & Schneidawind, C. 2019. Inhibition of DOT1L and PRMT5 promote synergistic anti-tumor activity in a human MLL leukemia model induced by CRISPR/Cas9. *Oncogene,* 38**,** 7181-7195.

Setten, R. L., Rossi, J. J. & Han, S. P. 2019. The current state and future directions of RNAi-based therapeutics. *Nat Rev Drug Discov,* 18**,** 421-446.

Sheppard, D. 1994. Dominant negative mutants: tools for the study of protein function in vitro and in vivo. *Am J Respir Cell Mol Biol,* 11**,** 1-6.

Shultz, L. D., Lyons, B. L., Burzenski, L. M., Gott, B., Chen, X., Chaleff, S., Kotb, M., Gillies, S. D., King, M., Mangada, J., Greiner, D. L. & Handgretinger, R. 2005. Human lymphoid and myeloid cell development in NOD/LtSz-scid IL2R gamma null mice engrafted with mobilized human hemopoietic stem cells. *J Immunol,* 174**,** 6477-89.

Shultz, L. D., Schweitzer, P. A., Christianson, S. W., Gott, B., Schweitzer, I. B., Tennent, B., McKenna, S., Mobraaten, L., Rajan, T. V., Greiner, D. L. & et al. 1995. Multiple defects in innate and adaptive immunologic function in NOD/LtSz-scid mice. *J Immunol,* 154**,** 180-91.

Siegel, R. L., Miller, K. D. & Jemal, A. 2020. Cancer statistics, 2020. *CA: A Cancer Journal for Clinicians,* 70**,** 7-30.

Silva, J. M., Li, M. Z., Chang, K., Ge, W., Golding, M. C., Rickles, R. J., Siolas, D., Hu, G., Paddison, P. J., Schlabach, M. R., Sheth, N., Bradshaw, J., Burchard, J., Kulkarni, A., Cavet, G., Sachidanandam, R., McCombie, W. R., Cleary, M. A., Elledge, S. J. & Hannon, G. J. 2005. Second-generation shRNA libraries covering the mouse and human genomes. *Nat Genet,* 37**,** 1281-8.

Stam, R. W., Schneider, P., Hagelstein, J. A., van der Linden, M. H., Stumpel, D. J., de Menezes, R. X., de Lorenzo, P., Valsecchi, M. G. & Pieters, R. 2010. Gene expression profiling-based dissection of MLL translocated and MLL germline acute lymphoblastic leukemia in infants. *Blood,* 115**,** 2835-44.

Stern, P., Astrof, S., Erkeland, S. J., Schustak, J., Sharp, P. A. & Hynes, R. O. 2008. A system for Cre-regulated RNA interference in vivo. *Proc Natl Acad Sci U S A,* 105**,** 13895-900.

Sun, D., Melegari, M., Sridhar, S., Rogler, C. E. & Zhu, L. 2006. Multi-miRNA hairpin method that improves gene knockdown efficiency and provides linked multi-gene knockdown. *Biotechniques,* 41**,** 59-63.

Takeda, S., Chen, D. Y., Westergard, T. D., Fisher, J. K., Rubens, J. A., Sasagawa, S., Kan, J. T., Korsmeyer, S. J., Cheng, E. H. & Hsieh, J. J. 2006. Proteolysis of MLL family proteins is essential for taspase1-orchestrated cell cycle progression. *Genes Dev,* 20**,** 2397-409.

Taub, J. W., Konrad, M. A., Ge, Y., Naber, J. M., Scott, J. S., Matherly, L. H. & Ravindranath, Y. 2002. High frequency of leukemic clones in newborn screening blood samples of children with B-precursor acute lymphoblastic leukemia. *Blood,* 99**,** 2992-6.

Tentler, J. J., Tan, A. C., Weekes, C. D., Jimeno, A., Leong, S., Pitts, T. M., Arcaroli, J. J., Messersmith, W. A. & Eckhardt, S. G. 2012. Patient-derived tumour xenografts as models for oncology drug development. *Nat Rev Clin Oncol,* 9**,** 338-50.

Terziyska, N., Castro Alves, C., Groiss, V., Schneider, K., Farkasova, K., Ogris, M., Wagner, E., Ehrhardt, H., Brentjens, R. J., zur Stadt, U., Horstmann, M., Quintanilla-Martinez, L. & Jeremias, I. 2012. In vivo imaging enables high resolution preclinical trials on patients' leukemia cells growing in mice. *PLoS One,* 7**,** e52798.

Thomas, M., Gessner, A., Vornlocher, H. P., Hadwiger, P., Greil, J. & Heidenreich, O. 2005. Targeting MLL-AF4 with short interfering RNAs inhibits clonogenicity and engraftment of t(4;11)-positive human leukemic cells. *Blood,* 106**,** 3559-66.

Tkachuk, D. C., Kohler, S. & Cleary, M. L. 1992. Involvement of a homolog of Drosophila trithorax by 11q23 chromosomal translocations in acute leukemias. *Cell,* 71**,** 691-700.

Townsend, E. C., Murakami, M. A., Christodoulou, A., Christie, A. L., Köster, J., DeSouza, T. A., Morgan, E. A., Kallgren, S. P., Liu, H., Wu, S. C., Plana, O., Montero, J., Stevenson, K. E., Rao, P., Vadhi, R., Andreeff, M., Armand, P., Ballen, K. K., Barzaghi-Rinaudo, P., Cahill, S., Clark, R. A., Cooke, V. G., Davids, M. S., DeAngelo, D. J., Dorfman, D. M., Eaton, H., Ebert, B. L., Etchin, J., Firestone, B., Fisher, D. C., Freedman, A. S., Galinsky, I. A., Gao, H., Garcia, J. S., Garnache-Ottou, F., Graubert, T. A., Gutierrez, A., Halilovic, E., Harris, M. H., Herbert, Z. T., Horwitz, S. M., Inghirami, G., Intlekofer, A. M., Ito, M., Izraeli, S., Jacobsen, E. D., Jacobson, C. A., Jeay, S., Jeremias, I., Kelliher, M. A., Koch, R., Konopleva, M., Kopp, N., Kornblau, S. M., Kung, A. L., Kupper, T. S., LeBoeuf, N. R., LaCasce, A. S., Lees, E., Li, L. S., Look, A. T., Murakami, M., Muschen, M., Neuberg, D., Ng, S. Y., Odejide, O. O., Orkin, S. H., Paquette, R. R., Place, A. E., Roderick, J. E., Ryan, J. A., Sallan, S. E., Shoji, B., Silverman, L. B., Soiffer, R. J., Steensma, D. P., Stegmaier, K., Stone, R. M., Tamburini, J., Thorner, A. R., van Hummelen, P., Wadleigh, M., Wiesmann, M., Weng, A. P., Wuerthner, J. U., Williams, D. A., Wollison, B. M., Lane, A. A., Letai, A., Bertagnolli, M. M., Ritz, J., Brown, M., Long, H., Aster, J. C., Shipp, M. A., Griffin, J. D. & Weinstock, D. M. 2016. The Public Repository of Xenografts Enables Discovery and Randomized Phase II-like Trials in Mice. *Cancer Cell,* 30**,** 183.

Trentin, L., Giordan, M., Dingermann, T., Basso, G., Te Kronnie, G. & Marschalek, R. 2009. Two independent gene signatures in pediatric t(4;11) acute lymphoblastic leukemia patients. *Eur J Haematol,* 83**,** 406-19.

Vick, B., Rothenberg, M., Sandhöfer, N., Carlet, M., Finkenzeller, C., Krupka, C., Grunert, M., Trumpp, A., Corbacioglu, S., Ebinger, M., André, M. C., Hiddemann, W., Schneider, S., Subklewe, M., Metzeler, K. H., Spiekermann, K. & Jeremias, I. 2015. An advanced preclinical mouse model for acute myeloid leukemia using patients' cells of various genetic subgroups and in vivo bioluminescence imaging. *PLoS One,* 10**,** e0120925.

Voellmy, R. 2005. Dominant-positive and dominant-negative heat shock factors. *Methods,* 35**,** 199-207.

Wightman, B., Ha, I. & Ruvkun, G. 1993. Posttranscriptional regulation of the heterochronic gene lin-14 by lin-4 mediates temporal pattern formation in C. elegans. *Cell,* 75**,** 855-62.

Wilkinson, A. C., Ballabio, E., Geng, H., North, P., Tapia, M., Kerry, J., Biswas, D., Roeder, R. G., Allis, C. D., Melnick, A., de Bruijn, M. F. & Milne, T. A. 2013. RUNX1 is a key target in t(4;11) leukemias that contributes to gene activation through an AF4-MLL complex interaction. *Cell Rep,* 3**,** 116-27.

Wiznerowicz, M. & Trono, D. 2003. Conditional suppression of cellular genes: lentivirus vector-mediated drug-inducible RNA interference. *J Virol,* 77**,** 8957-61.

Woiterski, J., Ebinger, M., Witte, K. E., Goecke, B., Heininger, V., Philippek, M., Bonin, M., Schrauder, A., Röttgers, S., Herr, W., Lang, P., Handgretinger, R., Hartwig, U. F. & André, M. C. 2013. Engraftment of low numbers of pediatric acute lymphoid and myeloid leukemias into NOD/SCID/IL2Rcγnull mice reflects individual leukemogenecity and highly correlates with clinical outcome. *Int J Cancer,* 133**,** 1547-56.

Xia, Z. B., Anderson, M., Diaz, M. O. & Zeleznik-Le, N. J. 2003. MLL repression domain interacts with histone deacetylases, the polycomb group proteins HPC2 and BMI-1, and the corepressor C-terminal-binding protein. *Proc Natl Acad Sci U S A,* 100**,** 8342-7.

Yagi, H., Deguchi, K., Aono, A., Tani, Y., Kishimoto, T. & Komori, T. 1998. Growth Disturbance in Fetal Liver Hematopoiesis of Mll-Mutant Mice. *Blood,* 92**,** 108-117.

Yang, Y., Hong, H., Zhang, Y. & Cai, W. 2009. Molecular Imaging of Proteases in Cancer. *Cancer Growth Metastasis,* 2**,** 13-27.

Yeoh, E. J., Ross, M. E., Shurtleff, S. A., Williams, W. K., Patel, D., Mahfouz, R., Behm, F. G., Raimondi, S. C., Relling, M. V., Patel, A., Cheng, C., Campana, D., Wilkins, D., Zhou, X., Li, J., Liu, H., Pui, C. H., Evans, W. E., Naeve, C., Wong, L. & Downing, J. R. 2002. Classification, subtype discovery, and prediction of outcome in pediatric acute lymphoblastic leukemia by gene expression profiling. *Cancer Cell,* 1**,** 133-43.

Yi, R., Qin, Y., Macara, I. G. & Cullen, B. R. 2003. Exportin-5 mediates the nuclear export of pre-microRNAs and short hairpin RNAs. *Genes Dev,* 17**,** 3011-6.

Yokoyama, A., Wang, Z., Wysocka, J., Sanyal, M., Aufiero, D. J., Kitabayashi, I., Herr, W. & Cleary, M. L. 2004. Leukemia proto-oncoprotein MLL forms a SET1-like histone methyltransferase complex with menin to regulate Hox gene expression. *Mol Cell Biol,* 24**,** 5639-49.

Yuan, T. L., Fellmann, C., Lee, C. S., Ritchie, C. D., Thapar, V., Lee, L. C., Hsu, D. J., Grace, D., Carver, J. O., Zuber, J., Luo, J., McCormick, F. & Lowe, S. W. 2014. Development of siRNA payloads to target KRAS-mutant cancer. *Cancer Discov,* 4**,** 1182-1197.

Yuan, Y., Zhou, L., Miyamoto, T., Iwasaki, H., Harakawa, N., Hetherington, C. J., Burel, S. A., Lagasse, E., Weissman, I. L., Akashi, K. & Zhang, D.-E. 2001. AML1-ETO expression is directly involved in the development of acute myeloid leukemia in the presence of additional mutations. *Proceedings of the National Academy of Sciences,* 98**,** 10398-10403.

Zeleznik-Le, N. J., Harden, A. M. & Rowley, J. D. 1994. 11q23 translocations split the "AT-hook" cruciform DNA-binding region and the transcriptional repression domain from the activation domain of the mixed-lineage leukemia (MLL) gene. *Proceedings of the National Academy of Sciences,* 91**,** 10610-10614.

Zeng, Y. & Cullen, B. R. 2005. Efficient processing of primary microRNA hairpins by Drosha requires flanking nonstructured RNA sequences. *J Biol Chem,* 280**,** 27595-603.

Zeng, Y., Wagner, E. J. & Cullen, B. R. 2002. Both natural and designed micro RNAs can inhibit the expression of cognate mRNAs when expressed in human cells. *Mol Cell,* 9**,** 1327-33.

Zhang, Y., Riesterer, C., Ayrall, A. M., Sablitzky, F., Littlewood, T. D. & Reth, M. 1996. Inducible site-directed recombination in mouse embryonic stem cells. *Nucleic Acids Res,* 24**,** 543-8.

Zhou, H., Spicuglia, S., Hsieh, J. J., Mitsiou, D. J., Høiby, T., Veenstra, G. J., Korsmeyer, S. J. & Stunnenberg, H. G. 2006. Uncleaved TFIIA is a substrate for taspase 1 and active in transcription. *Mol Cell Biol,* 26**,** 2728-35.

Zufferey, R., Donello, J. E., Trono, D. & Hope, T. J. 1999. Woodchuck hepatitis virus posttranscriptional regulatory element enhances expression of transgenes delivered by retroviral vectors. *J Virol,* 73**,** 2886-92.

7. List of publications

Publications

M. Carlet*, **K. Völse***, J. Vergalli, M. Becker, T. Herold, A. Arner, D. Senft, V. Jurinovic, W.-H. Liu, Y. Gao, V. Dill, B. Fehse, C. D. Baldus, L. Bastian, L. Lenk, D. M. Schewe, J. W. Bagnoli, B. Vick, J. P. Schmid, A. Wilhelm, R. Marschalek, P. J. Jost, C. Miehting, K. Riecken, M. Schmidt-Supprian, V. Binder, I. Jeremias
"*In vivo* inducible reverse genetics in patients' tumors to identify individual therapeutic targets"
Nature Communications 2021; 12(1):5655, doi: 10.1038/s41467-021-25963-z

W.-H. Liu, **K. Völse**, D. Senft, I. Jeremias
"A reporter system for enriching CRISPR/Cas9 knockout cells in technically challenging settings like patient models"
Scientific Reports 2021; 11(1):12649, doi: 10.1038/s41598-021-91760-9

J. M. Kempf*, S. Weser*, M. D. Bartoschek, K. H. Metzeler, B. Vick, T. Herold, **K. Völse**, R. Mattes, M. Schulz, L. E. Wange, M. Festini, E. Ugur, M. Roas, O. Weigert, S. Bultmann, H. Leonhardt, G. Schotta, W. Hiddemann, I. Jeremias, K. Spiekermann
"Loss-of-function mutations in the histone methyltransferase EZH2 promote chemotherapy resistance in AML"
Scientific Reports 2021; 11(1):5838, doi: 10.1038/s41598-021-84708-6

W.-H. Liu, P. Mrozek-Gorska, A.-K. Wirth, T. Herold, L. Schwarzkopf, D. Pich, **K. Völse**, M. C. Melo-Narváez, M. Carlet, W. Hammerschmidt, I. Jeremias
"Inducible transgene expression in PDX models *in vivo* identifies KLF4 as therapeutic target for B-ALL"
Biomarker Research 2020; 8:46, doi: 10.1186/s40364-020-00226-z

A. Moretti*, L. Fonteyne*, F. Giesert*, P. Hoppmann*, A. B. Meier*, T. Bozoglu, A. Baehr, C. M. Schneider, D. Sinnecker, K. Klett, T. Fröhlich, F. Abdel Rahman, T. Haufe, S. Sun, V. Jurisch, B. Kessler, R. Hinkel, R. Dirschinger, E. Martens, C. Jilek, A. Graf, S. Krebs, G. Santamaria, M. Kurome, V. Zakhartchenko, B. Campbell, **K. Voelse**, A. Wolf, T. Ziegler, S. Reichert, S. Lee, F. Flenkenthaler, T. Dorn, I. Jeremias, H. Blum, A. Dendorfer, A. Schnieke, S. Krause, M. C. Walter, N. Klymiuk, K. L. Laugwitz, E. Wolf#, W. Wurst#, C. Kupatt#

"Somatic gene editing ameliorates skeletal and cardiac muscle failure in pig and human models of Duchenne muscular dystrophy"

Nature Medicine 2020; 26(2):207-214, doi: 10.1038/s41591-019-0738-2

Abstracts

K. Völse, M. Carlet, D. Schewe, I. Jeremias

"MLL/AF4 plays an essential role for established ALL PDX tumors during their growth *in vivo* as detected by inducible knockdown in mice"

HemaSphere 2020; 4(S1):140, doi: 10.1097/HS9.0000000000000404

* These authors share first authorship.

# These authors share last authorship.

8. Declaration

Eidesstattliche Versicherung

Völse, Kerstin
_____
Name, Vorname

Ich erkläre hiermit an Eides statt,
dass ich die vorliegende Dissertation mit dem Thema

“Role of the t(4;11) fusion proteins MLL/AF4 and AF4/MLL for survival and growth of patient-derived xenograft leukemia cells *in vivo*”

selbständig verfasst, mich außer der angegebenen keiner weiteren Hilfsmittel bedient und alle Erkenntnisse, die aus dem Schrifttum ganz oder annähernd übernommen sind, als solche kenntlich gemacht und nach ihrer Herkunft unter Bezeichnung der Fundstelle einzeln nachgewiesen habe.

Ich erkläre des Weiteren, dass die hier vorgelegte Dissertation nicht in gleicher oder in ähnlicher Form bei einer anderen Stelle zur Erlangung eines akademischen Grades eingereicht wurde.

_____ _____

Ort, Datum Unterschrift Doktorand

9. Acknowledgements

Als erstes möchte mich bei Prof. Dr. Irmela Jeremias bedanken für die intensive Betreuung, für die Unterstützung bei den verschiedenen Projekten und für die zahlreichen fachlichen Diskussionen. Ich konnte mich fachlich und auch persönlich weiterentwickeln und möchte mich ganz herzlich für die gute Zusammenarbeit bedanken.

Besonders bedanke ich mich auch bei Prof. Dr. Arnd Kieser für die Betreuung meiner Doktorarbeit, für die immer offene Tür und die vielen wertvollen Ideen.

Mein großer Dank gilt auch den Mitgliedern meines Thesis Advisory Committees, Prof. Dr. Arnd Kieser, Prof. Dr. Olivier Gires, Prof. Dr. Irmela Jeremias und Dr. Michela Carlet für die zahlreichen wissenschaftlichen Diskussionen und den hilfreichen Input.

Außerdem möchte ich mich bei Dr. Michela Carlet und Dr. Wen-Hsin Liu bedanken für die hervorragende Betreuung und der stetigen Unterstützung.

Darüber hinaus bedanke ich mich bei meinen Kooperationspartnern Alexander Wilhelm und Prof. Dr. Rolf Marschalek für die sehr gute Zusammenarbeit und vor allem bei der Unterstützung der Analyse der MACE Seq Daten.

Vielen Dank auch an die ganze Abteilung Apoptose in Hämatopoietischen Stammzellen für die großartige Zusammenarbeit. Ich möchte mich herzlich bei den Technischen Assistenten bedanken für die tatkräftige Unterstützung in meinem Projekt. Ein riesiger Dank geht auch an meine Mit-Doktoranden zum einen für die fachliche Unterstützung, zum anderen für die vielen lustigen Momente aber auch dafür, dass ihr immer ein offenes Ohr hattet. Ich hätte mir keine besseren Kollegen wünschen können! Danke auch an allen Mitarbeitern der Tierhaltung für die Versorgung der Mäuse.

Zuletzt möchte ich mich bei meiner Familie und meinen Freunden bedanken für die stetige Unterstützung und Motivation. Vielen Dank dafür!